



MASTERARBEIT

Titel der Masterarbeit

Glycan Interactions in Amoebae

>1 von 1<

Verfasser

Stefan Mereiter BSc

angestrebter akademischer Grad

Master of Science (MSc)

Wien, 2013

Studienkennzahl lt.
Studienblatt:

A 066 834

Studienrichtung lt.
Studienblatt:

Molekulare Biologie

Betreuerin / Betreuer:

Univ.-Prof. Dr. Graham Warren

I. Acknowledgment

First of all I would like to thank my supervisor at the Vienna University of Natural Resources and Life Sciences, a.o. Univ. Prof. Dr. Iain B.H. Wilson, for the opportunity to carry out my master thesis in his laboratory, for his always supportive and friendly nature and his expertise which enabled me deep insights into the field of glycobiology.

Thank you to Dr. Alba Hykollari, who guided me through this master thesis, who continually availed herself with assistance and encouragement, and from whom I learned so much.

Thank you to Dr. Shi Yan for the stimulating scientific and collegial conversations we shared, for his attentive ear to any problem I wished to air and for our always entertaining lunch breaks.

Thank you to Dr. Martin Dragosits for sharing his experiences on cloning and helping me to solve so many minor problems along the way. Thank you Dipl.-Ing. Simone Kurz and Rhiannon Stanton, BSc, for being great labmates and Dr. Carmen Jimenez-Castells for sharing her precious chemicals.

I want to thank the scientific director of the Max F. Perutz Laboratories, Univ. Prof. Dr. Graham Warren, for accepting the official supervision of this thesis, despite of his many other duties.

Last but not least I want to thank my family for being my always reliable rock in turbulent waters, and my dear friends for both, challenging me to fight my inner couch-potato and also helping me to get my mind of the thesis when it was appropriate.

Table of Contents

MASTERARBEIT	1
I. Acknowledgment	2
II. Abstract	5
III. Introduction	6
3.1 <i>Dictyostelium discoideum</i>	6
3.2 Glycosylation	10
3.2.1 N-Glycosylation	11
3.2.2 Glycosylation in <i>Dictyostelium</i>	12
3.3 Lectins	13
3.3.1 Discoidin I	14
3.4 Mass Spectrometry	16
IV. Material and Methods	18
4.1 Cultivation of <i>Dictyostelium discoideum</i>	18
4.1.1 Maintenance on Agar Plate	18
4.1.2 Axenic Growth in Liquid Media	19
4.1.3 Protein Extraction	19
4.2 General Working Procedures with Lysates	20
4.2.1 SDS-PAGE (sodium dodecyl sulphate polyacrylamide gel electrophoresis)	20
4.2.2 Coomassie Staining	21
4.2.3 Western Blotting	21
4.2.4 Western Blotting with Inhibition by Neoglycoconjugates	23
4.2.5 Tryptic Digest Protocol for Purified Protein	24
4.2.6 Tryptic Digest of Excised Bands	24
4.2.7 PNGase A Digest	24
4.2.8 PNGase F Digest	25
4.2.9 Glycan Purification	25
4.2.10 Sepharose Matrix Affinity Chromatography	25
4.2.11 Acrylamide Matrix Affinity Chromatography	26
4.2.12 Magnetic Beads Immuno Precipitation	26
4.2.13 Methanol Protein Precipitation	27
4.2.14 Silver Staining	27
4.2.13 Tryptic Digest Protocol Subsequent to Silver Staining	28
4.2.14 Mass Spectrometry	28
4.3 Cloning	29
4.3.1 Reverse Transcription	29
4.3.2 PCR from cDNA	29

4.3.3 Band Purification after PCR.....	30
4.3.4 Digestion with Restriction Enzymes.....	30
4.3.5 Ligation.....	31
4.3.6 CaCl ₂ Competent <i>E. coli</i>	31
4.3.7 Transformation of Competent <i>E. coli</i> after Ligation.....	32
4.3.8 Screening for Transformed <i>E. coli</i>	32
4.3.9 Transformation of Competent <i>E. coli</i> with Purified Plasmid.....	32
4.3.10 Pilot Protein Expression.....	33
4.3.11 Large Scale Protein Expression.....	33
4.3.12 <i>E. coli</i> Lysis for Recombinant Protein.....	33
4.3.13 His-Tag purification.....	34
4.4 Websites and Software.....	34
V. Results.....	35
5.1 Western Blot Inhibition Assay.....	35
5.2 HRP Quality Control.....	38
5.3 Affinity Chromatography.....	41
5.3.1 Affinity Chromatography with Sepharose Matrix.....	41
5.3.2 Affinity Chromatography with Acrylamide Matrix.....	47
5.4 Investigation on Discoidin I.....	52
5.4.1 Cloning of Discoidin I.....	52
5.4.2 Cloning of Discoidin I N and C terminus.....	59
5.4.3 Binding affinity of Discoidin I A to HRP.....	61
VI. Discussion.....	62
VII. References.....	66
VIII. Appendix.....	72
8.1 Growth Kinetics of Ax3.....	72
8.2 Abstract in German.....	73
8.3 Curriculum Vitae of the Author.....	74

II. Abstract

Dictyostelium discoideum is a well-studied social amoeba that upon starvation undergoes a developmental shift in which it aggregates with thousands of other cells to form a real multicellular organism in which subsets of cells differentiate and specialize to perform certain tasks. During this developmental shift many of *D. discoideum*'s intra and extracellular properties change as for instance its N-glycome. The majority of N-glycans of single cellular *D. discoideum* carry an α -1,3-core-fucosylation, up to eight mannoses and intersecting and bisecting N-acetylglucosamines. These glycan structures change dramatically during cell differentiation leading to non-intersected and non-bisected N-glycans with in total only five mannoses, but the α -1,3-core-fucose remains. To date the biological function of the core-fucose and N-glycomic shift is a puzzle. It seems more than certain that at least one specific N-glycan-binding lectin exists in this organism. Here I show inhibition western blots that support this assumption. Hence I performed an affinity chromatographical screening for lectins by offering HRP, a plant protein carrying quite simple α -1,3-core-fucosylated N-glycans, to *D. discoideum* lysates. Subsequent MALDI-TOF mass spectrometry protein mass fingerprint analysis and MS/MS peptide sequencing identified isolated proteins. By this method the lectin discoidin I could be identified as a potential *D. discoideum*-N-glycan-binding protein. This protein is a well-known lectin of *D. discoideum* whose function is still unknown but whose expression starts after aggregation of the amoeba and therefore might play a role coordinated with the smaller N-glycan structures. Due to further investigations on the biochemical properties of Discoidin I, dscA-1, one of three Discoidin I chains occurring in the organism, has been expressed with an N-terminal His-tag in BL21 *E. coli* expression strains and purified on Ni-NTA columns. The so purified Discoidin I was then subject to simple examinations of its binding properties which led to unexpected results that might be due to the expression system chosen or the experimental set up. Additionally due to the complicated structure of discoidin I, actually consisting of 2 sugar-binding sites one at each terminus, two truncated discoidin I proteins comprising either only one of the binding sites were expressed. In this thesis I present evidence for a novel natural binding partner of discoidin I and provide expressed proteins which might render future scientific breakthrough on developmental research of *D. discoideum* possible.

III. Introduction

The model organism *Dictyostelium discoideum* is a well-studied social amoeba which inhabits soil, feeds on bacteria and is capable upon starvation to aggregate and form with about 10.000 to 50.000 other cells a real multicellular organism (Kessin, 2001). One developmental key stage of the multi-cellular *D. discoideum*, as a result of its slug-like shape commonly known as “slug”, is capable of chemotaxis and phototaxis, shows a simple form of immune system and consists of developmentally committed cells (Müller-Taubenberger et al., 2007 ; Chen et al., 2013) . Once an appropriate location has been reached the slug metamorphoses into a fruiting body composed of a rod expanding towards the air and spore cells on its top. By its unique switch from uni- to multicellularity and despite being a quite simple organism, *Dictyostelium discoideum* drew scientific interest in topics like development, aggregation and cell-cell-communication.

One of the fundamental differences between a unicellular life form and a multicellular is the high amount of cell-cell-communication that is required (Van Haastert, 1991). When a bunch of independent cells decide to start acting as a unit, the expression of a variety of surface proteins and glycans has to change in order to handle the new tasks such as uniform cell movement, adhesion, coordinated cell development and possibly substrate exchange.

Previous investigations on the N-glycome of *D. discoideum* have revealed that its major N-glycans are of oligomannosidic nature carrying α 1,3 core fucose as well as intersecting and bisecting N-acetylglucosamine (Schiller, 2009). The glycosylation profile shifts during development towards shorter N-glycans, with more accessible core-fucoses in the multicellular form. Even though the reason for this developmental change in N-glycan structure has not been elucidated yet, it may be associated with agglutination of this otherwise independent amoeba. Corresponding lectins for N-glycans of *D. discoideum* have not been identified. These lectins would help to clarify the role of glycosylation shifts, and enlighten the still not well understood aggregation of this fascinating creature.

3.1 *Dictyostelium discoideum*

Scientific classification	
Domain:	Eukarya
Kingdom:	Amoebozoa
Superphylum:	Conosa
Phylum:	Mycetozoa
Family:	Dictyosteliidae
Genus:	Dictyostelium
Species:	<i>D. discoideum</i>

Dictyostelium discoideum is a free living amoeba inhabiting soil rich in humus of the temperate zone and belongs to the phylum of mycetozoa (Raper, 1935). Due to the former misjudgement that mycetozoa are part of the fungal kingdom, they are in English commonly known as slime moulds. Today two ways of classification for mycetozoa exist, a stricter, monophyletic one, sometimes referred to as true slime moulds, and a wider, polyphyletic one (Stephenson and Stempen, 2000). The stricter classification of the mycetozoa phylum distinguishes between three classes, the plasmodial slime moulds, the cellular slime moulds, to which *Dictyostelium* belongs to, and the protostelids. In the wider classification also some non-amoebozoan classes are counted. What all mycetozoa have in common is a single cellular trophic stage lacking a cell wall in which they remain as long as food is abundant; as soon as they run out of food, they are able to form stalks that produce fruiting bodies releasing spores for spreading.

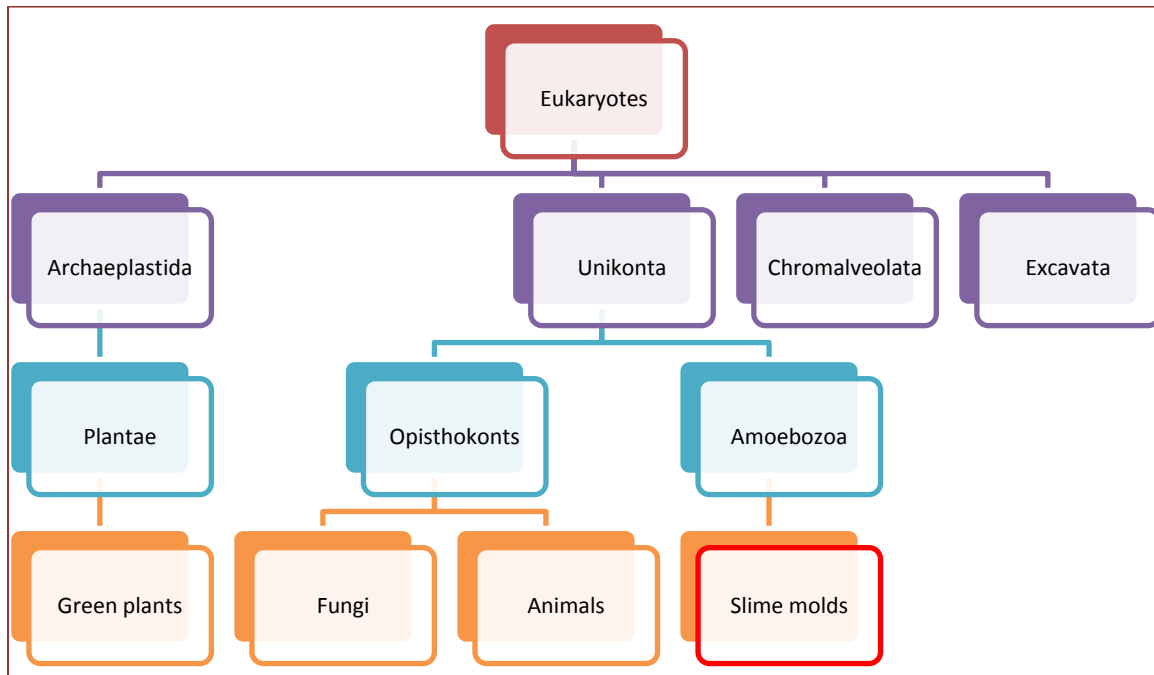


Figure 3.1: Phylogenetic tree adapted from Keeling et al., 2009, Tree of Life Web Project at <http://tolweb.org/Eukaryotes/3>

Figure 3.1 depicts the phylogenetic tree of eukaryotes showing that animals, fungi and slime moulds all belong to the unikonta. Many of the biological phenomena have been preserved since the last common ancestor, like signal transduction and pattern formation, leading to many homologies within the taxonomic group of unikonts. In some other regards slime moulds represent intermediates between plants and opistokonts; for instance, as intracellular storage compounds, both trehalose, used by fungi and plants, and glycogen, utilized by animals, are present in mycetozoa (Wright B. et al., 1968). The group of dictyostelia can be divided into four groups based on sequence analysis of rRNA (Schaap et al., 2006). Group 1, 2 and 3 are, from a

morphological point of view, quite similar. They can encyst upon rough environmental conditions and thereby turn into a dormant stage to endure life-threatening circumstances. Additionally they can also aggregate, form multi-cellular organisms and partly develop into spores. The main distinguishing feature of group 4, the group *D. discoideum* belongs to, is the use of different chemo-attractants for aggregation and the large numbers of spores encapsulated in the spore coat (Devreotes, 1989; Manahan et al., 2004).

The genome of *D. discoideum* was sequenced and published 2005 (Eichinger et al., 2005). The size of the genome is approximately 33.8 Mb, larger than *S. cerevisiae* (12 Mb) but still smaller than *A. thaliana* (123 Mb), *C. elegans* (103 Mb) or *D. melanogaster* (180 Mb). It carries around 12,500 genes which is more than half as much as humans (around 21,000 genes), with introns in most of its genes (70%). Many human disease encoding genes have highly similar orthologues in *D. discoideum*. Very surprising is the amount of A+Ts which make up 78.8% of the genome (Urushihara, 2009).

In their natural environment, slime moulds feed on bacteria or yeast, which contain all 20 genetically encoded, proteinogenic amino acids; therefore, they lack the ability to synthesise many by themselves (Payne, 2005). The following amino acids are essential for *D. discoideum*: arginine, histidine, isoleucine, leucine, lysine, methionine, phenylalanine, proline, threonine tryptophan and valin. Axenic strains which are able to grow in the absence of other living organisms have been isolated and are now widely used by the scientific community. Yeast extract and peptones are added to the media to meet the high demand for complex components. The transparent nature of uni- and multi-cellular stages allows the monitoring of protein expression, localization of proteins and visualization using different tags such as fluorescence (Maeda et al., 2003).

Aggregation of single cellular *D. discoideum* is due to the secreted, chemoattractant cAMP which binds to cAMP dependent G-Protein receptors (Konijn et al., 1969; Hereld, 2005). The extracellular use of cAMP is a unique feature of the dictyostelia family (Schaap, 2011). During this process cAMP is produced in periodical pulses and results in concentric cAMP circles that lead each cell to the centre of aggregation. The cells first aggregate into a mound and in response to the continued cAMP emission from its top, a tipped mound is formed. At this stage, the *D. discoideum* cells start to differentiate into either prespore or prestalk cells. The prestalk cells migrate to the top and the prespore cells migrate to the bottom, causing the mound to elongate. The so formed shape is called "finger". It soon falls over and starts migrating as a real multicellular organism in the so-called "slug" stage (figure 3.2). In this stage it seeks for a suitable location to sporulate, guided by its phototactical and chemotactical abilities. When such a location has been found the slug ultimately forms a fruiting body in which about 20% of the cells die in order to lift the spores; a process known as culmination.

Dictyostelium discoideum is also capable of sexual reproduction. If two different mating types meet under cool and dark conditions, they fuse to form a giant cell (Saga et al., 1983). This giant cell secretes cAMP to attract further amoeba, which are almost all consumed by the giant cell. Some of the amoebae, though, form a cellulose wall around the entire group. This is known as a macrocyst. The giant diploid cell eventually

undergoes recombination, meiosis and then further divides through mitosis to produce many haploid amoebae which hatch from the macrocyst (O'Day et al., 2011).

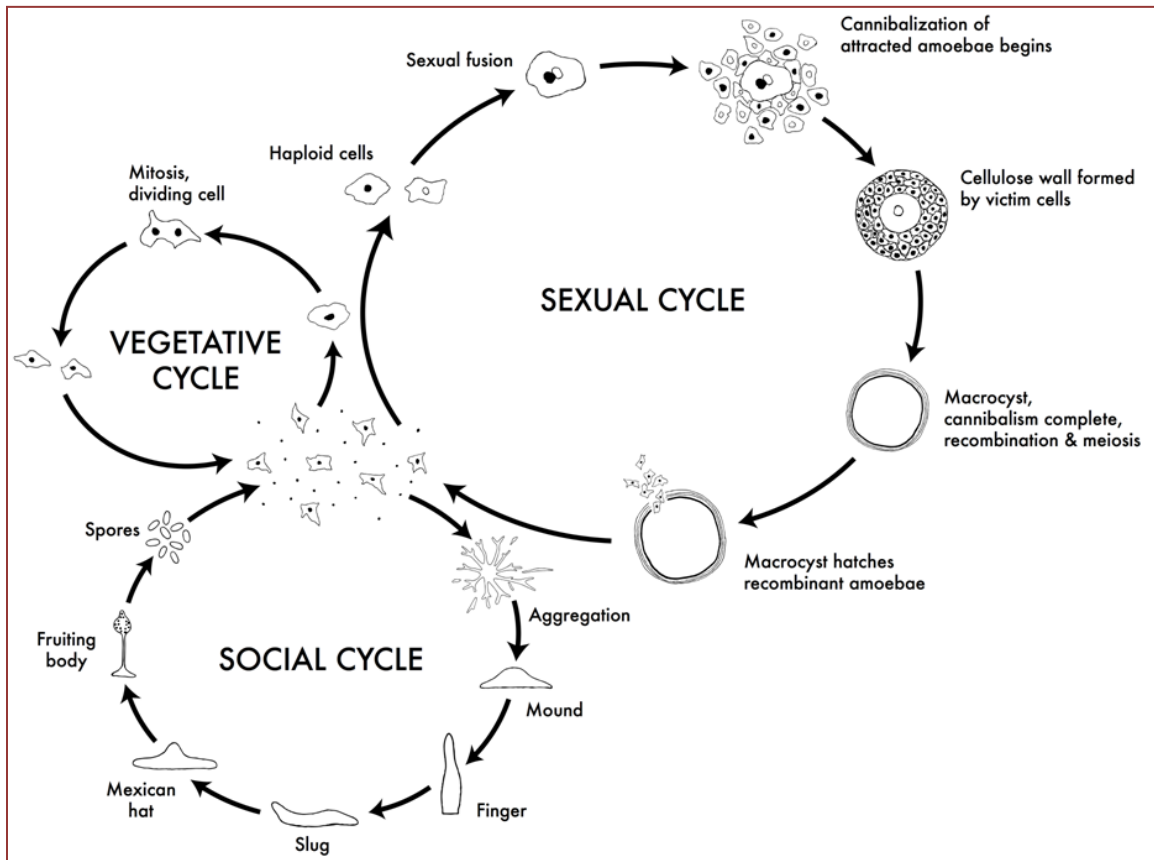


Figure 3.2: Life cycle of *Dictyostelium discoideum* from *Dictybase.org*

Dictyostelium discoideum is used as a cell biological model organism for cell-cell adhesion, eukaryotic chemotaxis, eukaryotic cell motility, organelle and protein dynamics, cytokinesis and it is also used as a model for biomedical research on cell migration in health and disease, innate immunity, legionnaires' disease and molecular basis of neurodegenerative diseases (Müller-Taubenberger et al., 2013). *D. discoideum* is easy to grow in liquid media and thus, a high cell number can fast be achieved. It is a comparatively robust amoeba and its spores can be kept at -80°C for long-term storage. The genome contains 6 chromosomes and is fully sequenced. *D. discoideum* is haploid and mutants can therefore easily be obtained. Many molecular genetic techniques are available, for instance: gene inactivation by homologous recombination, gene replacement, antisense strategies, RNA interference, restriction enzyme-mediated integration, library complementation and expression of GFP fusion proteins. Stocks of wild-type and mutant strains are available and commercially available kits for RNA extraction such as Trizol (Invitrogen) and RNeasy (QIAGEN) can be used (Gaudet et al., 2008).

3.2 Glycosylation

Glycosylation is a very common post-translational modification performed by all eukaryotic and many prokaryotic cells. In general it is an enzymatically-catalysed, site-specific addition of carbohydrate residues. The saccharides being used and the resulting so-called glycans depend on the enzymes present in the given cell and/or compartment and the target of the glycosylation reaction.

Each sugar residue is linked to one another via glycosidic bonds, which are formed between the anomeric carbon atom of one sugar and a hydroxyl-group of the other sugar (figure 3.2.1). Depending on the angle of the bond, the linkage is called α or β . Additionally the number of the linked carbon atom is stated.

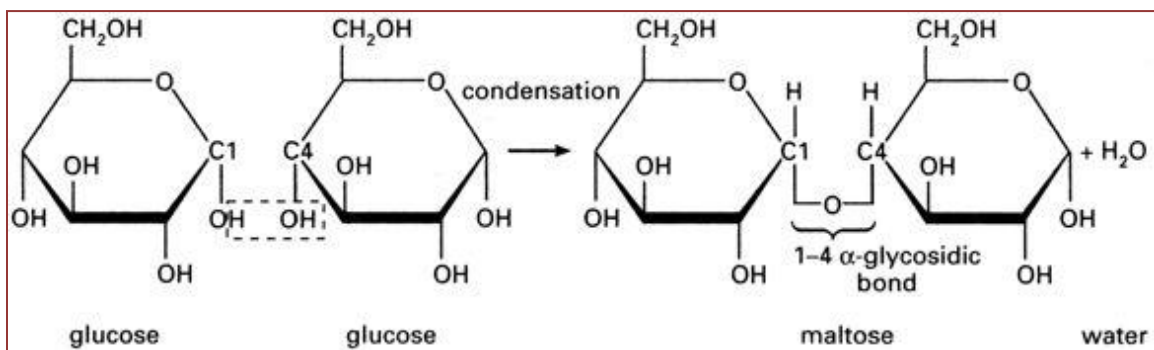


Figure 3.2.1: Glycosidic bond formation between the hydroxyl group of C1 and C4 of two glucose monosaccharides resulting in glucose disaccharide connected by an α -1,4-bond (with the trivial name maltose) via an oxygen atom.

Oligosaccharides can be attached to proteins or lipids. The quantity of glycosylation depends on the target. Examples for highly glycosylated proteins are proteoglycans, whose functions are associated with water retention, resistance to compressive and tensile forces as well as growth factor gradient formation (Yanagishita, 1993).

On proteins we distinguish between three classes of glycans: the O-glycans, the C-glycans and the N-glycans. Sugars of O-glycans are added one by one on a serine or threonine residue of proteins in the Golgi apparatus. C-glycans are rare modifications, where one mannose is added to the carbon atom of a tryptophan. On the other hand, the sugars of an N-glycan are attached as an oligosaccharide to asparagines of proteins in the endoplasmic reticulum. Protein glycosylation plays an important biological role. Glycosylation can be crucial for the correct folding of a protein, it can contribute in stability and solubility, and it can carry information for localisation and represents specific binding sites for lectins. Many enzymes involved in glycosylation are not expressed constitutively. Therefore the glycome of a single cell can vary depending on internal and external factors.

3.2.1 N-Glycosylation

The generation of an N-glycan is a multi-step process. The first steps are conserved among eukaryotes. N-glycosylation was also discovered in prokaryotes, but there is still not so much known about it (Wacker et al., 2002).

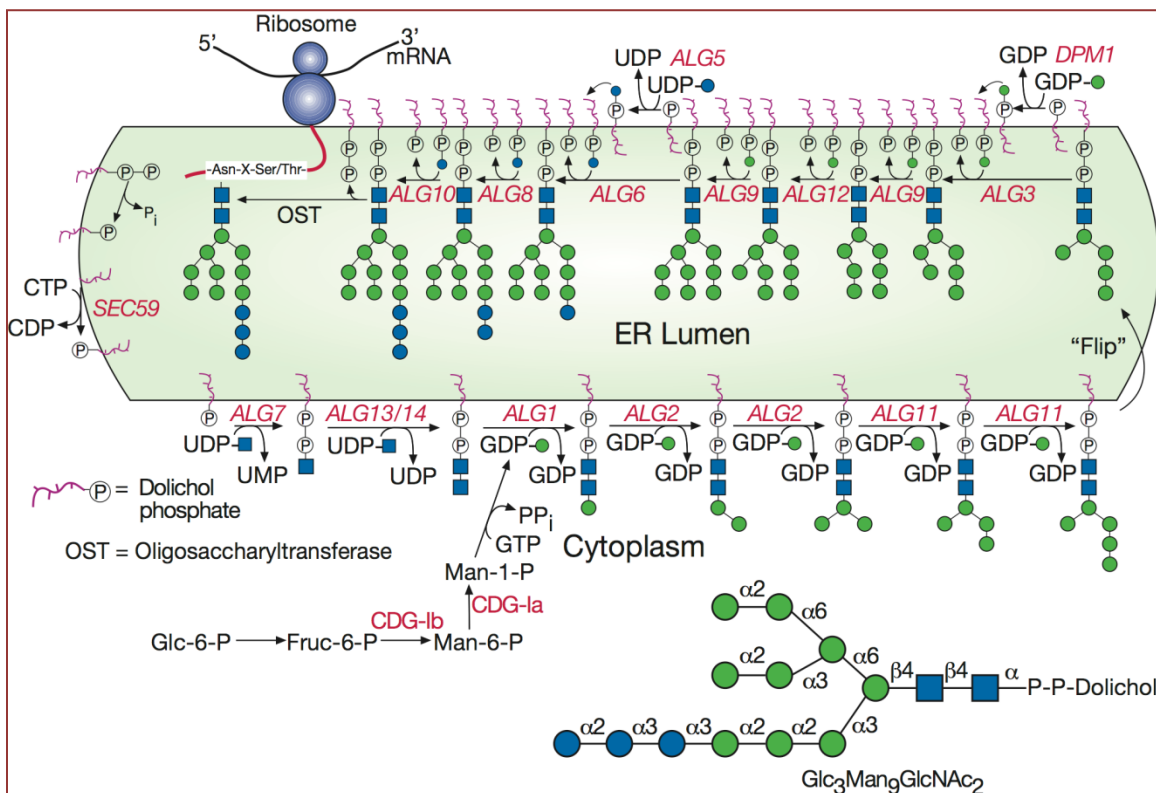


Figure 3.2.1.1 Process of precursor assembly at the ER membrane and all involved enzymes. Taken from *Essentials of Glycobiology, Second Edition, Chapter 8*

In eukaryotes the formation of N-glycans starts on the cytosolic face of the rough endoplasmic reticulum, where a glycan structure consisting of five mannoses (Man) and two N-acetylglucosamines (GlcNAc) is carried by a dolichol pyrophosphate. This structure is then flipped to the inside of the ER lumen where further mannoses and glucoses are added in order to build the so-called precursor with the formula $\text{GlcNAc}_2\text{Man}_9\text{Glc}_3$ (figure 3.2.1.1). The oligosaccharyltransferase (OST) transfers the whole precursor glycan to a nascent polypeptide carrying the peptide sequence Asn-X-Ser/Thr or rarely Asn-X-Cys (Helenius and Aebi, 2004). Though this mechanism is highly conserved, a few parasitic organisms have lost some glycosyltransferases activities, resulting in truncated precursor structures (Samuelson et al., 2005). After the precursor is transferred to the target protein, its glucoses are removed in the ER, a process related to quality control. One glucose is reattached to incorrectly folded proteins till they fold

correctly or are degraded (Hersovics, 1999). Before the correctly folded protein is transferred to the Golgi one mannose is removed (Tremblay and Hersovics, 1999). In the Golgi several N-glycan modification steps occur which differ from organism to organism.

3.2.2 Glycosylation in Dictyostelium

Except for the absence of sialic acid, the *D. discoideum* overall carbohydrate composition is similar to that of animals (West et al., 2005). Still the typical oligomannosidic structures of *D. discoideum* have proven to be quite complicated with charged N-glycans carrying sulphate and methyl phosphate (Feasly et al., 2010; Hykollari et al., 2013) and with neutral N-glycans carrying both intersecting and bisecting N-acetylglucosamine residues (figure 3.2.2.1) and a core α 1,3-fucose (Schiller et al., 2009).

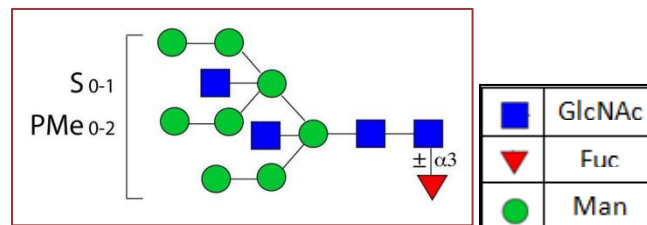


Figure 3.2.2.1 Typical N-glycan structure found in *D. discoideum*

A fascinating feature of *D. discoideum* is a developmental shift of the N-glycome. The degree of sulphate and phosphate modifications decreased during late tip formation, and whereas N-glycans from single cellular *D. discoideum* were endoglycosidase Endo H resistant, they became sensitive during aggregation and culmination (Ivatt et al. 1981). Recently it has been shown by mass spectrometry that the major neutral N-glycan structure shifts from $\text{Man}_8\text{GlcNAc}_4\text{Fuc}_1$ towards $\text{Man}_5\text{GlcNAc}_2\text{Fuc}_1$ (figure 3.2.2.2) (Schiller et al., 2009).

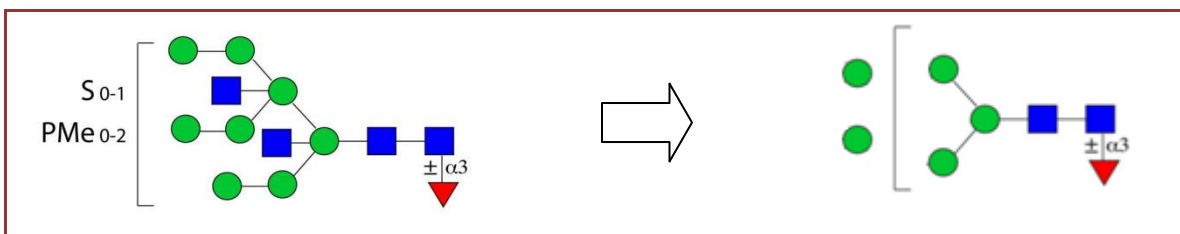


Figure 3.2.2.2 N-Glycan trend during the development of *D. discoideum*

A unique glycosylation feature of *D. discoideum* is a pentasaccharide O-glycan linked to hydroxyproline (Teng-umnuay et al., 1998). This unique Gal- α 1,6-Gal- α 1-Fuc- α 1,2-Gal- β 1,3-GalNAc glycosylation has been found on the protein SKP1, a protein related to ubiquitination. The biosynthetic pathway has been partly revealed showing that it takes

place in the cytoplasm only (Ercan et al., 2006) and that it is important for oxygen sensing (Xu et al., 2012).

Although not a form of protein glycosylation, still noteworthy are polysaccharides used by *D. discoideum*. *D. discoideum* is capable of cellulose production, which it uses for stalk and spore coat formation and during encystment (Zhang et al., 2001; O'Day et al., 2012; Grimson et al., 1996). Even more particular is a heteropolysaccharide produced by *D. discoideum* during spore formation, which consists of galactose and N-acetylgalactosamine (West et al., 2009). This galactose-rich polysaccharide (GPS) is important for spore integrity due to regulation of protein content of the coat and its role in crystalline cellulose formation.

3.3 Lectins

The word lectin is derived from the Latin word legere and means “to select”. They were first defined as proteins capable of binding reversibly to carbohydrates (Boyd and Shapleigh, 1954). Today a protein must meet four conditions to be classified as a lectin (Gabius et al., 2004):

1. A lectin is a protein that contains a carbohydrate recognition domain (CRD)
2. A lectin is not an immunoglobulin
3. A lectin does not modify the carbohydrates to which it binds
4. A lectin is no carrier for free mono- or oligosaccharides

Lectins are a very crucial class of protein and occur ubiquitously in nature. Their biological function in eukaryotic cells is manifold, from regulation of cell adhesion over binding of soluble extra- and intercellular glycoproteins, to intracellular signalling and control of protein levels. Concanavalin A was the first lectin which was purified in large scale and which is used till today extensively for purification and characterization of sugar-containing molecules.

In animals the main functions of lectins are to enable cell-cell contact and to act in innate immunity. Usually they contain two or more binding sites for carbohydrates via a number relatively weak interactions that ensure specificity on the one hand but reversibility on the other hand.

Plants and bacteria also contain lectins. In Plants they often act as strong insecticides, whereas in bacteria many lectins contribute in adherence and are therefore often associated with host-pathogen interactions. For example *E. coli* uses lectins to adhere to epithelial cells in the gastrointestinal tract of mammals.

Due to the phylogenetically closer relation of *D. discoideum* towards animals and the presence of homologues lectins, *D. discoideum* lectin function is presumably similar to that of animals. The variety of functions of membrane-bound animal lectins is depicted in figure 3.3.1.

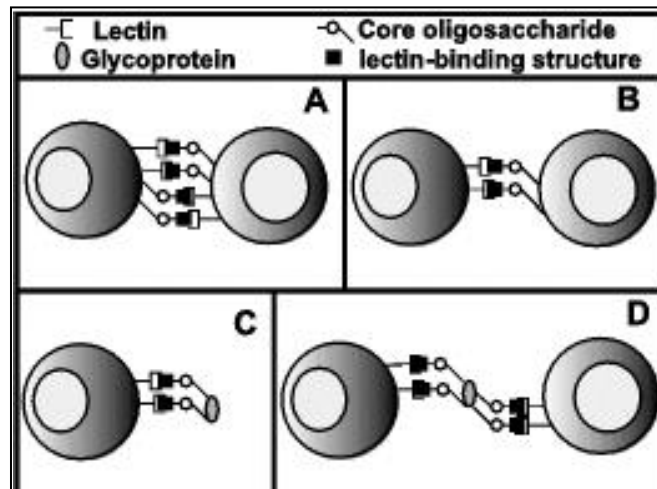


Figure 3.3.1 Possible function of membrane bound lectins.

Taken from *Essentials of Glycobiology, 2nd edition* (Varki et al., 2009). **A and B.)** Cell-cell interactions facilitated by lectin-glycan binding. **C.)** Binding of soluble glycoproteins present in the environment. **D.)** Cell-cell interaction facilitated by a mediating glycoprotein.

3.3.1 Discoidin I

Discoidin I is an often investigated, but in regards of its function or its natural binding partner, never conclusively understood lectin of *Dictyostelium discoideum*. During the single cell stage of *D. discoideum* when its food sources are abundant, discoidin I is hardly detectable, but as soon as aggregation starts the expression of discoidin I is to such an extent upregulated that it constitutes around 1% of the total protein in *D. discoideum* (Rosen et al., 1973; Frazier et al., 1975). Discoidin I can immunohistochemically be already detected during early aggregation and was shown to be intracellularly located in multilaminar bodies, from which it is released into the extracellular space (Barondes et al., 1985). On the other hand in later developmental stages starting from the slug, discoidin I is exclusively located on the surface of the multicellular organism, but neither intracellularly nor intercellularly (Barondes et al., 1983). The polymorphic nature of discoidin I is due to it actually being a product of a small, coordinately regulated multigene family consisting of three isoforms: *dscA*, *dscC* and *dscD*. The three isoforms differ in total 12 amino acids from each other, most of them located N-terminally. All three isoforms are located on the 2nd chromosome and are duplicated on the same chromosome in the laboratory strains Ax3 and Ax4 (Poole et al., 1981; Tsang et al., 1981). Its expression is transcriptionally regulated by cAMP, PSF (prestarvation factor) and CMF (conditioned medium factor), the three signalling key players for regulating the initialization of aggregation upon starvation (Blusch et al., 1995). DscI is 253 amino acids long and contains an N-terminal discoidin domain and a C-terminal H-type lectin domain (figure 3.3.1.1). Additionally it has an RGD (Arginine-

Glycine-Aspartic acid) motif which is a common cell binding site in adhesive proteins (Ruoslahti, 2003). The identified receptor for the RGD motif in *D. discoideum* is a 67 kDa cell-surface glycoprotein (Gabius et al., 1985).

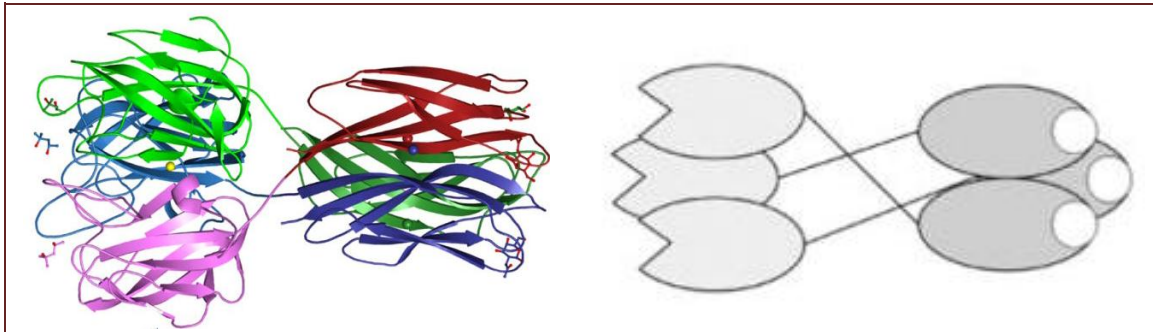


Figure 3.3.1.1: Crystal structure of discoidin I trimer (left) and a schematic graphic of it (right). N-terminal discoidin domains are in light colours, C-terminal H-type lectin domains are in dark colours. Taken from Mathieu et al. (2010).

The discoidin domain is a functionally diverse motif found in numerous proteins in both eukaryotes and prokaryotes (Baumgartner et al., 1998). It shows interactions with a wide range of molecules and is mainly involved in cell-surface-mediated regulatory events and glycoconjugates binding. Two famous, medically highly relevant examples of proteins carrying the discoidin domain are the blood coagulation factors V (Jenny et al., 1987) and VIII (Wood et al., 1984). Due to the conservation of the motif, serious physiological consequences of related disorders and the ability to interact with a broad range of ligands, it has become an intensively researched motif (Kiedziarska et al., 2007). Some examples of eukaryotic proteins carrying the discoidin domain are shown in figure 3.3.1.2). As shown in this figure it is present in a variety of very different protein families, often in multi-domain proteins, sometimes in repeats and frequently in combination with a signal peptide.

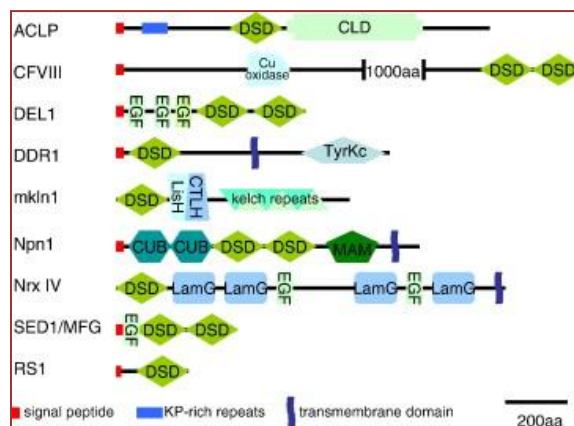


Figure 3.3.1.2: Shows a series of phylogenetically and functionally not related proteins carrying the discoidin domain (DSD). Taken from Kiedziarska et al. (2007).

Crystal structural analysis of discoidin I showed that the discoidin domain binding sites are formed by surface loops protruding from a β -barrel (Mathieu et al., 2010). These surface loops are highly variable in length in homologous proteins carrying this domain, explaining the great variety of binding partners and biological functions. Those structural homologues of discoidin that also form trimers are F-type fucose binding lectins such as *Anguilla anguilla* agglutinin (AAA).

The H-type lectin domain has been closer characterized very recently in the snail *Helix pomatia* (Sanchez et al., 2006). Besides *Dictyostelium discoideum* and *Helix pomatia*, such a domain was also identified in corals. Even though binding affinities of the H-type lectin domain towards GalNAc monosaccharides and α GalNAc-containing oligosaccharides were described, its function is still very uncertain. Glycan array analysis and microcalorimetric analysis showed that in discoidin I affinity for Gal β 1-3GalNAc and GalNAc β 1-3Gal are actually 10-fold stronger than for GalNAc monosaccharides (Mathieu et al., 2010).

3.4 Mass Spectrometry

Mass spectrometry (MS) is an analytical technique to determine the mass composition of molecules in a sample. It gives information about the chemical composition of samples and sometimes about their structure. First the compound is ionized to generate charged molecules and molecule fragments and then the mass-to-charge ratio is measured. In this thesis the mass spectrometric technique called matrix-assisted-laser-desorption-ionization time-of-flight time-of-flight (MALDI-TOF-TOF) was used (Harvey, 2008). MALDI describes the ionization method, in which the analyte is covered by a matrix. The sample/matrix crystal is targeted by a laser beam. The matrix transfers the energy needed for ionization from the laser light to the sample molecules (figure 3.4.1).

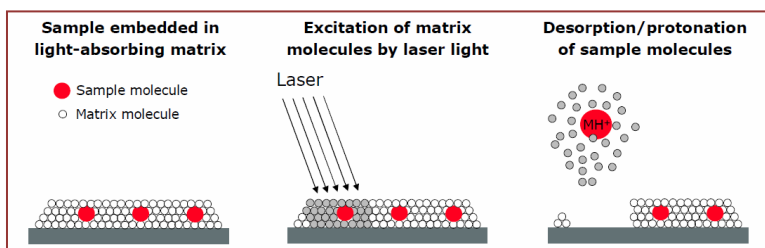


Figure 3.4.1 Depicts the MALDI ionization procedure

The used lasers are mostly nitrogen lasers and Nd:YAG lasers (Holle et al., 2009). Many different matrixes are used for MALDI depending on what kind of sample is ionized. Each matrix type has its own specific energy threshold and has thus advantages and disadvantages ionizing given sample. For peptides, for example, α -Cyano-4-hydroxy-

cinnamic acid (ACH) matrix can be used, whereas for glycans 2-azathiothymine (ATT) often shows better results.

In TOF after the ionization an electric field accelerates the sample and the time is measured that the sample needs to reach the detector. The acceleration and therefore the time needed to reach the detector depends on the analytes mass to charge ratio. The bigger m/z is, the slower the ion flies. To improve the resolution of the mass spectrogram pulsed ion extraction and a reflector can be used (figure 3.4.2). The reflector is usually not used when the analytes (such as intact proteins) are not stable enough to survive the energetic stress of deceleration and reacceleration in a high kV electric field within nanoseconds.

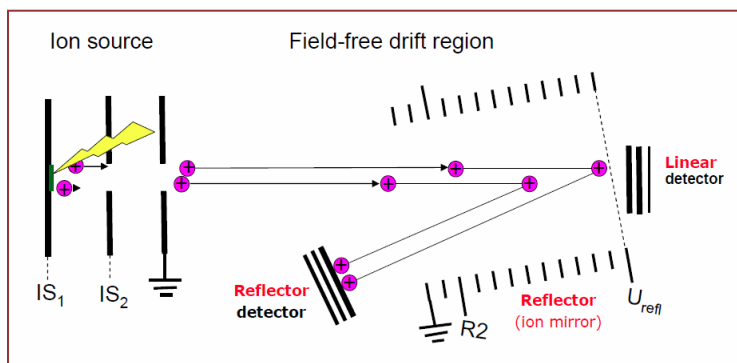


Figure 3.4.2 Depicts the linear TOF and TOF with reflector

TOF/TOF is a type of MS/MS which fragments a mother ion in order to get further details about chemical composition and structure. Ions can be fragmented via various methods, but most commonly collision-induced dissociation (CID), which is a post-source fragmentation, and laser induced dissociation (LID), which is an in-source fragmentation, are used. CID induces fragmentation due to collision with gas molecules. LID induces fragmentation directly by high laser energy. Since fragments fly with the same speed as their mother ion, the fragments of one mother ion can be separated from other fragments by a timed ion gate that lets only ions of a specific time window pass. Afterwards the fragments are accelerated again causing them to separate according to their m/z .

IV. Material and Methods

4.1 Cultivation of *Dictyostelium discoideum*

Dictyostelium discoideum is relatively easy to grow. They can be cultivated both on solid substrata covered with bacteria, which is closer to *D. discoideum*'s natural way of living, or in rich liquid media, which yields higher cell numbers. Since *D. discoideum* is a free living organism, it does not require controlled nitrogen or carbon dioxide conditions. The cells can be grown at room temperature, not exceeding 25°C. The only strain which was used in this master thesis was the AX3 strain which was obtained from the Dicty stock center and is a "pseudo" wild type strain capable of axenic growth.

4.1.1 Maintenance on Agar Plate

In order to maintain the Ax3 strain, besides keeping a spore stock at -80°C, they have been kept in their fruiting body developmental stage on an agar plate (Fey et al., 2007). Their spores remain under dark, dry and room temperate conditions stable for about one month and could be used to start a new liquid media culture line if needed.

First a colony of *E. coli* (OP50) was inoculated in sterile water. Then two or three spore heads either from previous Ax3 agar plates or from a -80°C stock were added to the bacterial suspension. In order to disperse the spores the suspension was vortexed for several minutes, then spread over an SM plate (table 4.1.1.1) and incubated at room temperature. The bacteria grow faster and expand to a lawn on the agar. After around 40 hours the bacterial lawn is consumed by Ax3 cells and the social developmental cycle starts. After a further 24 hours, fruiting bodies are formed in which the spores remain stable for about one month.

Table 4.1.1.1 1l SM agar

Glucose	2 g
Bacto peptone	2 g
Yeast extract	0.2 g
MgSO ₄	0.1 g
KH ₂ PO ₄	1.9 g
K ₂ HPO ₄	1 g
Agar	15 g
Adjust to	pH 6.5

4.1.2 Axenic Growth in Liquid Media

The experimental procedure is according to Fey et al., 2007. To start an axenic culture two to three spore heads of an agar plate with developed *D. discoideum* (as described in 4.1.1) were picked up by a sterile platinum wire and inoculated into a 24 well plate with 1 ml HL 5 (table 4.1.2.1) and 50 µg/ml streptomycin sulphate (Sigma) in each well. Cells were grown at room temperature without shaking. It took about 3 – 7 days, depending on the age of the spores, till the cells started slowly to grow. The media of those wells that showed good cell growth were transferred to a flask with HL 5 and 50 µg/ml streptomycin sulphate shaking at 100 rpm at room temperature to start exponential growth.

To maintain axenic growth around 2×10^4 cells of in log phase cells growing (i.e. below 8×10^6 cell per ml (Watts and Ashworth, 1970)), were transferred from the old flask to a new one containing 15 ml HL 5 and 50 µg/ml streptomycin sulphate and incubated at room temperature shaking at 100 rpm.

Table 4.1.2.1 1l HL 5 medium

Proteose peptone	5 g
Thiotone E peptone	5 g
Glucose	10 g
Yeast extract	5 g
Na ₂ HPO ₄ *7H ₂ O	0.35 g
KH ₂ PO ₄	0.35 g
dihydrostreptomycin-sulphate	0.05 g
Adjust to	pH 6.5

4.1.3 Protein Extraction

1.25×10^4 cells per µl lysate were used. Cells were counted and the desired amount of cells in HL5 was transferred from a shaking flask to a fresh Eppendorf tube. Cells in HL5 were centrifuged on 2000 g for 5 minutes; the supernatant was discarded and washed 2 times with KK2 buffer (table 4.1.3.1) with repeated centrifugation in between. The cell pellet was resuspended in lysis buffer (table 4.1.3.2) to a final concentration of 1.25×10^4 cells per µl and left on ice with occasional vortexing for 30 minutes. In order to get rid of cell fragments, the lysate was centrifuged with a benchtop centrifuge at 14.000 rpm, 4°C and for 30 minutes. The supernatant was transferred to a new Eppendorf tube and stored at -20°C.

Table 4.1.3.1 1l KK2 Buffer

KH ₂ PO ₄	2.2 g
K ₂ HPO ₄	0.7 g

Table 4.1.3.2 Lysis Buffer Recipe

Tris	50 mM
1M HCl	Adjust to pH 7.5
NaCl	150 mM
Triton X-100	0.5%
Protease inhibitor cocktail	1% (added before use)

4.2 General Working Procedures with Lysates

4.2.1 SDS-PAGE (sodium dodecyl sulphate polyacrylamide gel electrophoresis)

The cell extracts were mixed 1:1 with a 2x sample buffer (Table 4.2.1.1) and cooked for 10 minutes at 95°C. The 12.5% resolving gels were mixed (Table 4.2.1.2), poured between the glass plates, overlaid by 20% ethanol and left to polymerize for 45 minutes. After the stacking gels were mixed, the ethanol was removed. Then the stacking gel was poured on top of the resolving gel, the comb was put into place and left to polymerize for 30 minutes. The finished gel was placed into the electrophoresis apparatus which was then filled with electrode buffer (Table 4.2.1.3) and the comb was removed. The pockets were filled depending on the protein concentration with 2 – 15 µl sample or 1.5 µl protein ladder (Figure 4.2.1.1). The SDS-PAGE ran for around 50 minutes under 200 V.

Table 4.2.1.1 2x Sample Buffer Recipe

Sodium dodecyl sulphate (SDS)	200 mg
Dithioerythritol (DTE)	155 mg
Stacking gel buffer	5 ml
87% Glycerol	3.6 ml
dH ₂ O	1.9 ml
Bromophenol blue (1% in 48% ethanol)	1 drop

Table 4.2.1.2 Preparation of 2 gels

	Resolving gel	Stacking gel
30% Acrylamide	3.75 ml	0.76 ml
1% Bis-Acrylamide	1.17 ml	0.52 ml
Resolving gel buffer (1.5 M Tris/HCl, pH 8.8)	2.25 ml	/
Stacking gel buffer (0.5 M Tris/HCl, pH 6.8)	/	1.0 ml
dH ₂ O	1.71 ml	1.71 ml
10 % sodium dodecyl sulfate (SDS)	90 µl	40 µl
10% ammonium persulfate (APS)	54 µl	32 µl
N,N,N',N'-tetramethyl-ethylenediamine (TEMED)	5.4 µl	3.2 µl

Table 4.2.1.3 Electrode Buffer Recipe

	Resolved in dH ₂ O
Tris(hydroxymethyl)aminomethane (Tris)	3 g/l
Glycine	14.4 g/l
Sodium dodecyl sulfate (SDS)	1 g/l

4.2.2 Coomassie Staining

The gel was released from the glass plates and the stacking gel part was discarded. The remaining resolving gel was washed shortly with dH₂O, proteins were immobilized by incubation in fixation solution (Table 4.2.2.1) for 30 minutes and afterwards again washed shortly with dH₂O. Then the gel was placed in Coomassie staining solution (0.04% Coomassie Brilliant Blue G (Sigma) in 3.5% (w/v) perchloric acid) with rocking for 1 hour. Destaining was performed by rocking the stained gels in 5% (v/v) acetic acid until the background disappeared and the bands were clearly visible.

Table 4.2.2.1 Fixation Solution Recipe For 1 l Solution

Methanol	0.5 l
Acetic acid	0.07 l
dH ₂ O	0.43 l

4.2.3 Western Blotting

After SDS-PAGE the separated proteins were blotted in blotting buffer (table 4.2.3.1 and 4.2.3.2) from the gel on a nitrocellulose membrane via semi-dry blotting for 40 minutes and 20 V. The membrane was then reversibly stained by Ponceau to control the blotting

success and destained by H₂O. The membrane was blocked in 0.5% BSA. Rabbit anti-HRP antibody (1:10.000) was added and incubated for 1 hour at room temperature. Afterwards the membrane was washed 3 times 5 minutes with 5% TTBS (table 4.2.3.3 and 4.2.3.4), and incubated with an alkaline-phosphate-conjugated goat anti-rabbit antibody (1:2000) for 1 hour at room temperature, washed again 3 times 5 minutes with 5% TTBS. Detection was carried out using SigmaFAST™ BCIP/NBT.

Table 4.2.3.1 10x Blotting-buffer Resolved in dH₂O

Tris/HCl	250 mM
Glycine	1.92 M

Table 4.2.3.2 Blotting-buffer For 1 l Solution

10x Blotting-buffer	0.1 l
Methanol	0.2 l
dH ₂ O	0.7 l

Table 4.2.3.3 10x Tris-buffered saline (TBS) Resolved in dH₂O

Tris-Base	0.5 M
Adjust with 37% HCl	pH 7.4
NaCl	1.5 M

Table 4.2.3.4 Tween Tris-buffered saline (TTBS) For 1 l Solution

10x TBS	0.1 l
dH ₂ O	0.9 l
Tween 20	0.5 ml

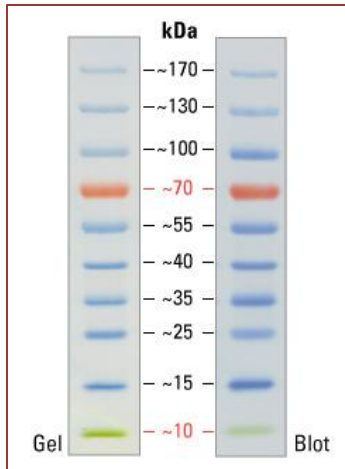
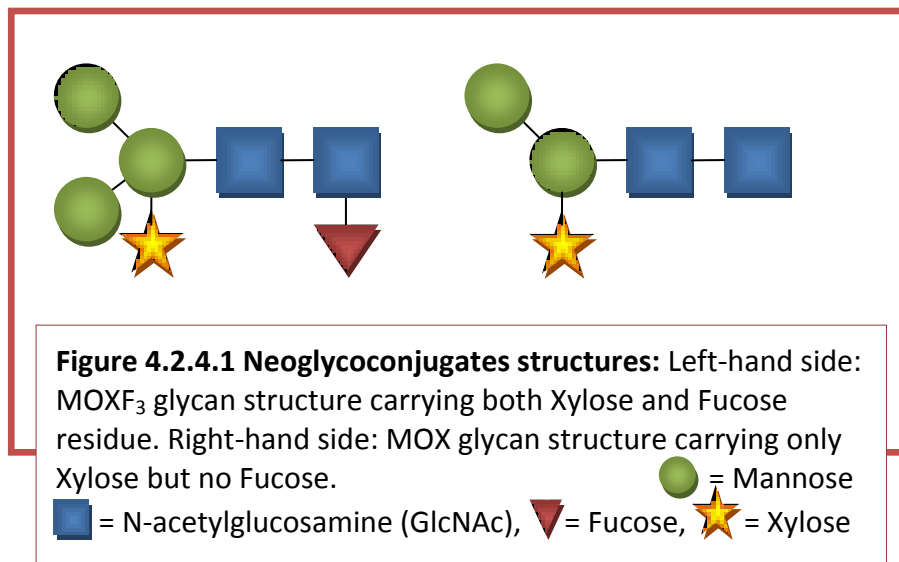


Figure 4.2.3.1: Standard protein ladder used in this master thesis

4.2.4 Western Blotting with Inhibition by Neoglycoconjugates

Two different neoglycoconjugates (glycans cross-linked to BSA) have been used to inhibit anti-horseradish peroxidase binding to specific epitopes. On the one hand MOXF₃ has been used which fully occupies the binding site of the anti-horseradish peroxidase and therefore fully inhibits its binding properties. On the other hand MOX has been used which occupies only the binding site of anti-horseradish peroxidase for xylose, and therefore makes the antibody specific for fucose only.



4.2.5 Tryptic Digest Protocol for Purified Protein

10 μl of protein solution (between 0.1 and 1.0 mg/ml) were mixed with 15 μl of 50mM NH_4HCO_3 and 1.5 μl of 100mM DTT. The samples were then incubated for 5 minutes at 95°C. 3 μl of freshly prepared 100mM iodoacetamide were added to the samples and incubated in the dark for 20 minutes. 5 μl of Trypsin working solution are added and incubated at 37°C for 3 hours.

4.2.6 Tryptic Digest of Excised Bands

First the Coomassie stained bands were excised from the SDS-PAGE gel and cut into small pieces (1mm³). Then the pieces were destained by washing with 50 μl HQ H₂O for 5 minutes, 50 μl 50% acetonitrile for 15 minutes, 50 μl 100% for 15 minutes, 50 μl freshly dissolved 100mM NH_4HCO_3 for 5 minutes, 50 μl 100% acetonitrile for 15 minutes. Each step was at room temperature and after each step the supernatant was discarded. At the end the samples were dried with a SpeedVac for 10 minutes. For alkylation, for 50 μl 10 mM DTT (dithiothreitol) in 100 mM NH_4HCO_3 were added to the sample and incubated for 60 minutes at 56°C; the supernatant was discarded and 50 μl 50 mM IAA (iodoacetamide) in 100 mM NH_4HCO_3 was added and incubated at room temperature for 45 minutes in the dark. Then gel pieces were again washed twice with 50 μl 50% acetonitrile for 15 minutes and 50 μl 100% acetonitrile for 15 minutes. The samples were dried by a SpeedVac for 10 minutes. The samples were then digested by adding 30 μl 12.5 ng/ μl trypsin in 20 mM NH_4HCO_3 , incubated with shaking at 37°C for 30 minutes. The gel absorbs the trypsin solution, therefore at least 20 μl more 12.5 ng/ μl trypsin in 20 mM NH_4HCO_3 were added to fully cover the sample and the incubation was continued at 37°C for 16 hours. The supernatant was transferred to a fresh tube, 50 μl 50% acetonitrile with 0.1% TFA was added, and incubated for 30 minutes shaking at room temperature. The combined supernatants were dried with a SpeedVac for 1 hour. Finally the sample was dissolved in 20 μl HQ H₂O and spotted for MALDI MS.

4.2.7 PNGase A Digest

After the tryptic digest, samples were dissolved in about 15 – 20 μl HQ H₂O. The trypsin was inactivated by heating up to 95°C for 5 minutes. First 15 μl of 50 mM NH_4Ac (pH 5.0) was added and then 0.5 μl PNGase A (Roche) and incubated overnight at 37°C.

4.2.8 PNGase F Digest

After the tryptic digest, samples were dissolved in about 15 – 20 μl HQ H_2O . The trypsin was inactivated by heating up to 95°C for 5 minutes. First 15 μl of 50 mM NH_4HCO_3 (pH 8.0) was added and then 0.2 μl PNGase F (NEB) and incubated overnight at 37°C.

4.2.9 Glycan Purification

First a Dowex-LiChroprep mini-column was prepared. A column tip was filled with 40 – 50 μl of Dowex in 1% HAc, and was washed once with 250 μl of 1% HAc. Then 2 – 3 mm LiChroprep in pure MeOH was stacked on top and was washed by 3 x 100 μl MeOH. The column was equilibrated with 5 x 100 μl of 1% HAc. If the sample was a PNGase F product it needed to be acidified with 10% HAc before application. The sample was dissolved in HQ H_2O till a total volume of 200 μl and applied on the column. The flow through was collected (approx. 200 μl). Then the sample was eluted by 250 ml HQ H_2O and collected. Additionally the sample was further eluted by 2 x 250 μl of 10% MeOH and also collected. The fractions were dried with a SpeedVac, dissolved in HQ H_2O and examined by MALDI MS.

4.2.10 Sepharose Matrix Affinity Chromatography

287 mg CNBr-activated Sepharose 4B powder (GE Healthcare) was suspended in 2 ml 1 mM HCl. After the sepharose medium swelled to about 1 ml volume it was washed with about 60 ml 1mM HCl to remove additives. 10 mg HRP lyophilized powder was dissolved in 1 ml coupling buffer (0.1 M NaHCO_3 , pH 8.3, containing 0.5 M NaCl). 1 ml of the HRP containing coupling solution was mixed with about 1 ml sepharose medium and mixed end-over-end for 1 hour at room temperature. Excess ligands were washed away by 5 ml coupling buffer. Remaining active groups were blocked by 1 ml 1 M Tris-HCl buffer, pH 8.0, for 2 hours. The medium is then washed by three cycles of alternating pH consisting of 5 ml 0.1 M acetic acid / sodium acetate, pH 4.0 containing 0.5 M NaCl followed by 5 ml 0.1 M Tris-HCl, pH 8.0 containing 0.5 M NaCl. 150 μl HRP-sepharose beads were equilibrated with 1.5 ml TBS and incubated with 500 μl freshly prepared Ax3 lysate (see 4.1.3) rotating over night at 4°C. Remaining HRP-sepharose beads were stored at 4°C after adding 1:500 NaN_3 . Flow through and the washing step with 1.5 ml TBS (4.2.10.1) were collected. Beads were then mixed with 100 μl SDS-PAGE sample buffer and boiled at 95°C for 10 minutes to release proteins bound to the matrix. Proteins from input, flow through, final washing step and bead samples were separated by SDS-PAGE.

4.2.10.1 Tris-Buffered Saline

Tris-Base	50 mM
Adjust with 1M HCl	pH 7.4 – 8.0
NaCl	150 mM

4.2.11 Acrylamide Matrix Affinity Chromatography

2 mg HRP lyophilized powder was dissolved in coupling buffer (4.2.11.1) and added to an Eppendorf tube containing 150 mg acrylamide beads (Thermo Scientific, UltraLink Biosupport). The beads were incubated with HRP rotating for 1 hour. The tube was centrifuged on 1200 g for 5 – 10 minutes and the supernatant removed. The beads were then blocked by 1.5 ml 1 M Tris-HCL buffer, pH 8.0, rotating for 2.5 hours. The tube was centrifuged on 1200 g for 5 – 10 minutes and the supernatant removed. Then the beads were washed by 1.5 ml PBS, 1.5 ml 1M NaCl, 1.5 ml PBS and again 1.5 ml PBS shaking for 15 minutes, respectively. After each washing step the tube was centrifuged on 1200 g for 5 – 10 minutes and the supernatant removed. The beads were then equilibrated with 1.5 ml TBS. 500 µl lysate was added and incubated over night on 4° C. On the next day the supernatant was collected and the beads were washed twice with 1.5 ml TBS. This wash was also collected. The beads were then cooked in SDS-Loading dye on 95° C for 5 minutes. All collected fractions were separated by SDS-PAGE.

4.2.11.1 Coupling Buffer

NaHCO ₃	0.1 M
Adjust with 1M HCl	pH 8.3
NaCl	0.5 M
Sodium citrate	0.6 M

4.2.12 Magnetic Beads Immuno Precipitation

The magnetic beads were commercially obtained (Pierce®Crosslink Magnetic IP/Co-IP Kit) and the procedure was according to the attached manual. The bottle with magnetic beads was vortexed and 25 µl beads were transferred to Eppendorf tubes. The solution was discarded and the beads were washed two times with 500 µl 1x Modified Coupling Buffer (4.2.12.1). The beads were coupled with 5 µg antibody in 100 µl 1x Modified Coupling Buffer for 15 minutes at room temperature and unbound antibody were washed away by once 100 µl and two times 300 µl 1x Modified Coupling Buffer. The cross linking step was optional and unless stated otherwise omitted. Cross linking contained of one 30 minutes incubation step with 20 µM DSS (disuccinimidyl suberate)

followed by washing steps with three times 100 µl Elution Buffer and two times Lysis/Wash Buffer. The antibody coupled beads were incubated for 3 hours at room temperature with 500 µl lysate. Unbound proteins were cleared by 2 times washing with 50 µl Washing Buffer and one time washing with 50 µl HQ H₂O. Bound proteins were eluted by elution buffer with pH 2 and the eluate was subsequently neutralized by a supplied neutralization buffer.

4.2.12.1 Modified Coupling Buffer

20x Coupling Buffer	0.1 ml
Lysis/Wash Buffer	0.1 ml
HQ H ₂ O	1.8 ml

4.2.13 Methanol Protein Precipitation

To any protein solution that was desired in a higher protein concentration this procedure was applied. First a 100% methanol volume 5 times the volume of the protein solution was added and incubated at least 20 minutes at -20°C. Then the solution was centrifuged 11.000 g for 30 minutes at 4°C. The supernatant was removed and in case of high salt content 50 µl 100% methanol was added and centrifuged once more. Supernatant was removed and the sample was dried at 60°C.

4.2.14 Silver Staining

The experimental procedure is according to Shevchenko et al., 1996. This is a SDS-PAGE following protocol for whole-protein staining with higher sensitivity than Coomassie. After SDS-PAGE the gel was fixated by 50% methanol and 5% acetic acid in water for 20 minutes, and washed by 50% methanol. Followed by sensitization via 0.02% sodium thiosulfate for 1 minute, which enhances the resolution. Sensitization solution was rinsed twice by HQ H₂O. The gel was stained by incubation with cold 0.1% silver nitrate for 20 minutes at 4°C. The staining solution was washed away by rinsing twice with HQ H₂O and the gel was developed in 0.04% formalin in 2% sodium carbonate. As soon as the developer turned yellow it was replaced by fresh one. The development was terminated by discarding the developing solution and washing with 5% acetic acid. Stained gels could be stored in 1% acetic acid at 4°C.

4.2.13 Tryptic Digest Protocol Subsequent to Silver Staining

The experimental procedure is according to Shevchenko et al., 2007. First the gel was rinsed in water for several hours to remove remaining acid. Then the desired bands were excised, sliced into mm³ large cubes and transferred to Eppendorf tubes. 500 µl of acetonitrile was added, and the gel pieces shrank for 10 minutes. Acetonitrile was discarded and the gel pieces were vacuum dried for 10 minutes. To reduce the disulfide bonds, 50 µl of 10 mM DTT in 100 mM NH₄HCO₃ was added and incubated at 56°C for 30 minutes. The DTT solution was then exchanged by acetonitrile and the gel pieces shrank for 10 minutes. Acetonitrile was discarded and gel pieces were vacuum dried for 10 minutes. The thiol groups of cysteine residues were chemically modified and thus inactivated by 50 µl of 50 mM iodoacetamide in 100 mM NH₄HCO₃ incubated for 20 minutes. The gel pieces were once more shrunk by acetonitrile and vacuum dried. Trypsin working solution consists of a 3:9:1 (vol/vol/vol) mixture of 12.5 ng/µl trypsin, 20 mM NH₄HCO₃ and acetonitrile. The gel pieces were swollen in the trypsin working solution for 30 minutes on ice. If necessary more trypsin working solution was added on top of the gels so that they were completely covered and left for another 90 minutes on ice. Then the trypsin working solution was discarded and the wet gel pieces were covered with ammonium bicarbonate buffer and stored over night at 37°C.

4.2.14 Mass Spectrometry

The MS and the MS/MS analysis were performed with a Bruker Autoflex Speed MALDI-TOF-TOF. This MALDI instrument has a SmartBeam laser, which is a modified Nd:YAG laser emitting a wave length of 355 nm and is capable of laser induced dissociation (LID), an MS/MS fragmentation by post-source decay. For analysis 1 µl of the tryptic digest peptide fragments were spotted on a carrier plate, air dried for 5 minutes and covered by 1 µl of α-Cyano-4-hydroxycinnamic acid (ACH) matrix (Table. 4.2.14.1), which also crystallized within few minutes.

The MS/MS fragmentation analysis has an m/z window of ± 0.6% m/z of the selected peak. Two peaks that were closer than ± 0.6% m/z were not fragmented separately.

4.2.14.1 ACH Matrix

ACH	0.5%
Acetonitrile	50%
TFA	0.1%

4.3 Cloning

4.3.1 Reverse Transcription

The reverse transcription was performed with 2 µg RNA template. 1 µl of 10 mM dNTP, 0.5 µl of 100 µM T18 primer and 11.5 µl of nuclease free water were added. The mixture was heated to 65°C for 5 minutes and then cooled down on ice for 1 minute. 1 µl of RNaseOUT, 4 µl of RT 5 x buffer, 1 µl of 1 M DTT and 1 µl of Superscript MMLV-RT were added to the mixture. The reverse transcription ran at 50 °C for 1 hour. The reaction was stopped and the enzymes inactivated by heating up the mixture to 70°C for 15 minutes.

4.3.2 PCR from cDNA

By reverse transcription produced cDNA was used as a template. Following primers were used:

Discoidin I Primer		Anealing T	Restriction
Forward	5'-GTGCCATGGCTACCCAAGGTTTAGTTC-3'	51°C	NcoI Site
Reverse	5'-GACTCGAGTTATTCCAAAGCGGTAGC-3'		XhoI Site
Q-GAPDH Primer			
Forward	5'-CCGTGGGTTGAATCATATTTGAAC-3'	60°C	/
Reverse	5'-GGTTGTCCCAATTGGTATTAATGG-3'		/
Discoidin I N-terminal Primer			
Forward	5'-GTGCCATGGCTACCCAAGGTTTAGTTC-3'	51°C	NcoI Site
Reverse	5'-TACCTCGAGTTAGCTTTGTACTGGTTGAGTGAGA-3'		XhoI Site
Discoidin I C-terminal Primer			
Forward	5'-GTGCCATGGTACAAAGCTCAGTCACTCAA-3'	51°C	NcoI Site
Reverse	5'-GACTCGAGTTATTCCAAAGCGGTAGC-3'		XhoI Site

The primers were ordered from Sigma-Aldrich. The PCR working solution was prepared as shown in table 4.3.2.1 and the PCR programme is shown in table 4.3.2.2.

4.3.2.1 PCR working solution

HQ H ₂ O	14.2 µl
5x Expand PCR buffer	4 µl
Primer forward	0.5 µl
Primer reverse	0.5 µl
10 mM dNTPs	0.4 µl
cDNA	0.2 µl
Expand PCR Polymerase	0.2 µl

4.3.2.2 PCR programme

95°C	120 s	once
51°C	30 s	
72°C	60 s	10 cycles
95°C	30 s	
51°C	30 s	
72°C	60 s + 5 s/cycle	20 cycles
95°C	30 s	
72°C	300 s	once

4.3.3 Band Purification after PCR

As soon as the PCR was finished, a 6x SDS/DNA Loading Dye was added to the amplified PCR mix and everything was loaded on a 1% agarose gel. The separation was performed until the front marker migrated over 80% of the gel length. Under short observation in the UV-light, the PCR bands were cut out and the contained DNA was isolated with a GFX DNA purification kit (Illustra). The DNA was diluted in 20 µl of provided TRIS buffer. Finally the DNA concentration was determined with the Nano-Drop spectrometer.

4.3.4 Digestion with Restriction Enzymes

The PCR amplified DNA fragment and the pET30a vector were digested in parallel (4.3.4.1 and 4.3.4.2 respectively). The restriction mixtures were incubated for 3 hours at 37°C in which after 2 hours and 15 minutes 1 µl of shrimp alkaline phosphatase (Promega) was added to the plasmid restriction mixture and also incubated for the remaining 45 minutes. The mixtures were then heat inactivated at 65°C for 20 minutes

and the DNA was isolated with a GFX DNA purification kit (Illustra). The fragment DNA was diluted in 12 μl HQ H₂O, the plasmid DNA in 15 μl HQ H₂O and subsequently the concentration was determined with the Nano-Drop spectrometer.

4.3.4.1 Restriction mixture for PCR amplified DNA fragment

Fragment DNA	15 μl
NEB Buffer 4	3 μl
100x BSA	0.3 μl
NcoI Restriction Enzyme	0.75 μl
XhoI Restriction Enzyme	0.75 μl
HQ H ₂ O	10.2 μl

4.3.4.2 Restriction mixture for Plasmid

pET30a Plasmid	7 μl
NEB Buffer 4	3 μl
100x BSA	0.3 μl
NcoI Restriction Enzyme	0.75 μl
XhoI Restriction Enzyme	0.75 μl
HQ H ₂ O	18.2 μl

4.3.5 Ligation

Using the determined DNA concentrations of DNA fragment and plasmid the reaction ligation was set up. Around 150 ng of pET30a was used with an equimolar or slightly excess amount of DNA fragment. Since the cloned gene discoidin I is around 7 times smaller than the used pET30a plasmid, at least 20 ng of this fragment was used. The calculated amounts of plasmid and fragment were mixed, 1 μl 10x T4 DNA buffer was added, and the mixture was made up to 9 μl with HQ H₂O. Finally 1 μl of T4 DNA ligase was added and incubated at 14°C overnight.

4.3.6 CaCl₂ Competent *E. coli*

In order to transform *E. coli* by heat-shock they have to be made competent first. 2 ml of 10 ml LB overnight culture are transferred to fresh 200 ml LB and left shaking at 37°C

till the OD600 reaches 0.5. Then the cells are transferred to sterile centrifugation tubes and left on ice for 10 minutes. The cells are centrifuged for 10 minutes with 4000 g at 4°C and resuspended in 6 ml of 0.1 M CaCl₂. 1.15 ml of sterile 87% glycerol was added. The solution was aliquoted to 200 µl per sterile microcentrifugation tube, snap-frozen in liquid nitrogen and stored at -80°C.

4.3.7 Transformation of Competent *E. coli* after Ligation

In this thesis competent JM109 *E. coli* were used for cloning the vector. 200 µl competent JM109 cells were thawed on ice, mixed with the ligation mixture and left for further 15 minutes on ice. The heat-shock was performed for 1 minute at 42°C and afterwards the cells were returned on ice for 2 minutes. The *E. coli* transformation tube was made up to 1 ml with SOC medium and put at 37°C for 1 hour. To remove the excess liquid the cells were pelletized via full speed centrifugation for 30 seconds. The cell pellet was taken up again in the remaining 200 µl of media and plated on kanamycin containing plates. Colonies were allowed to grow overnight at 37°C.

4.3.8 Screening for Transformed *E. coli*

E. coli colonies from the ligation/transformation were inoculated with a sterile toothpick into 4 µl HQ H₂O of which 1 µl is used to set a point on the master plate, which is a kanamycin LB plate streaked with all possibly positive transfectants. To the remaining 3 µl inoculated HQ H₂O 1 µl of discoidin I forward and reverse primer respectively, and 5 µl green taq polymerase mix is added. With this mixture a PCR is performed and loaded on a 1% agarose gel to check for the presence of the amplified discoidin I gene. Those *E. coli* that are seemingly successfully transformed with a plasmid carrying a fragment are further analysed. The plasmid was isolated via mini prep method (QIAprep Spin Miniprep Kit, QIAGEN) and 15 µl of 50 – 100 ng/µl plasmid were sent in for sequencing (Eurofins MWG operons).

4.3.9 Transformation of Competent *E. coli* with Purified Plasmid

In this thesis competent BL21 *E. coli* were used for recombinant protein expression. They were thawed on ice, mixed with 1µl of purified plasmid carrying the fragment and left for further 15 minutes on ice. The heat-shock was performed for 1 minute at 42°C and returned on ice for 2 minutes. The *E. coli* transformation tube was made up to 1 ml with SOC media and incubated at 37°C for 1 hour. To remove the excess liquid the cells were pelletized via full speed centrifugation for 30 seconds. The cell pellet was taken up again in remaining 200 µl of media and plated on kanamycin containing plates. Colonies were allowed to grow overnight at 37°C.

4.3.10 Pilot Protein Expression

500 µl BL21 cells of an overnight culture were added to 10 ml LB containing 34 µg/ml chloramphenicol and 50 µg/ml kanamycin for each expression series performed. Usually 4 expression series are performed in parallel: two different temperatures (24°C and 16°C) and each with or without 0.5 mM IPTG. The cells were grown until the OD600 reached a value between 0.5 and 0.8. As a zero point sample 1 ml of aliquot is removed and stored at -80°C. After that 0.5 mM IPTG was added, except for the controls, and the cells were placed in the incubator with the intended temperature (24°C and 16°C). At each time point, which was usually every hour for cells at 24°C and every two hours and one sample overnight for cells at 16°C, 1 ml of aliquot was taken and stored at -80°C. As soon as all the samples were collected they were thawed on ice, supernatant after centrifuging at 16.000 g was discarded and the cells were lysed in 200 µl Lysis Buffer for 20 min at 37°C under constant shaking and with subsequent sonification. Full-speed centrifugation for 5 minutes separated the soluble from the insoluble fraction. The result of the pilot expression was visualized on SDS-PAGE with Coomassie staining as well as with western blotting to detect the His-Tag.

4.3.11 Large Scale Protein Expression

2.5 ml BL21 cells of overnight culture were added to 50 ml LB containing 34 µg/ml chloramphenicol and 50 µg/ml kanamycin. The cells were grown until the OD600 reached a value between 0.5 and 0.8. Then 0.5 mM IPTG was added and the cells were placed in an incubator with the temperature that has been shown by the pilot expression to yield most recombinantly expressed and indentured protein. Also the ideal duration of expression was determined by the pilot expression. After that the lysis procedure (described 4.3.12) was repeated.

4.3.12 *E. coli* Lysis for Recombinant Protein

Before the *E. coli* lysis buffer was used, Phenylmethylsulfonyl fluoride (PMSF) was added to a final concentration of 0.1mM. The harvested *E. coli* samples from the large scale expression were thawed on ice and mixed with 200 µl *E. coli* lysis buffer (table 4.3.11.1) with PMSF for each ml of *E. coli* suspension harvested. The pellet was resuspended in the lysis buffer and incubated for around 20 minutes at 37°C with constant shaking. Finally the solid phase was separated from the liquid phase by maximum speed (over 16.000 rpm) centrifugation for 5 minutes and stored in different tubes at -80°C.

4.3.12.1 *E. coli* lysis buffer

Tris	50 mM
Adjust with HCl	pH 7.4
EDTA	0.5 mM
Trion X-100	0.1 %
MgCl ₂	5 mM
Lysozyme	100 µg / ml
DNase	1.2 u / ml

4.3.13 His-Tag purification

1 ml of 50% Ni-NTA slurry was transferred to a 2 ml microcentrifuge tube. The beads were spun down and the supernatant removed. The beads were washed four times by 1 ml of lysis buffer. After transferring the beads to a 15 ml falcon tube, lysates containing His-tagged protein was added and constantly shaken for 60 minutes at 4°C. The lysate-Ni-NTA mixture was moved to a 1 ml column and the flow-through was collected. The column was then washed twice with 1 ml lysis buffer and twice with 2 ml wash buffer. The proteins were then eluted with 4 times 0.5 ml elution buffer and stored at -80°C.

4.4 Websites and Software

TRIS buffer calculator: <http://www.cytographica.com/lab/HHTris.html>

Alignment: <http://multalin.toulouse.inra.fr/multalin/>

MS fingerprint: <http://prospector.ucsf.edu/prospector/cgi-bin/msform.cgi?form=msfitstandard>

Reverse and complementary sequence:

http://www.bioinformatics.org/sms/rev_comp.html

Sequence translation: <http://web.expasy.org/translate/>

Protein Mass and pI: http://web.expasy.org/compute_pi/

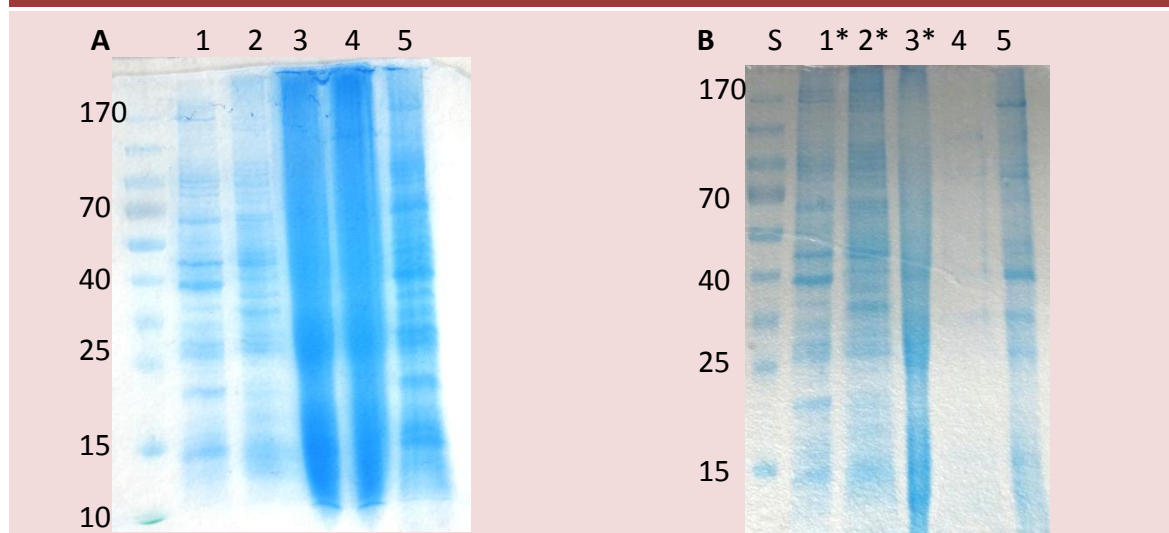
V. Results

5.1 Western Blot Inhibition Assay

High mannosidic N-glycans of *D. discoideum* have been shown to be anti-HRP positive due to a core- α -1,3-fucose (Schiller et al., 2009). Western blotting experiments that underline the presence, and show the distribution, of the anti-HRP epitope were performed.

First in order to normalize the application volumes of different lysates from several different organisms, SDS-PAGE with subsequent Coomassie staining was performed. The used lysates were from *Dictyostelium discoideum* strain Ax3, *Caenorhabditis elegans* strain N2 and *Acanthamoeba castellanii* strain Neff (Fig 5.1.1.A). This procedure was repeated with additional crude-extracts from *Drosophila melanogaster* strain Canton-S and after several adjustments normalization of the lysates could be achieved (Fig 5.1.1.B). Sample marked by asterisk and concentration shown have been used for further blotting experiments.

Figure 5.1.1 Normalization of lysates

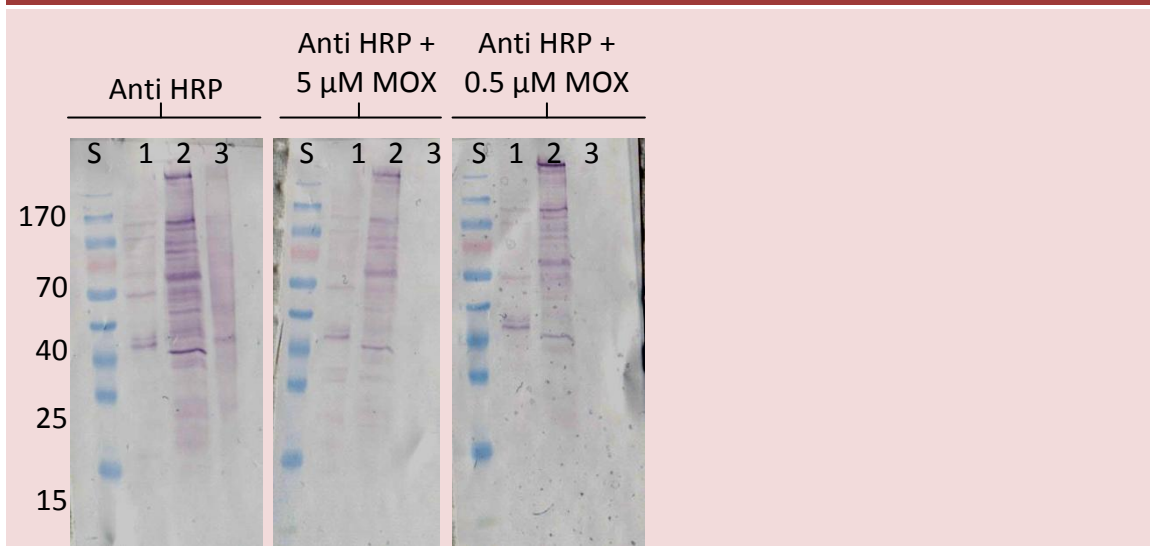


The application volumes of the lysates were normalized by SDS-PAGE with subsequent Coomassie staining. **A.)** 1: Ax3; 2: N2; 3: Neff; 4: Neff; 5: Ax3. 5 μ l of each sample has been applied **B.)** 1: Ax3, 12 μ l; 2: N2, 15 μ l; 3: Neff, 4 μ l; 4 and 5: Canton-S, 15 and 10 μ l respectively. Samples marked by an asterisk were used for further western blotting experiments.

Next I performed western blot experiments with the normalized lysates of *D. discoideum* strain Ax3, *C. elegans* strain N2 and *A. castellanii* strain Neff detected with anti-HRP primary antibody (figure 5.1.2 and 5.1.3). The anti-HRP antibody used here is specific for the N-glycans of horseradish peroxidase; in particular it binds the

oligosaccharide MMXF₃ epitope (Paschinger et al., 2008). This antibody has proven to be a useful tool for the identification of these N-glycans in all kind of samples carrying this and also very similar epitopes, e.g. it can bind to MOXF, MOF and MMF epitopes as well. As shown by these western blots all three evolutionary very distinct organisms carry an epitope recognized by the Anti-HRP antibody (figure 5.1.2 and 5.1.3). This is true for *D. discoideum* and *C. elegans* because of core- α -1,3-fucosylated N-glycans (Schiller et al., 2009; Yan et al., 2009), and in case of *A. castellanii* it is due to β -1,2-xylose (Schiller et al., 2012). To further probe these glycan structures, inhibition experiments were routinely performed. Western blot-inhibition assays give additional information about the binding epitope and have been well established for the anti-HRP antibody. The basis of this experiment is that before the blotted sample is incubated with the primary antibody, the primary antibody is inhibited by an antigenic molecule, in this case the BSA neoglycoconjugates carrying MOX or MOXF (described in 4.2.4). If the binding site with which the primary antibody detects the sample is blocked by the inhibitor, bands which were visible in the normal western blot will disappear. On the other hand, if the binding site is not or only partially blocked, bands will remain or slightly fade compared to the uninhibited western blot.

Figure 5.1.2 Western Blot with anti-HRP and with or without MOX inhibition

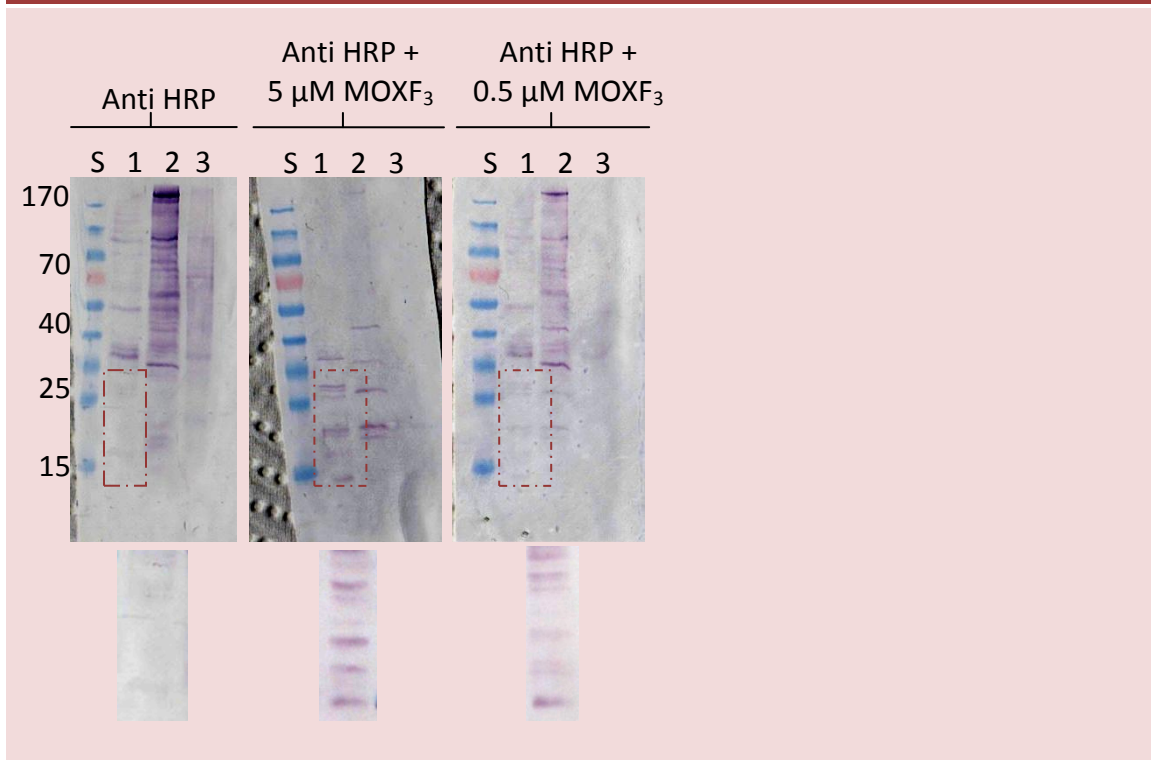


Applied on each blot are the normalized volumes of 1: Ax3, 12 μ l; 2: N2, 15 μ l; 3: Neff, 4 μ l. The blots were incubated for 1 hour with rabbit anti-HRP primary antibody, and then for 1 hour with goat anti-rabbit secondary antibody coupled to alkaline phosphatase. For detection the membrane was rinsed in BCIP/NBT solution for about 1 minute. In case of the 5 μ M and the 0.5 μ M inhibited blots the primary antibody was mixed for 1 hour with the given concentration of MOX glycoconjugate before it was added to the blots.

The MOX inhibitor clearly specifically inhibited the binding of anti-HRP to glycoprotein of *A. castellanii* (figure 5.1.2). This is consistent with the fact that out of the used samples only *A. castellanii* carries the β -1,2-xylose moiety and thus cannot be recognized by the

antibody after blocking its xylose recognition site. By the inhibition western blotting with MOXF in contrast it was expected that the detection of all three samples is cleared. Although the bands detected by the normal anti-HRP western blot disappeared, surprisingly low molecular mass bands appeared which had not been detected before (figure 5.1.3).

Figure 5.1.3 Western Blot with anti-HRP and with or without MOXF inhibition



Applied on each blot were normalized volumes of 1: Ax3, 12 μ l; 2: N2, 15 μ l; 3: Neff, 4 μ l. The blots were incubated for 1 hour with rabbit anti-HRP primary antibody, and then for 1 hour with goat anti-rabbit secondary antibody coupled to alkaline phosphatase. For detection the membrane was incubated in BCIP/NBT solution for about 1 minute. In case of the 5 μ M and the 0.5 μ M inhibited blots the primary antibody was mixed for 1 hour with the given concentration of MOXF glyco-conjugate before it was added to the blots. Regions shown in the red boxes are enlarged beneath and visually enhanced.

We hypothesized that these low molecular proteins were lectins that were able to bind the multivalent MOXF, which in turn is bound by anti-HRP antibody. Three reasons led to this conclusion: 1. The detected proteins cannot be detected by the anti-HRP antibody directly, but only indirectly in presence of a glycoconjugate that is bound by the antibody. It is likely that the detected protein therefore bound the glycoconjugate itself. 2. The detected proteins were below 40 kDa. Lectins are often protein of low molecular mass; for example ConA, a mannose binding lectin is 25 kDa in mass or AAL, a fucose binding lectin, is 36 kDa in mass. 3. In previous experiments it was shown that

small lectins can retain even under denaturing conditions of an SDS-PAGE their binding properties or at least regain them afterwards (West and McMahon, 1977).

5.2 HRP Quality Control

Horseradish peroxidase (HRP) from the plant *Armoracia rusticana* was commercially obtained in pure and lyophilized form (Sigma Aldrich). To confirm the quality, purity and correct glycosylation of the protein for our purposes several tests have been performed. Via SDS-PAGE and Coomassie staining the correct size and the presence of only one protein were shown (figure 5.2.1). I then confirmed via MALDI-TOF spectrometry that the tryptically digested protein shows the correct peptide mass fingerprint (PMF, figure 5.2.2) when compared to the *in silico* digest (table 5.2.1). It is therefore confirmed that our commercially obtained protein is indeed pure HRP. Next we analysed the glycosylation of our HRP by performing a PNGase digest (figure 5.2.3) with subsequent MALDI-TOF and MS-MS. I hereby confirmed that the purchased HRP carries the desired MMXF₃ sugar.

Figure 5.2.1 SDS-PAGE of HRP

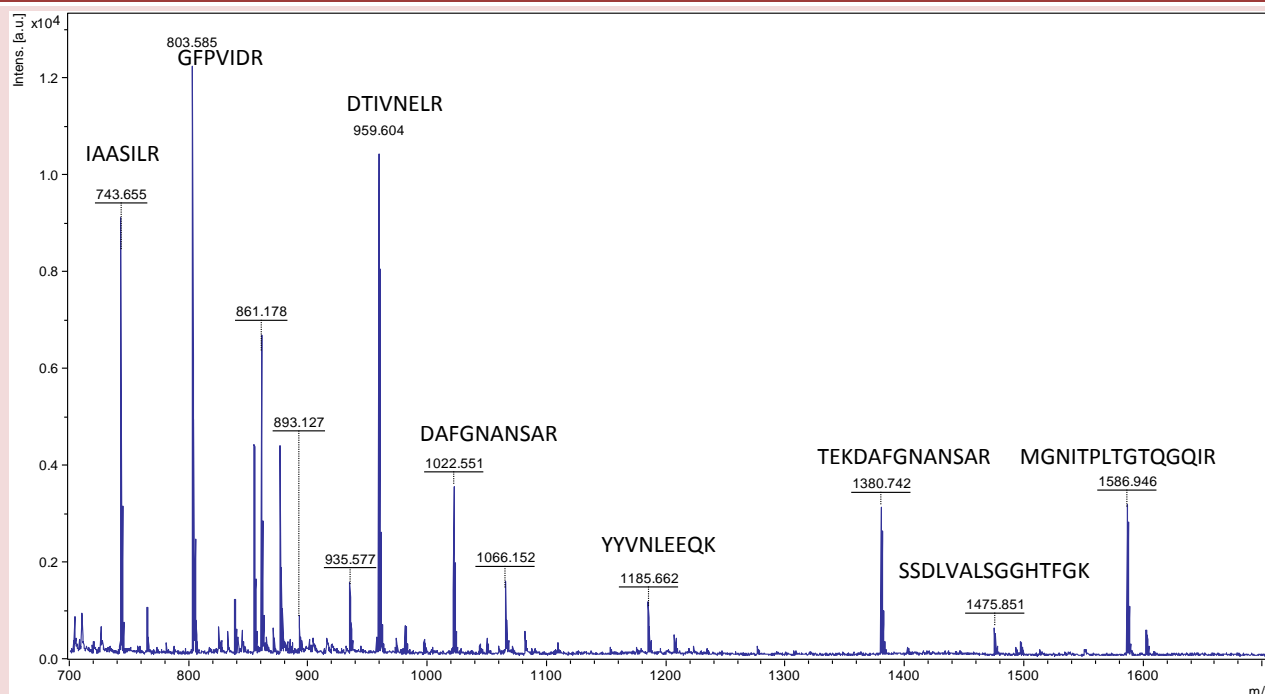


The commercially obtained HRP was diluted 0.5 µg / µl dH₂O, mixed 1:1 with loading buffer and loaded on the gel. On lane 1, 2 µl have been loaded (1 µg HRP). On lane 2, 10 µl have been loaded (5 µg HRP).

Table 5.2.1 In silico tryptic digest prediction of HRP (#MC, missed cleavages)

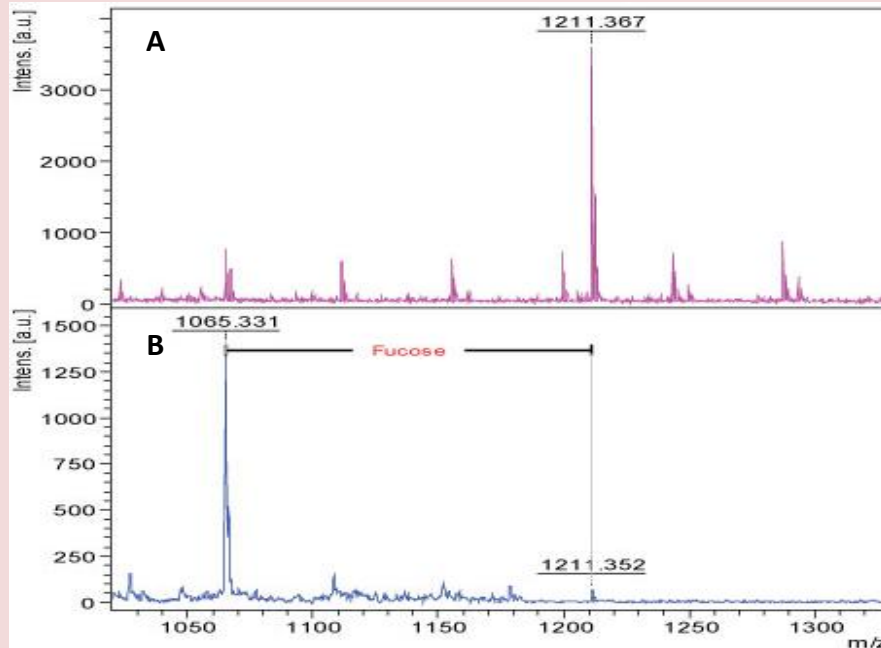
mass	position	#MC	peptide sequence	mass	position	#MC	Peptide sequence
2900.57	125-150	1	RDSLQAFDLANANLPAPFFTLPLQLK	1185.58	234-242	0	YYVNLEEQK
2833.46	208-233	1	GLCPLNGNLSALVDFDLRTPITFDNK	1182.55	176-184	1	NQCRFIMDR
2744.46	126-150	0	DSLQAFDLANANLPAPFFTLPLQLK	1177.61	151-160	1	DSFRNVGLNR
2725.25	40-63	0	LHFHDCFVNGCDASILLDNTTSFR	1162.57	84-94	1	MKAAVESACPR
2642.35	185-207	0	LYNFSNTGLPDPTLNNTTYLQTLR	1105.54	300-309	1	LNCRVVNSNS
2545.31	95-119	0	TVSCADLLTIAAQQSVTLAGGPSWR	1062.58	77-85	1	GFPVIDRMK
2501.29	243-265	0	GLIQSDQELFSSPNATDTIPLVR	1022.46	67-76	0	DAFGNANSAR
2299.08	1-20	0	MQLTPTFYDNSCPNVSNIVR	959.52	21-28	0	DTIVNELR
2182.99	266-284	0	SFANSTQTFNFAVEAMDR	935.48	226-233	0	TPTIFDNK
2129.11	155-175	1	NVGLNRSSDLVALSGGHTFGK	903.44	86-94	0	AAVESACPR
2102.04	226-242	1	TPTIFDNKYYVNLEEQK	803.44	77-83	0	GFPVIDR
2073.07	285-303	1	MGNITPLTGTQGQIRLNCR	743.48	33-39	0	IAASILR
1976.96	161-179	1	SSDLVALSGGHTFGKNQCR	697.45	120-125	1	VPLGRR
1916.99	208-225	0	GLCPLNGNLSALVDFDLR	681.34	180-184	0	FIMDR
1806.89	67-83	1	DAFGNANSARGFPVIDR	672.38	155-160	0	NVGLNR
1586.83	285-299	0	MGNITPLTGTQGQIR	619.30	304-309	0	VVNSNS
1475.75	161-175	0	SSDLVALSGGHTFGK	541.35	120-124	0	VPLGR
1414.73	21-32	1	DTIVNELRSDPR	524.25	151-154	0	DSFR
1380.65	64-76	1	TEKDAFGNANSAR	520.23	176-179	0	NQCR
1198.69	29-39	1	SDPRIAASILR	505.26	300-303	0	LNCR

Figure 5.2.2 MALDI-TOF analysis of typically digested HRP



The HRP sample was in-gel digested over night by trypsin. The obtained PMF (Peptide Mass Fingerprint) shown here was compared with the *in silico* digest and the peptide sequences were assigned accordingly. The protein mass coverage of peptides with no missed cleavages was around 29%.

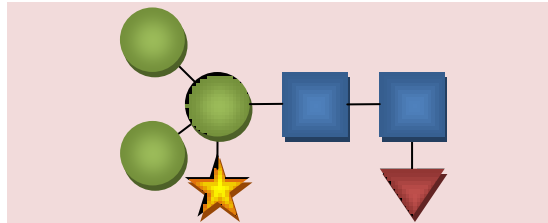
Figure 5.2.3 MS and MS/MS glycan analysis of HRP



Peptides of tryptically digested HRP were further treated with PNGase A and the released carbohydrates were purified as described in 4.2.6. **A.)** The carbohydrates were then analysed by MS showing a peak at 1211.4, which is the mass of an MMXF₃ sugar. **B.)** The 1211.4 peak was further analysed by MS/MS fragmentation and showed the characteristic fragmentation of 1065.331 caused by the loss of fucose.

HRP is carrying an MMXF₃ N-glycan which is an immunogenic epitope. I proved that the purchased HRP also carries this oligosaccharide. Plant N-glycans are known to carry a core β -1,2-xylose on the mannose and a core α -1,3-fucose on the proximal GlcNAc (as shown in figure 5.2.4). This was necessary to confirm on the purchased HRP because it was, due to its N-glycan moieties, used as a ligand to isolate and identify lectins.

Figure 5.2.4 Typical core-N-glycan of plants



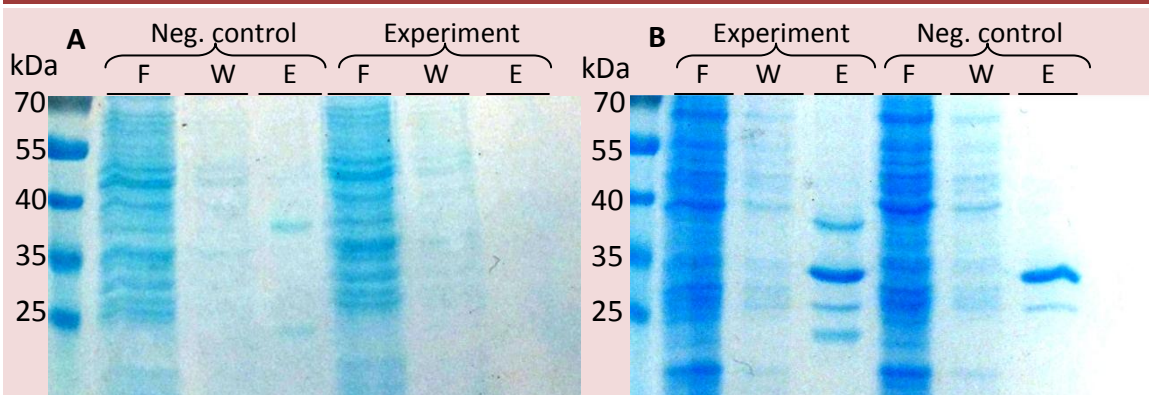
5.3 Affinity Chromatography

It has been described previously that lectins that bind core fucosylated N-glycans can be isolated via HRP coupled affinity chromatography (Schubert et al., 2012). In order to identify a lectin in *D. discoideum* that also binds this glycan moiety I performed two different types of affinity chromatography. One was based on a sepharose matrix as described in Schubert et al., and one was based on an acrylamide matrix.

5.3.1 Affinity Chromatography with Sepharose Matrix

The working procedure can be found at chapter 4.2.10. In this experiment sepharose beads were coupled with HRP and then incubated with *D. discoideum* Ax3 lysate. For comparative reasons this experiment was performed with N2 lysates in parallel. In addition as a negative control beads, that were not coupled to HRP but in the remaining steps treated similarly, were used. By this method two proteins of the N2 lysate and four proteins of the Ax3 lysate could be isolated (figure 5.3.1.1). The Ax3 negative control showed comparatively similar binding strength of two proteins from the actual experiment (33 kDa and 27 kDa). The other two Ax3 proteins (37 kDa and 24 kDa) showed similar sizes to the two proteins isolated from N2 lysate (also 37 kDa and 24 kDa).

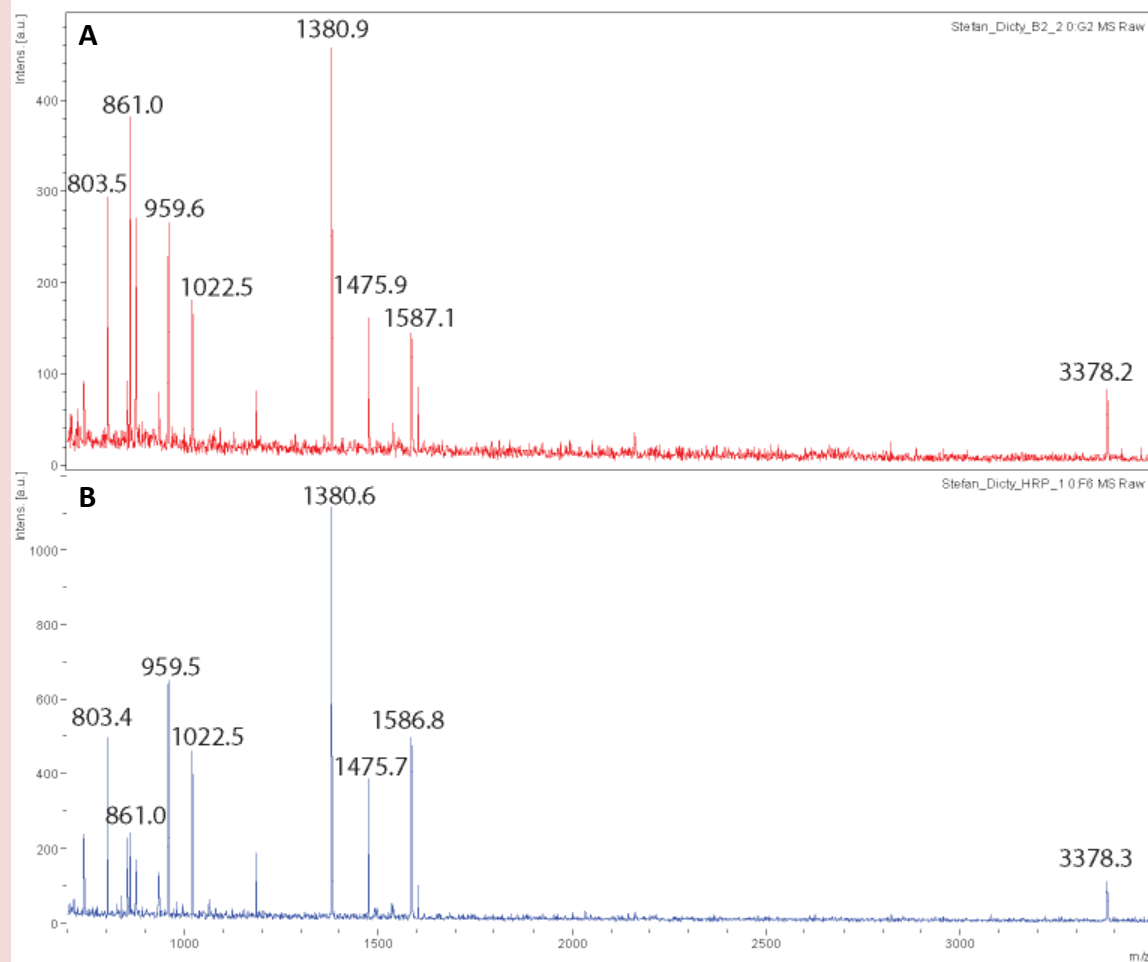
Figure 5.3.1.1 Sepharose Affinity Chromatography



Sepharose beads were coupled with HRP and incubated with *C. elegans* N2 lysate (A), or *D. discoideum* Ax3 lysate (B). Negative controls were sepharose beads not coupled to HRP. The annotation E, W and F stand for elution, wash and flow-through respectively. A.) Two proteins with the approximate sizes of 37 kDa and 24 kDa eluted in the experiment. The elution in the negative control is free of protein. B.) Four proteins with approximate sizes of 37 kDa, 33 kDa, 27 kDa and 24 kDa eluted in the experiment. In the negative control the 33 kDa protein and the 27 kDa protein eluted as well.

To identify those proteins they were excised, washed and the peptides were digested in-gel with trypsin. Subsequently PMFs were obtained by MALDI-TOF analysis and screened by the online software “MS-FIT” (see chapter 4.4). For the highest molecular weight bands of Ax3 and N2 (both 37 kDa) no hits in databases comprising *D. discoideum* or *C. elegans* PMFs could be found. But it stood out that both mass fingerprint spectra showed highly similar trypsin digestion pattern to each other and to HRP tryptic digests (figure 5.3.1.2). Due to the agreement of the size of the protein they have been identified as HRP eluted from the beads.

Figure 5.3.1.2 PMF of 37 kDa Band of Affinity Chromatography with Sepharose Matrix

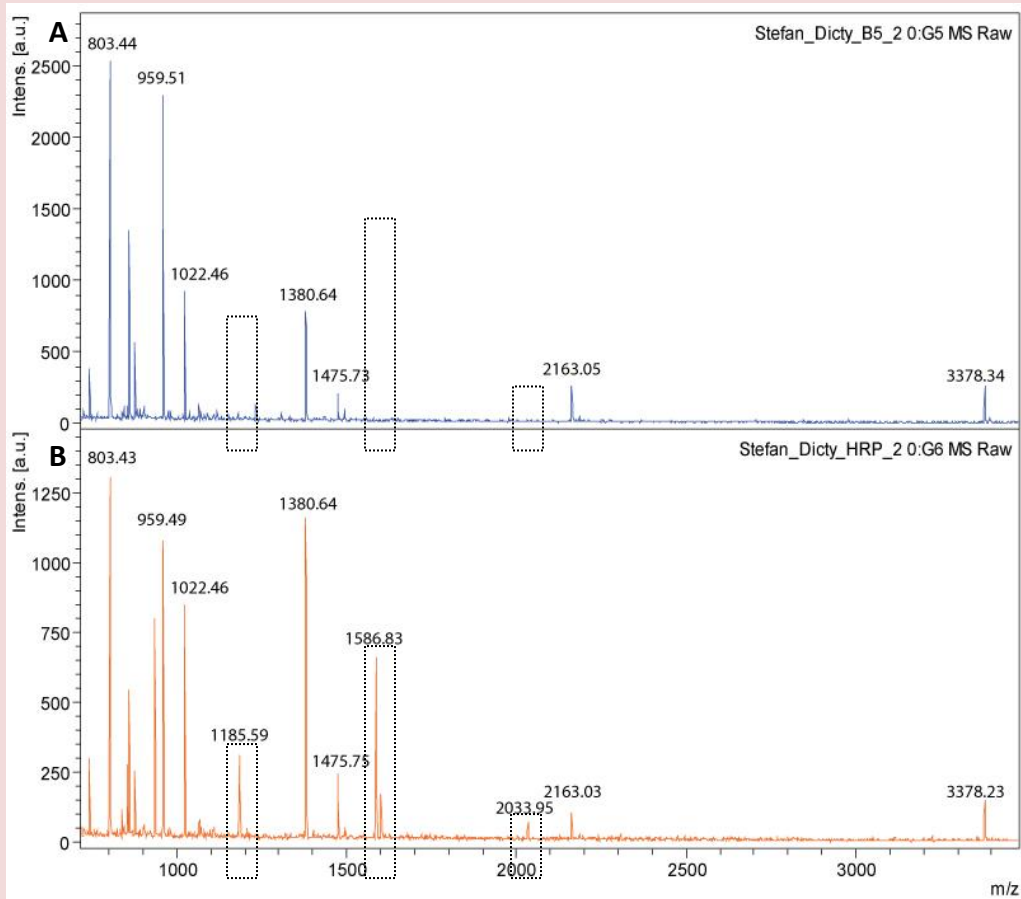


Trypsin digestion mass fingerprints of the 37 kDa protein isolated by sepharose coupled with HRP affinity chromatography and incubated with *D. discoideum* lysate (A) and purified HRP (B). The two spectra are evidently highly similar showing identical mass fingerprints. Thus the 37 kDa protein was identified as HRP.

Surprisingly the lowest molecular weight bands of Ax3 and N2 (both 24 kDa) also showed similar PMFs as HRP, but three peaks (1185.59 m/z; 1586.83 m/z; 2033.95 m/z)

were missing (figure 5.3.1.3). In addition HRP is 10 kDa larger than the 24 kDa protein. Comparison of present and missing peptides and their location on the HRP primary sequence solved the riddle. All those PMFs that were found in both HRP and 24 kDa protein are located N-terminally, whereas all those PMFs that are solely found in HRP are located C-terminally. In between lies a region that if proteolytically cleaved would lead to a 24 kDa protein (figure 5.3.1.4). This strongly suggests that the 24 kDa protein is in fact a truncated HRP protein.

Figure 5.3.1.3 PMF of 24 kDa Band of Affinity Chromatography with Sepharose Matrix



Trypsin digestion mass fingerprints of the 24 kDa protein isolated by sepharose coupled with HRP affinity chromatography and incubated with *D. discoideum* lysate (A) and purified HRP (B). The two spectra are evidently very similar, but some peptides in the spectrum of intact HRP are absent from the spectrum of the 24 kDa band. Those peptides were marked by boxes.

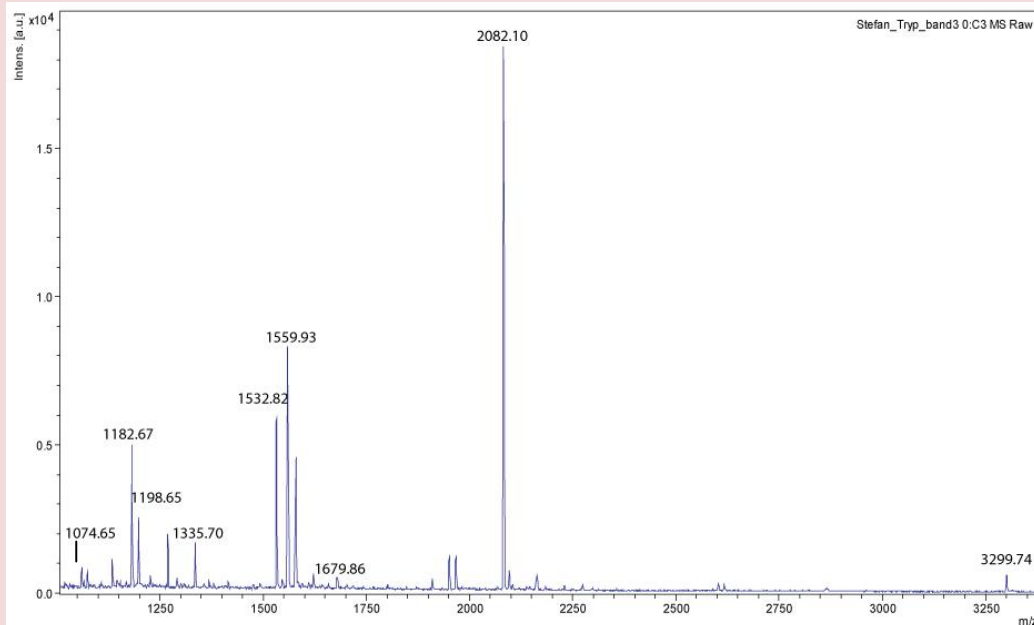
Figure 5.3.1.4 HRP protein with annotated regions

MQLTPTFYDNSCPNVSNIVRDTIVNELRSDPRIAASILRLHFHDCFVNGCDASILLDNTTSFRTEKDAFG
NANSARGFPVIDRMKAAVESACPRTVSCADLLTIAAQQSVTLAGGPSWRVPLGRRDSLQAFLDLANANLP
APFFTLPLQPKDSFRNVGLNRSSDLVALSGGHTFGKNCQRFIMDRLYNFSNTGLPDPPTLNTTYLQTLRGLC
PLNGNLSALVDFDLRTPTIFDNKYVYNLEEOKGLIQSDQELFSSPNATDTIPLVRSFANSTQTFNFAFVE
AMDRMGNITPLTGTGOIIRLNCRVVNSNS

Primary sequence of the HRP protein starting from the N-terminus. Underlined in red are those peptides cut by trypsin which are present in both HRP and 24 kDa band. Underlined in blue are those peptides that are solely found in tryptic digest of HRP but not in tryptic digest of the 24 kDa band. The regional separation indicates strongly that the 24 kDa protein is a truncated HRP protein lacking the C-terminal region. In the green box is the possible cleavage area which could lead to a polypeptide with a mass of 24 kDa.

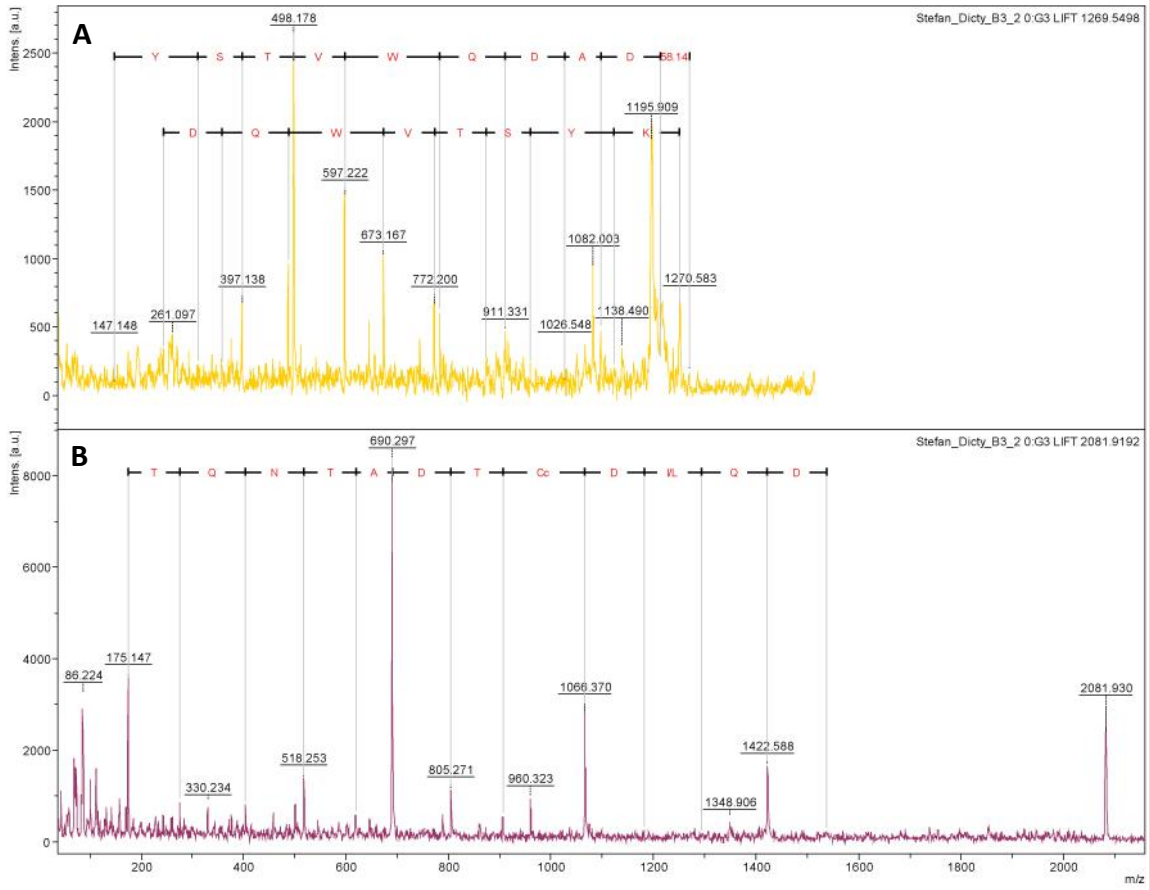
The two bands appearing exclusively in the Ax3 sample (33 kDa and 27 kDa) were shown by the negative control to have an affinity to the sepharose matrix itself. PMF analysis of the tryptically digested 33 kDa band showed in highly significant agreement that it is discoidin I (figure 5.3.1.5 and table 5.3.1.1). To prove the correct identification the 1269.6 m/z peptide and the 2081.9 m/z peptide were fragmented by MS/MS (figure 5.3.1.6). The thereby ascertained amino acid sequence confirmed the correct assignment.

Figure 5.3.1.5 PMF of 33 kDa Band of Affinity Chromatography with Sepharose Matrix



Trypsin digestion mass fingerprints of the 33 kDa protein isolated by sepharose coupled with HRP affinity chromatography and incubated with *D. discoideum* lysate. PMF analysis identified highly significant discoidin I (MOWSE Score 10981; protein mass coverage of 40%). All those peaks annotated with a masses were determined peptides of discoidin I.

Figure 5.3.1.6 MS/MS analysis of Discoidin I peptides to assure the correct identification



MS/MS analysis of tryptic digest discoidin I peaks 1269.55 m/z (A) and 2081 m/z (B). A.) Shows evidently the existence of DADGWVTSYK sequence by its y and b fragments. B.) Shows evidently the y fragments of DQIDCcDATNQT peptide

Table 5.3.1.1 PMF hits of 33 kDa Band with Discoidin I

m/z Submitted	MH ⁺ Matched	Delta ppm	Start	End	#MC	Sequence
1074.65	1074.55	89.0	105	115	0	(R)NGAAITGVTD(R)
1182.67	1182.58	81.7	70	79	0	(R)TFMC(Carbamidomethyl)VALQGR(G)
1335.70	1335.60	74.8	80	90	0	(R)GDHDQWVTSYK(I)
1532.82	1532.70	78.7	93	104	0	(R)YSLDNVTWSEYR(N)
1559.93	1559.80	84.4	116	128	0	(R)NTVVNHFFDTPIR(A)
1679.86	1679.72	86.5	227	239	0	(K)GFDC(Carbamidomethyl)VFYTWENK(V)
2082.10	2081.96	70.3	198	215	0	(K)VALNFDQIDC(Carbamidomethyl)TDATNQTR(I)
3299.74	3299.50	73.4	40	69	0	(K)GTNTIDGSEAWC(Carbamidomethyl)SSIVDTNQYIVAGC(Carbamidomethyl)EVPR(T)

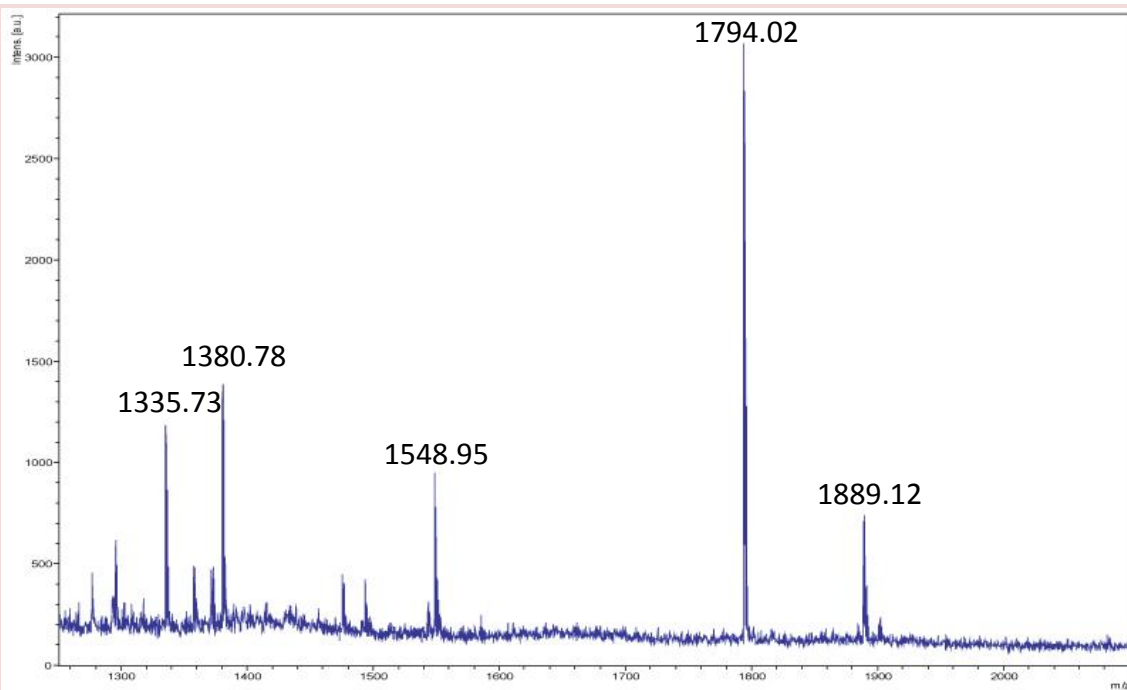
#MC, missed cleavages; 40% protein mass coverage

Similarly the tryptically digested 28 kDa band was identified in good PMF agreement as discoidin II (figure 5.3.1.7 and table 5.3.1.2). Even though only two peptides were assigned (1335.75 m/z and 1793.87 m/z) the subsequent MS/MS analysis revealed a correct amino acid sequence, confirming discoidin II as the 28 kDa protein (Fig. 5.3.1.8).

Discoidin I and discoidin II are two often investigated lectins of *D. discoideum*, whose function or natural binding partner were never conclusively understood. They are known to have high affinity to galactose and galactose-containing polymers such as sepharose, explaining their isolation even by the negative control.

Discoidin I and discoidin II have both approximately 28 kDa determined by the sum of their amino acid masses, but discoidin I displayed on the SDS-PAGE gel an apparent molecular weight of 33 kDa. The reason for that is unknown but it might be because of posttranslational modifications.

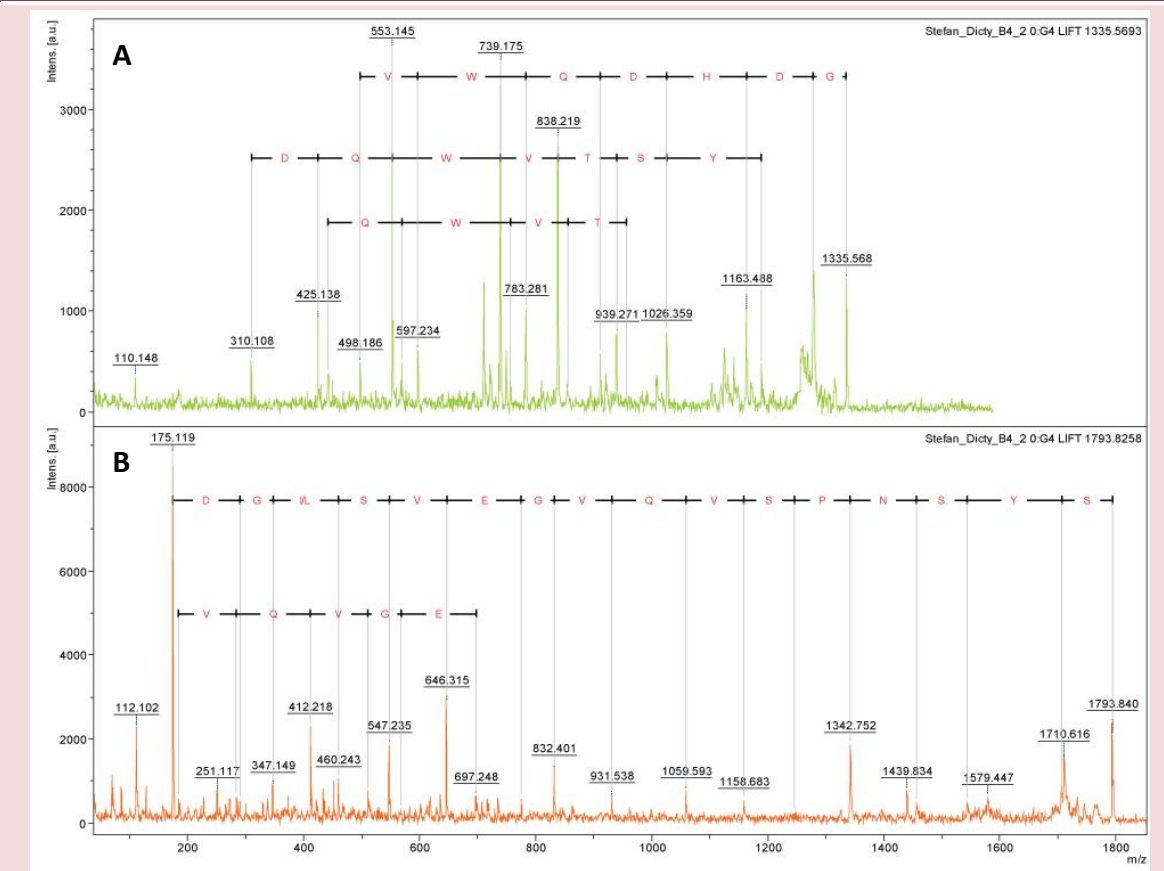
Figure 5.3.1.7 PMF of 28 kDa Band of Affinity Chromatography with Sepharose Matrix



Trypsin digestion mass fingerprint of the 28 kDa protein isolated by sepharose coupled with HRP affinity chromatography and incubated with *D. discoideum* lysate. PMF analysis identified discoidin II with a protein mass coverage of 12.5%. The two peaks 1335.73 m/z and 1794.02 m/z were determined peptides of discoidin II.

Table 5.3.1.2 PMF hits of 28 kDa Band with discoidin II						
m/z Submitted	MH ⁺ Matched	Delta ppm	Start	End	Missed Cleavages	Sequence
1335.7233	1335.5964	95.0	82	92	0	(R)GDHDQWVTSYK(L)
1794.0191	1793.8664	85.1	158	174	0	(K)SYNPSVQVGEVSIGDR(S)

Figure 5.3.1.8 MS/MS analysis of discoidin II peptides to assure the correct identification



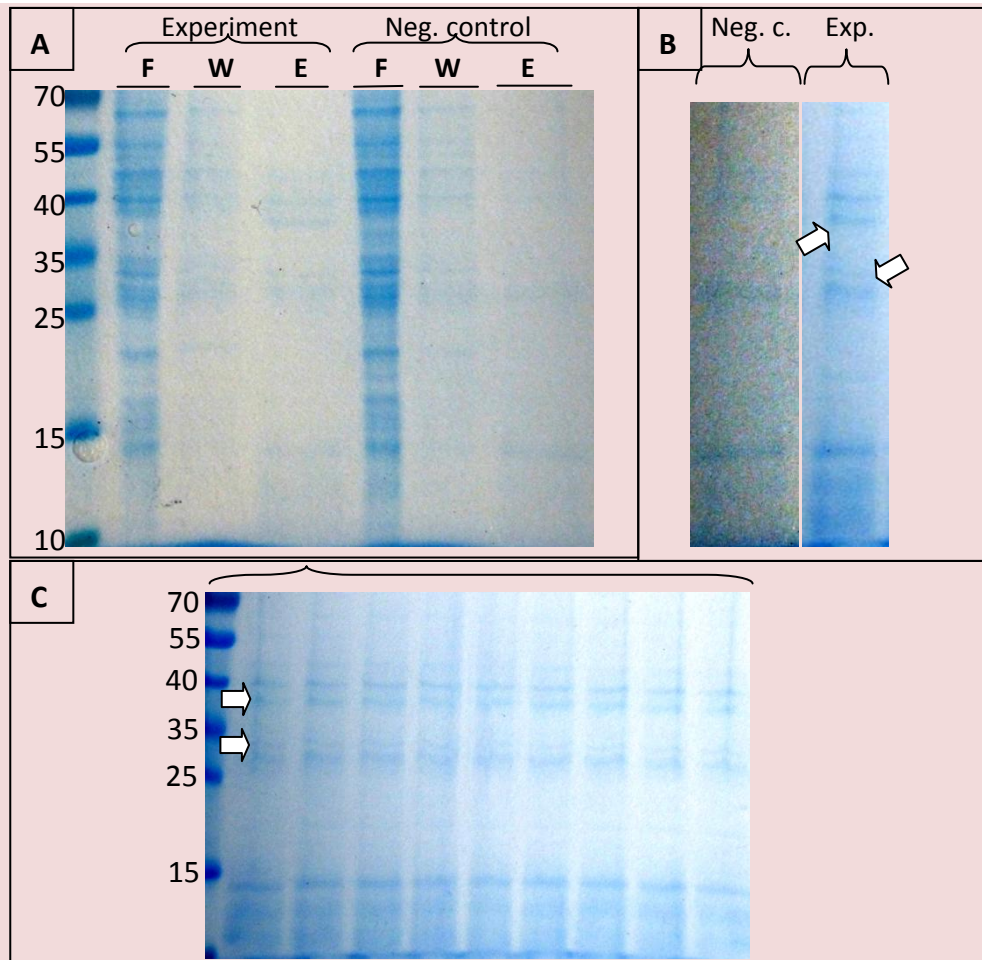
MS/MS analysis of tryptic digest discoidin II peaks 1335.75 m/z (A) and 1793.87 m/z (B). A.) Proof of the correct identification of the discoidin II peptide by showing the GDHDQWVTSY amino acid sequence by its a, b and y fragments. B.) Proves also the correct identification of discoidin II by showing the SYNPSVQVGEVSIGD amino acid sequence by its b and y fragments.

5.3.2 Affinity Chromatography with Acrylamide Matrix

In this experiment acrylamide beads were coupled with HRP and then incubated with *D. discoideum* Ax3 lysate as described in 4.2.1.1. In addition as a negative control beads, that were not coupled with HRP but in the remaining steps treated similarly, were used.

By this method low amounts of several proteins could be isolated (figure 5.3.2.1). The masses of these proteins were around 40 kDa, 37 kDa, 33 kDa, 28 kDa and 15 kDa. Of these proteins only the 37 kDa protein and the 33 kDa protein seemed to be missing from the negative control. In-gel tryptic digests of the three largest proteins (40 kDa, 37 kDa and 33 kDa) with subsequent MS analysis of the PMF revealed their identity.

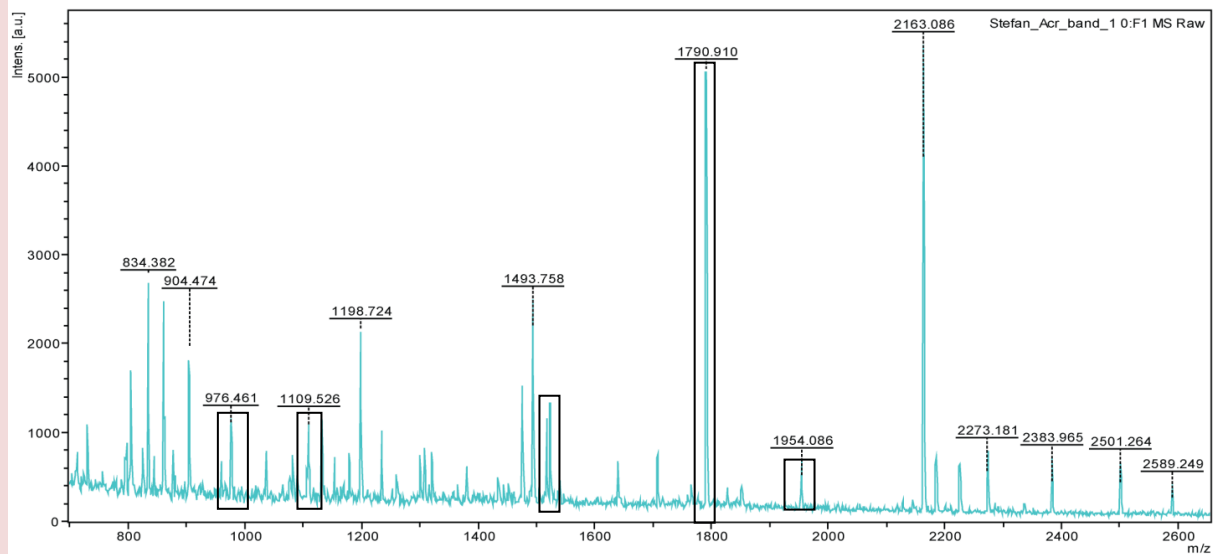
Figure 5.3.2.1 Acrylamide affinity chromatography



Acrylamide beads were coupled with HRP and incubated with *D. discoideum* Ax3 lysate (A). Negative controls were acrylamide beads not coupled to HRP. The annotation E, W and F stand for elution, wash and flow-through respectively. Slightly enhanced visualization of the elution of control and experiment (B). Even though the signal strength was quite low 2 proteins exclusively present in the elution of the experiment were found (marked by two arrows). In order to obtain enough material for protein determination by PMF several lanes were loaded with the elution of the experiment (C), revealing more clearly the two proteins (marked by arrows).

The 40 kDa protein is actin. This was revealed by MS PMF analysis and confirmed by MS/MS (figure 5.3.2.2). An interaction of actin with glycans or acrylamide is very unlikely and has never been published before. It can be found also on the negative control. It is presumably background, due to the high actin concentration in lysates of eukaryotic cells. It still remains unclear why actin so dominantly persists after washing whereas other abundant proteins were cleared away.

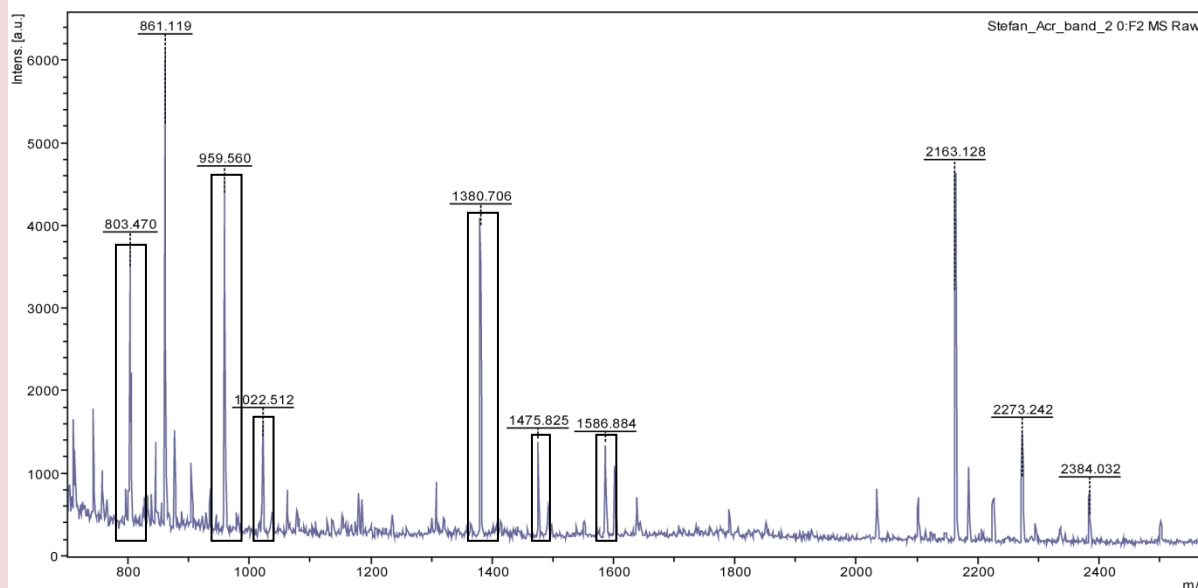
Figure 5.3.2.2 MS PMF analysis of 40 kDa band of acrylamide affinity chromatography



In-gel tryptic digest of a protein with a mass of 40 kDa isolated by affinity chromatography with HRP coupled acrylamide. Due to low protein amounts, trypsin autolysis and other background peaks are relatively abundant. Framed peaks are unique peaks of that spectrum (compared to the spectra of the other bands). MS-Fingerprint analysis revealed highly significant an Actin-protein (MOWSE score of 3431). The protein mass is also suiting (estimated: around 40kDa, actin: 41kDa). MS/MS analysis confirmed that result.

The 37 kDa protein was identified as HRP protein by its PMF (figure 5.3.2.3). The co-elution of HRP from HRP-coupled beads was experienced already with sepharose beads (chapter 5.4.1). This explains its absence from the negative control, in which beads not couple to HRP were used.

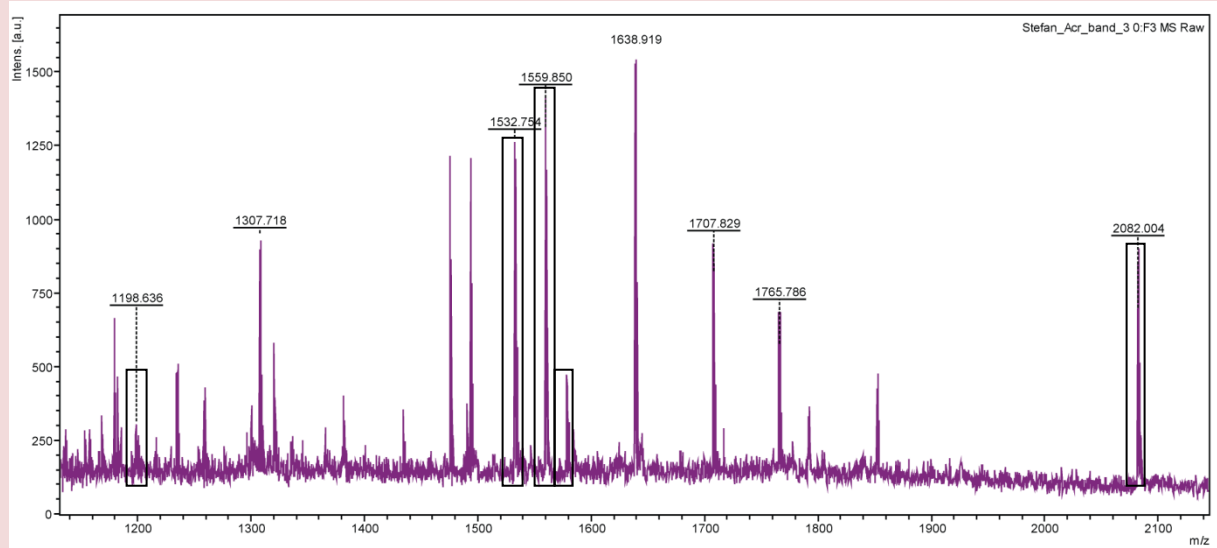
Figure 5.3.2.3 MS PMF analysis of 37 kDa band of acrylamide affinity chromatography



In-gel tryptic digest of a protein with a mass of 37 kDa isolated by affinity chromatography with HRP coupled acrylamide. Due to low protein amounts trypsin autolysis and other background peaks are relatively abundant. Framed peaks are unique peaks of that spectrogram (compared to the spectra of the other bands). MS-Fingerprint analysis revealed highly significant the HRP-protein (MOWSE score of 3431). MS-Fingerprint analysis revealed highly significant HRP (MOWSE score of 838). Mass is suiting (estimated: around 37kDa, HRP without posttranslational modifications: 34kDa). MS/MS analysis confirmed that result.

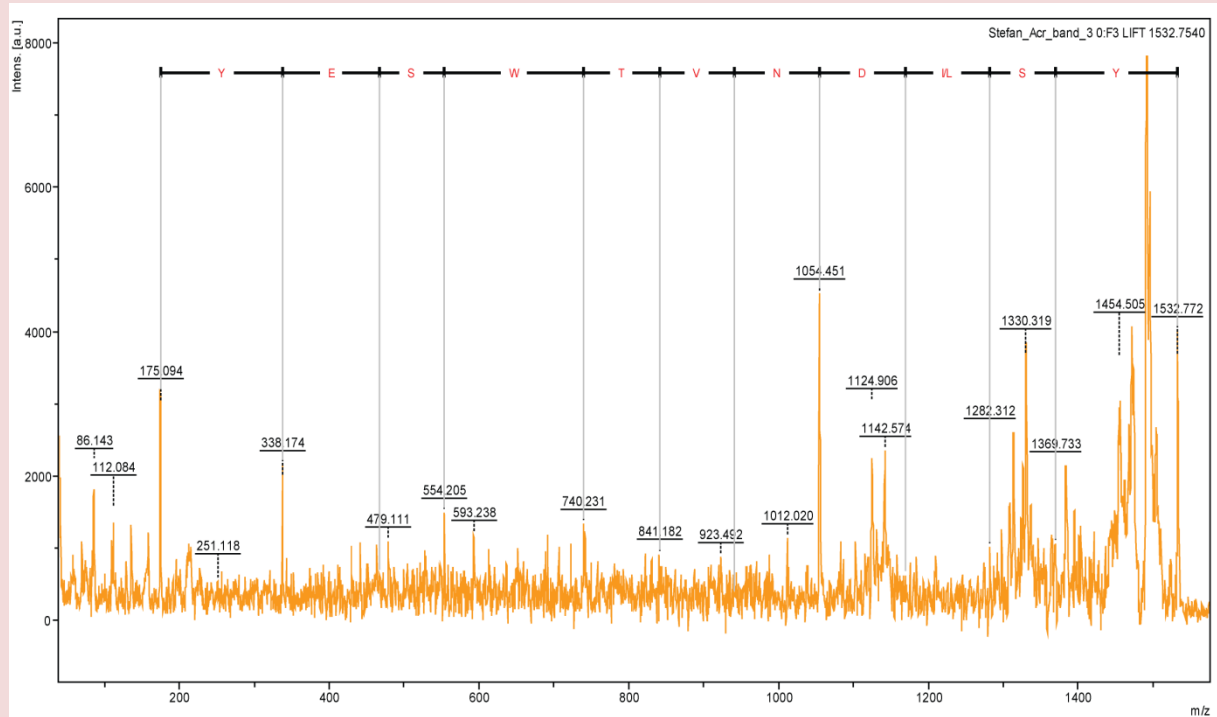
The 33 kDa protein was identified as discoidin I by its PMF (figure 5.3.2.4). On acrylamide matrix this lectin eluted solely on HRP coupled beads. The mass of discoidin I as sum of its amino acid masses (28 kDa) is again slightly smaller than estimated by the gel (33 kDa). This might be due to posttranslational modifications, or due to inaccuracy of the estimation. That the 33 kDa band is truly discoidin I was confirmed by MS/MS peptide sequence analysis of peak 1532.75 m/z (figure 5.3.2.5).

Figure 5.3.2.4 MS PMF analysis of 33 kDa band of acrylamide affinity chromatography



In-gel tryptic digest of a protein with a mass of 33 kDa isolated by affinity chromatography with HRP coupled acrylamide. Due to low protein amounts trypsin autolysis and other background peaks are relatively abundant. Framed peaks are unique peaks of that spectrogram (compared to the spectra of the other bands). MS-Fingerprint analysis revealed highly significant discoidin I (MOWSE score of 441). Mass is suiting (estimated: around 33kDa, Disc1: 28kDa). MS/MS analysis confirmed result.

Figure 5.3.2.5 MS/MS analysis of discoidin I peptides to assure the correct identification



MS/MS analysis of tryptic digest discoidin I peak 1532.75 m/z. Proves the correct identification of the discoidin I peptide by showing the YSIDNVTWSEY amino acid sequence by its y fragments.

5.4 Investigation on Discoidin I

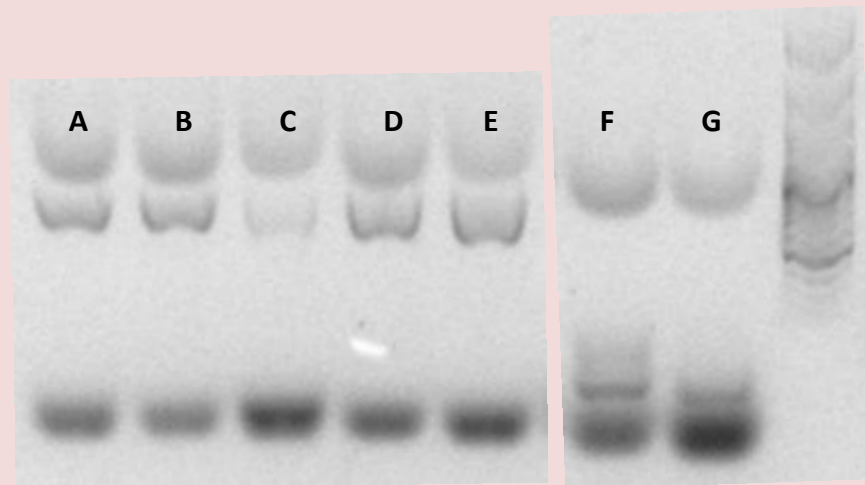
The identification of the lectin discoidin I (DscI, described in detail in 3.3.1) as a protein that may bind to MOXF₃ glycan structures aroused our interest. In order to confirm these binding properties and to investigate more deeply the biochemical characteristics of discoidin I, there was a need for high amounts of tagged protein. I therefore started cloning the open reading frame of discoidin I with the aim of obtaining an *E. coli* expression strain transfected with an expression vector encoding N-terminal His tagged discoidin I.

5.4.1 Cloning of Discoidin I

Wild type *D. discoideum* possesses 3 paralogous *discoidin I* genes, the so called A-Chain (*dscA-1*), B/C-Chain (*dscC-1*) and D-Chain (*dscD-1*). All 3 gene products consist of a 253 amino acid chain and they differ in less than 5% of their primary sequence. In *D. discoideum* Ax3 cells all three paralogues are present duplicated, with no further mutation. Since all three *discoidin I* genes seemed to have the same or at least extremely similar binding properties, there was no preference in which of these *discoidin I* genes were actually cloned. Besides it was not possible to design selective primer for only one paralogue, the obtained form had to be determined after cloning it.

First total RNA of Ax3 supplied by Alba Hykollari was reverse transcribed. The resulting cDNA had a concentration of 843.3 ng/μl (nano-drop). Then a PCR was performed as described in 4.3.2 with an annealing temperature gradient and with either a pair for discoidin I or, as a positive control, a GAPDH primer pair (figure 5.4.1.1).

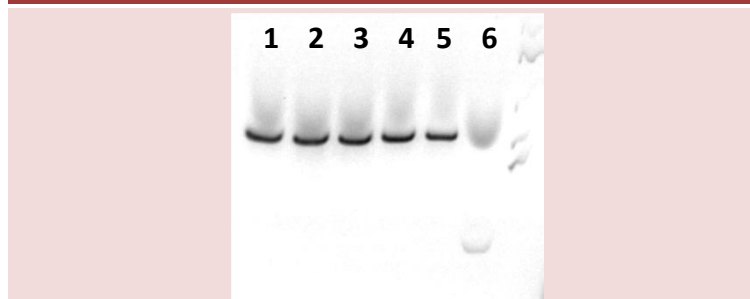
Figure 5.4.1.1 Gradient PCR with Discoidin I primers



A-E.) Gradient PCR with discoidin I primer. Annealing temperatures from A to E were 49°C; 51°C; 53,8°C; 56,6°C; 59,1°C respectively. It is not clear what the band above the specific PCR product is, but it could be seen in all samples, independent of primers or template. The specific bands show the correct size of around 760 bp. F and G.) The positive control with GAPDH primers with the freshly prepared cDNA template (F) and with an older cDNA template that has been proven to work (G)

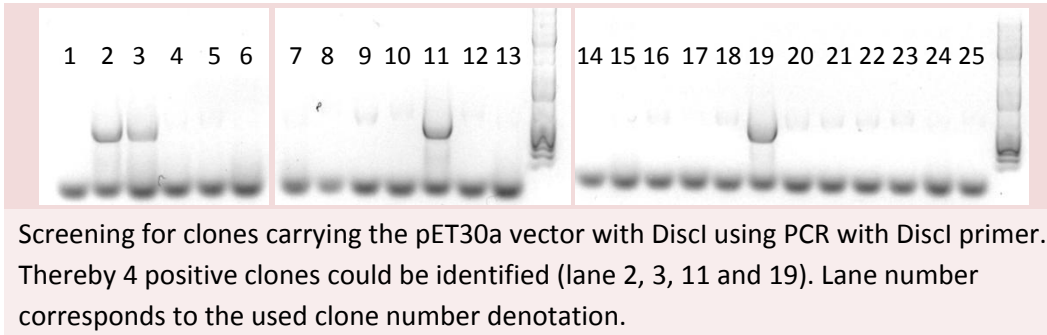
Seemingly annealing temperatures from 49°C to 59.1°C all lead to specific amplification of the discoidin I genes. In all further PCR amplifications 51°C was used. Another PCR was started to obtain large amounts of amplified discoidin I product (figure 5.4.1.2). Gel pieces containing the band of the size expected for the discoidin open reading frame were excised, and the DNA was purified. DNA concentration measurement with Nano-Drop revealed a concentration of 5.0 ng/μl. 25 μl of discoidin I DNA (around 120 ng) and 2 μl of pET30a vector (176 ng) were then digested with NcoI and XhoI and incubated together with ligase. The whole ligation mix was added to competent JM101 *E. coli* cells, heat shock treated and grown under kanamycin selection. All grown colonies were screened via PCR for the presence of discoidin I gene. Through this procedure four positive clones could be isolated (figure 5.4.1.3).

Figure 5.4.1.2 PCR for large amounts of amplified discoidin I



Lane 1 to 5: Discl amplifying PCR from Ax3 cDNA.
Lane 6: Control PCR with GAPDH primer.

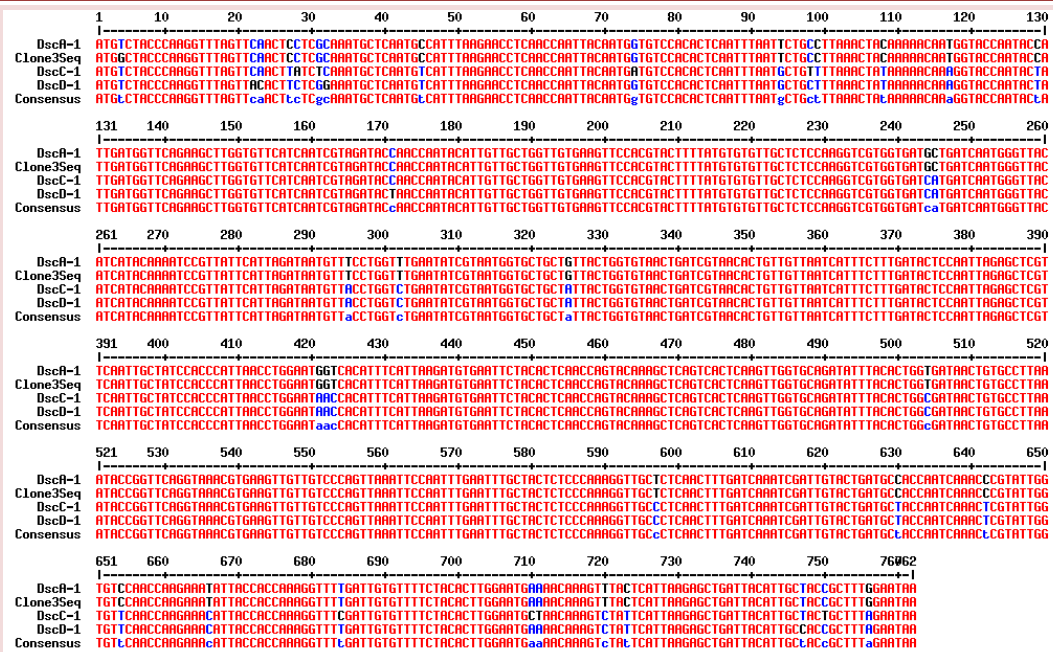
Figure 5.4.1.3 PCR screening for positive clones



Screening for clones carrying the pET30a vector with DscI using PCR with DscI primer. Thereby 4 positive clones could be identified (lane 2, 3, 11 and 19). Lane number corresponds to the used clone number denotation.

Clone number 2, 3, 11 and 19 were successfully transfected with a vector carrying the discoidin I fragment. After overnight culturing of the four clones in 4 ml LB each, the plasmids were collected via miniprep. The yield was 50 µl of 90.8 ng/µl, 86.2 ng/µl, 97.0 ng/µl and 81.8 ng/µl respectively. The inserts of the plasmids were sequenced in both directions using T7 promoter and T7 terminator primer. The sequence analysis showed that in all 4 cases the open reading frame of the A-Chain was cloned (figure 5.4.1.4)

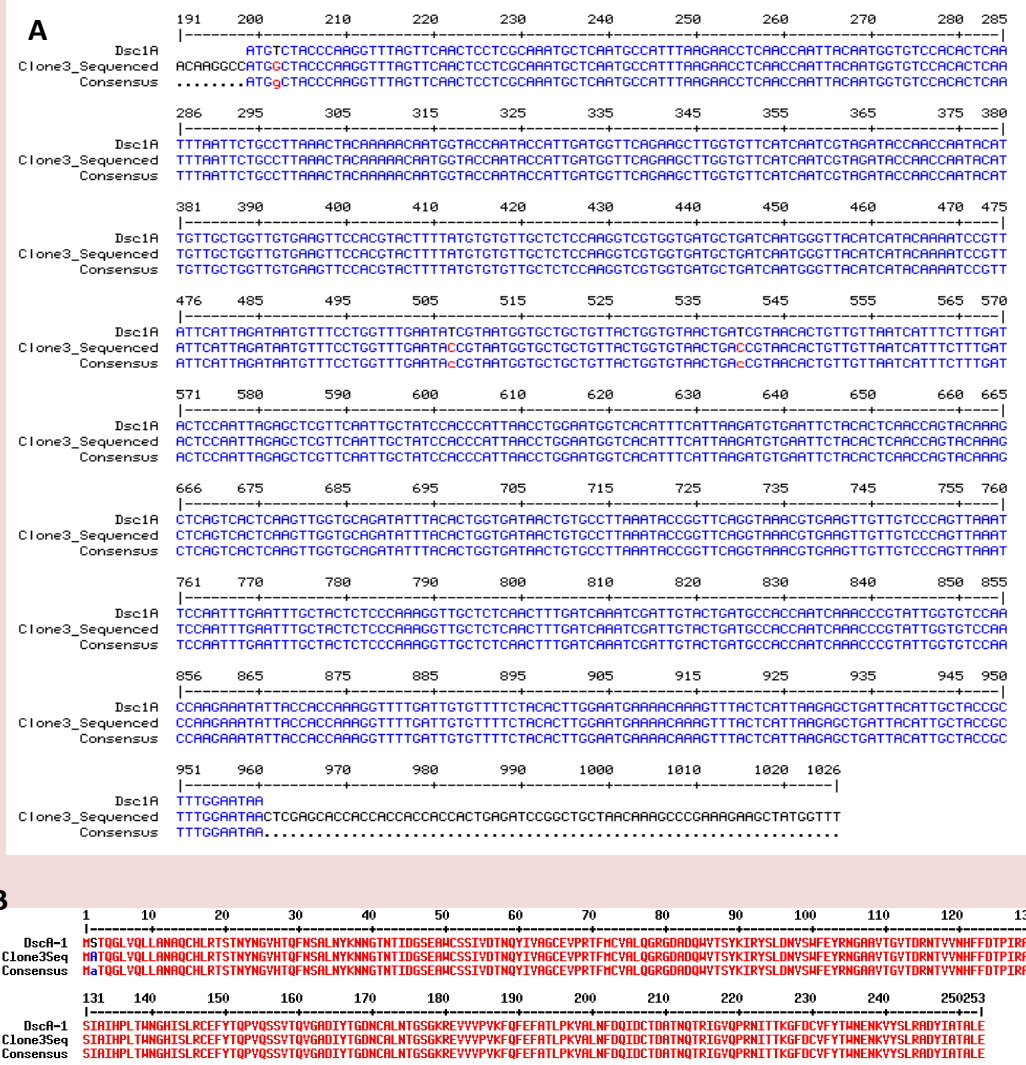
Figure 5.4.1.4 Alignment of the three Discoidin I Chains and the Discoidin I Sequence of Clone 3



Sequence alignment of the three discoidin I chains and the discoidin I sequence of clone 3 showing high similarity between the cloned sequence and the A chain with only 3 different bases, one of them inevitably caused by the primer sequence, the two other are silent mutations. With the C and D chain the cloned sequence has 32 and 30 differences respectively.

Whereas Clone 2, 11 and 19 unfortunately had missense mutations, Clone 3 showed two silent mutations at position 309 and 342, which happened both to be in wobble positions (figure 5.4.1.5 A). As proven by in-silico translation the primary amino acid sequence of *dscA-1* and the fragment are identical except the one amino acid substitution caused by the primer sequence (figure 5.4.1.5 B).

Figure 5.4.1.5 Alignment of Discoidin I A-Chain and the Discoidin I Sequence of Clone 3

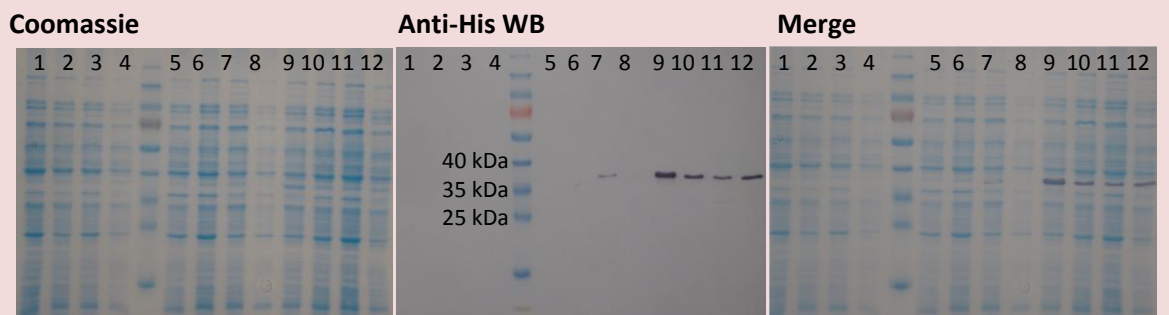


A.) The alignment between *dsc1* A-chain and the *dsc1* sequence of clone 3 reveals the 3 different bases. At position 4 the change from T to C causes a change from serine to alanine in the translated protein; this mutation was due to the primer in order to have an N-terminal in frame restriction site. The mutations at position 309 and 342, both T to C, caused no change in the amino acid sequence. B.) Primary sequence alignment of discoidin I and the cloned version showing only one mutation at the very N-terminal end.

Clone 2 showed a mutation in position 383 which leads in the protein to a substitution of an arginine by an isoleucine at position 128. This amino acid is located in the beta-sheet of the N-terminal domain.

The plasmids of clone 2 and 3 were used to transfect the expression strain BL21. From the grown plate, 4 colonies were picked for pilot expression at 16°C and 24°C. Western blot and Coomassie staining of the soluble fraction of the lysates showed that the dscA-1 of clone 2, which carried a missense point mutation, had problems being expressed (figure 5.4.1.6). On the other hand, dscA-1 from clone 3 carrying the silent mutation was expressed to high amounts and was soluble at 24°C as well as on 16°C.

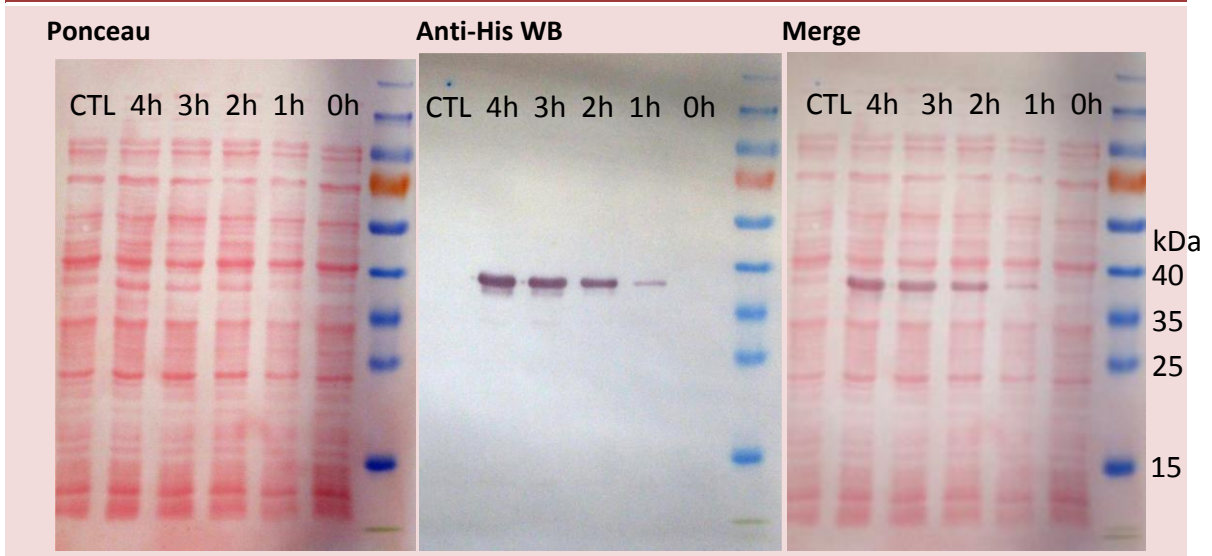
Figure 5.4.1.6 Pilot expression



Discoidin I pilot expression of clone 2 and 3. Soluble fractions of lysates are shown Coomassie stained and anti-His western blotted. **Lanes: 1 – 4:** controls, **1:** clone 2, 24°C, 4h; **2:** clone 2, 16°C, o.n.; **3:** clone 3, 24°C, 4h; **4:** clone 3, 16°C, o.n.; **5 – 7:** three different colonies of clone 2 IPTG induced, 24°C, 4h; **8:** clone 2 IPTG induced, 16°C, o.n.; **9 – 11:** three different colonies of clone 3 IPTG induced, 24°C, 4h; **12:** clone 3 IPTG induced, 16°C, o.n.

A time series was performed with the most efficiently expressing clone of the previous pilot expression experiment (figure 5.4.1.7). Due to the good results of 24°C, yielding high amounts of soluble protein, this condition was used for the large scale expression. The time series also showed that the amount of soluble protein increases even after 4 hours, indicating that the BL21 strain has no problems expressing DscA-1 that may have been caused by toxicity of the lectin itself or by strong formation of inclusion bodies.

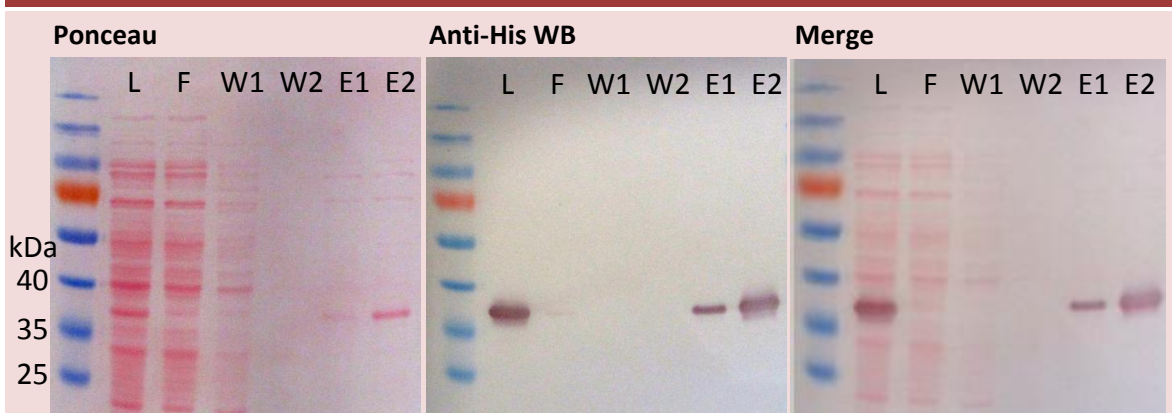
Figure 5.4.1.7 Pilot expression clone 3 I



Pilot expression of discoidin I of clone 3 with a 24°C time series. The control was not induced with IPTG but grown under the same conditions for 4 hours. The time series shows how the amount of discoidin I increases with the time after induction. The amount of *E. coli* proteins remains more or less unchanged. The optimal discoidin I expression seems to be at 24°C for at least 4 hours with clone 3.

The large scale expression was performed for 4 hours at 24°C. The soluble fraction of the lysate was collected and discoidin I protein was isolated by His-tag purification using a Ni-NTA column. This procedure yielded 2 ml of highly purified and concentrated discoidin I (2 µg/µl) (figure 5.4.1.8).

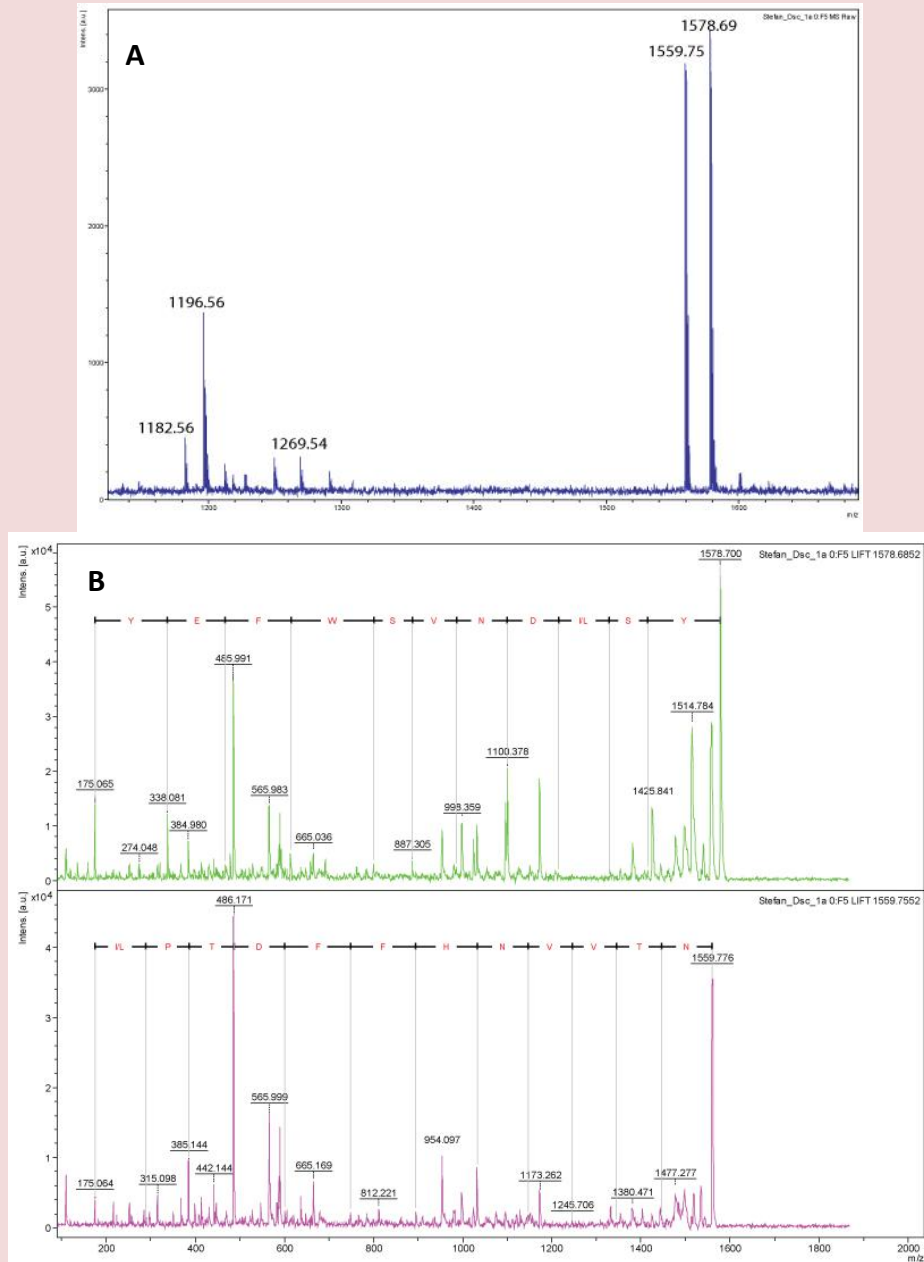
Figure 5.4.1.8 Large scale expression



Large scale expression of discoidin I of clone 3 for 4 hours at 24°C. The soluble fraction of the lysate was loaded onto a Ni-NTA column, washed several times, and eluted with an imidazole containing buffer. The annotation L, F, W and E stand for lysate, flow-through, wash and elution respectively. Through this procedure highly purified and concentrated discoidin I was obtained.

DscA-1 with His-tag expressed in *E. coli* showed the predicted size of around 38 kDa. A final PMF and MS/MS sequence analysis confirmed that the purified protein was discoidin I (figure 5.4.1.9).

Figure 5.4.1.9 Recombinant Discoidin 1 A fingerprint



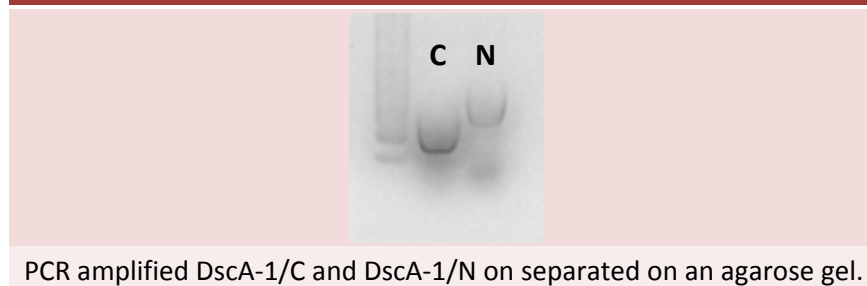
A.) PMF confirms that the expressed protein is discoidin I A. The 1182 m/z, 1196 m/z, 1559 m/z and 1578 m/z peaks were also found in the spectra for native discoidin I. B.) MS/MS digest of peak 1578.69 m/z and 1559.75 m/z emphasizes the correct identification. The mass of the peaks are within the 0.6% window, and therefore there is some overlap in the MS/MS spectra. Anyway the sequence for both peaks could be sequenced (YSIDNVSWF EY and NTVVNHFFD TPI) and further approved the correct PMF.

5.4.2 Cloning of Discoidin I N and C terminus

Discoidin I is a lectin carrying two sugar binding motifs. On the N-terminus it has the so called discoidin domain, which is a widely distributed domain amongst eukaryotes whose exact binding properties vary from protein to protein; the C-terminus is an H-type lectin domain, known to have affinity towards Gal, GalNAc and their polymers. In order to make a more specific analysis of discoidin binding properties and biological function in the future the two domains were cloned separately.

As a template for discoidin I A-Chain C-terminus and N-terminus, henceforth referred to as DscA-1/C and DscA-1/N respectively, pET30a vector with cloned DscA-1 gene was used (described in chapter 5.4.1). The primers and the PCR programme are described in chapter 4.3.2. After the PCR of the 485 bp large DscA-1/N and 319 bp large DscA-1/C (figure 5.4.2.1) the gel containing the fragments were excised and the DNA purified. Both fragments and the pET30a vector were cut by NcoI and XhoI and ligated.

Figure 5.4.2.1 PCR amplified discoidin I C-terminus and N-terminus



The whole ligation mix was added to competent JM101 *E. coli* cells, heat shock treated and grown under kanamycin selection. All grown colonies were screened via PCR for the presence of DscA-1/C or N fragment. Through this procedure 12 positive clones carrying DscA-1/C and 6 positive clones carrying DscA-1/N could be identified (figure 5.4.2.2).

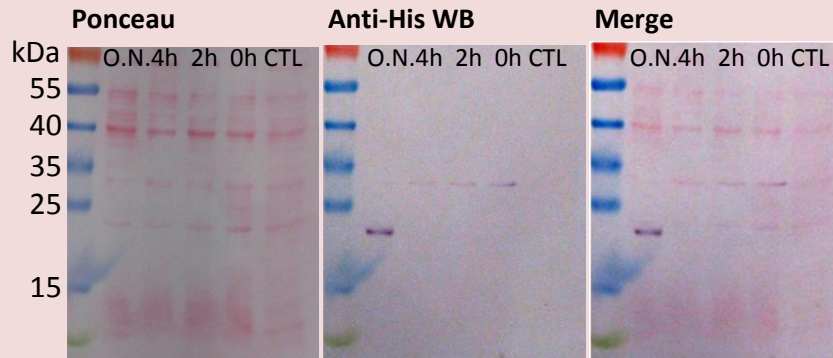
Figure 5.5.2.2 PCR screening for positive clones



Screening for clones carrying the pET30a vector with either DscA-1/N or DscA-1/C using PCR with respective primer pair. Thereby 6 positive clones for N-terminus (lane 1, 3, 6, 8, 9 and 10) and 12 positive clones for the C-terminus (all). Lane number corresponds to the used henceforth used clone number denotation.

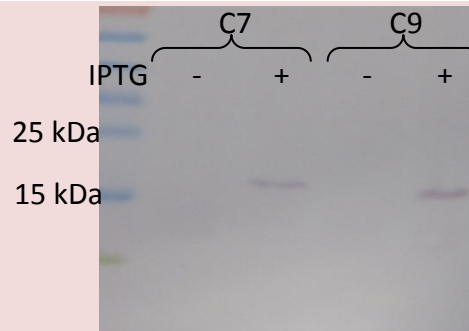
The plasmids of DscA-1/N clone 1 and DscA-1/C clone 7 and 9 were used to transfect the expression strain BL21. Of the overnight grown LB kanamycin plate one colony per clone was picked for pilot expression at 16°C and 24°C. Western blot and Coomassie staining of the soluble fraction of the lysates were analysed. At 24°C no protein was found in the soluble phase, neither for DscA-1/N nor for C (data not shown). However, at 16°C soluble DscA-1/N (figure 5.4.2.3) and DscA-1/C (figure 5.4.2.4) were obtained.

Figure 5.4.2.3 Pilot expression DscA-1/N soluble fraction



Soluble fraction of the DscA-1/N clone 1 pilot expression at 16°C. The control was not induced with IPTG but grown under the same conditions over night. The time series shows that detectable amount of DscA-1/N was achieved by overnight expression. The amount of *E. coli* proteins remains more or less unchanged.

Figure 5.4.2.4 Pilot expression DscA-1/C soluble fraction

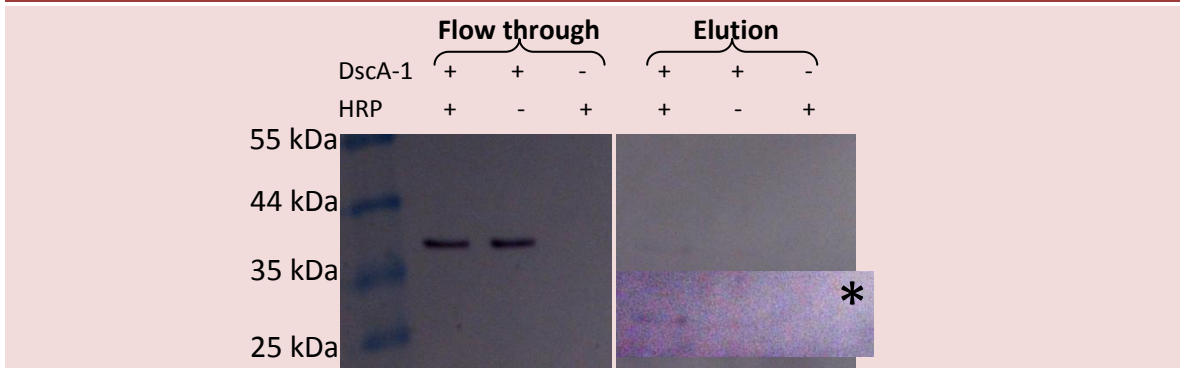


Soluble fraction of the DscA-1/C clone 7 and clone 9 pilot expression at 16°C overnight. Soluble DscA-1/C was expressed by both clones under these conditions.

5.4.3 Binding affinity of Discoidin I A to HRP

After the His-Tag purification of recombinant DscA-1 via a Ni-NTA column and the confirmation that the correct protein was expressed judging from its size on SDS-PAGE and parts of its peptide sequence revealed by MS/MS, the next step was to confirm the binding property of the recombinant DscA-1 towards the N-glycan of HRP. For this purpose I coupled acrylamide beads with HRP and performed an affinity chromatography using the His-tag purified DscA-1 as the analyte. This experiment displayed very weak binding interaction between DscA-1 and HRP.

Figure 5.4.2.1 HRP Acrylamide Affinity Chromatography with recombinant DscA-1



Acrylamide beads coupled with HRP and incubated for 1 hour at room temperature with His-tag purified recombinant DscA-1. The flow through shows that weak binding interactions exist between the recombinant DscA-1 and HRP resulting in only a small amount of DscA-1 detected in the elution fraction. Picture section marked by asterisk is the elution fraction better visualized due to higher contrast.

Repetition of this experiment as well as modifying the experimental parameters did not enhance the outcome. Possible reasons for the low binding affinity of the recombinant discoidin I are addressed in the discussion part.

VI. Discussion

Dictyostelium discoideum is one of the oldest still used molecular biological model organisms. First results concerning chemotaxis, aggregation and development date back to the year 1947 (Bonner, 1947). Since that time many researchers revealed one molecular biological puzzle piece by one, slowly but constantly helping to assemble the big picture of development in *D. discoideum*. Even though many data have been collected over the past 60 years, some crucial links are still missing making development in *D. discoideum* not understood throughout the whole process. As for example many spatio-temporal gene expression changes have been identified (Rosen et al., 1973; Mathieu et al., 2010), but their functions are still unknown. Another example is that an N-glycomic shift from single to multi-cellular stage is proven, without any hint for a reason (Schiller et al., 2009). To solve the latter uncharted issue, it would be necessary to identify a compound that is able to interact specifically with these glycans, in all likelihood a specifically binding lectin.

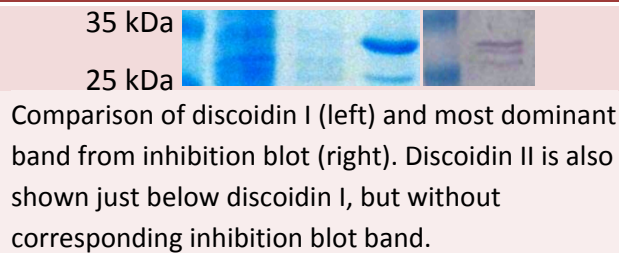
The glycosylation profile shifts during development towards shorter N-glycans, with more accessible core-region and core- α 1,3-fucoses in the multicellular form. This leads to an Endo-H sensitivity of the otherwise resistant *D. discoideum* glycans during aggregation and culmination (Ivatt et al. 1981). Especially the core- α 1,3-fucose drew our interest, because it is a moiety that appears in many, very different species, for example in nematodes, plants and slime moulds (Paschinger et al., 2008; Sturm et al., 1992; Schiller et al., 2009), but in some evolutionary more closely related organisms it is lost, as in *Acanthamoeba* (Schiller et al., 2012), which happens to be like *D. discoideum* also an amoebozoan, or in snails (Van Kuik et al., 1985) that just as nematodes are member of the protostomia clade of animals.

It is without doubt that this fucose moiety possesses a function, simply due to its reoccurrence all across the eukaryotic domain. In *D. melanogaster* for example, core- α 1,3-fucosylation occurs specifically in the embryonic nervous system. A spatio or temporal change of the core- α 1,3-fucose expression leads to a series of disorders (Rendic et al., 2010). Also as shown before in *D. discoideum* mutant strains lacking core- α 1,3-fucose growth rate was reduced, the germination of older spores was impaired and the slime sheath accumulation delayed (Schiller et al., 2009; Gonzales-Yanes et al., 1989; Champion et al., 1995). This may correlate with my experiment with a glucosidase II inhibitor shown to decrease doubling time of inhibited cells by more than 60% (see appendix).

The core-region of N-glycans in *D. discoideum* and in plants is quite similar. They differ by only one xylose moiety that exists in plants. The similarity is to such an extent that antibodies specific for the N-glycan of HRP (a plant peroxidase) are strongly cross-reacting with that of *D. discoideum*. Using HRP N-glycans to identify lectins that may bind the core-region of *D. discoideum* is therefore an admissible procedure and has been successfully used to identify a similar fungal lectin before (Schubert et al., 2012). The performed inhibition blots hinted at the existence of lectins that bind this core-

region. It was shown by West and McMahon (1977) that some lectins are in fact able to refold after SDS-PAGE and recover their binding specificity. Interestingly the protein examined in that study with this refolding property is discoidin I. As a matter of fact the strongest band revealed by the inhibition blot shows to have the same molecular mass as the discoidin I isolated by affinity chromatography (figure 6.1).

Figure 6.1



Lectin binding strengths are, compared to that of antibodies, very low. Bound lectins are easily washed away rendering affinity purification for lectins a challenging task. In natural environments binding strength of lectins often arises through avidity rather than affinity. The low concentration of a lectin in the total absence of more abundant proteins as yielded by affinity chromatography with acrylamide matrix can therefore be deemed as a significant evidence for specific binding towards the presented glycan.

It is rather difficult to determine a protein mass with an accuracy of ± 5 kDa by its appearance on an SDS-PAGE gel. That also applies for discoidin I when identified in-gel. The databases predict a molecular mass of approximately 28 kDa but on the SDS-PAGE that followed the affinity chromatography it appeared to be around 33 kDa. A reasonable suspicion, because discoidin II happens also to have approximately 28 kDa but definitely showed to be around 5 kDa smaller than discoidin I (figure 6.1). Post-translational modifications have not been reported for discoidin I, but they might very well exist. Phosphorylation may occur, but with a molecular mass of 80 Da per phosphate even multiple phosphorylations cannot be accountable for a shift of 5 kDa. Ubiquitination and sumoylation two highly conserved protein modification processes also occurring in *D. discoideum* seem also improbable (Clark et al., 1997; Sobko et al., 2002), because they usually add a mass of 8 to 12 kDa per protein, which would cause a stronger shift. On the other hand single or multiple glycosylations could theoretically cause a 5 kDa shift. For example the major N-glycan structure found in *D. discoideum* comprises a mass of around 2.5 kDa (H8N4F). Discoidin I carries no terminal signal sequence and has been shown to leave the cell via multilaminar bodies (Barondes et al., 1985). There are also signs for transport via normal secretory vesicles besides multilaminar body though (Fukuzawa and Ochiai, 1993). However, due to the lack of a signal sequence discoidin I seems not to enter the ER and should therefore not carry any N-glycosylation. Another not particularly likely possibility would be O-glycosylation which can be assembled on cytoplasmic proteins in *D. discoideum* (Teng-umnuay et al., 1998). This question must be left unanswered in this thesis, but the mass shift and post-

translational modification on discoidin I in general should be investigated in the future, as they might have a strong influence on its specificity and function. An attempt to examine the size of native discoidin I by MALDI-TOF MS was not successful, although the recombinant protein could be analyzed by this technique (data not shown).

Discoidin I, which is a potential N-glycan-core binding protein, was expressed for confirmation of this prediction and further examination in an *E. coli* expression strain BL21. *E. coli* expression lacks post translational modification of eukaryotes, and comprises different intracellular conditions, but due to its speed of execution it was the method of choice. Besides, discoidin I has been expressed before in *E. coli* by Mathieu et. al. (2010) and yielded fully folded proteins suitable for crystallographic studies. During the cloning procedure 2 silent mutations occurred, besides the one mutation that was introduced during PCR to achieve a restriction site. This N-terminal point mutation was shown to have no influence on the folding in discoidin I (Mathieu et al., 2010). In addition our recombinantly expressed discoidin I carried a 4.9 kDa N-terminal tail containing His-tag and S-tag resulting in a 33 kDa protein. Polyhistidine affinity tags are routinely used for purification of recombinantly expressed proteins and have shown to rarely influence protein structure or function (Lichty et al., 2005). Also the S-tag is known to usually leave structure and function of the target protein uninfluenced but to increase its solubility (Raines et al., 2000). Despite the experience that these tags rarely interfere with the target protein function, it cannot be excluded, especially because the tag constitutes around 17% of the mass of the relatively small target protein, discoidin I. For examination of the binding affinity of the recombinant protein the initial experiment using a HRP coupled acrylamide affinity chromatography, with which discoidin I was identified as a potential HRP N-glycan binding protein, was conducted. This resulted in only very low binding by recombinant discoidin I, close to the limit of detection of the subsequent western blot analysis. Undoubtedly the affinity of the recombinant protein was much weaker than that of in *Dictyostelium discoideum* expressed discoidin I. There is a series of reasons that could be responsible for that: First, as mentioned above, could the 4.9 kDa large N-terminal His- and S-Tag interfere with folding and lectin binding, especially if the N-glycan binding domain is on the N-terminal domain. Second, *E. coli* as an expression strain lacks correct post-translational modifications which are often required for proteins to function. Third, discoidin I is known to form trimers, but it is not known whether a monomer is sufficient for specific oligosaccharide binding or only the trimer. An inability of the recombinant discoidin I to form trimers, be it due to the lack of post-translational modifications, or tags that disturb the protein-protein-interaction, or simply because of an improper chemical environment, could explain the loss of binding affinity. Fourth, it was not possible to distinguish via MS and MS/MS which of the three discoidin I isoforms bound to the HRP coupled column. The binding affinities of the isoforms may differ and the expressed discoidin I A isoform may therefore lack the required MOXF₃ binding ability.

Future studies can address these questions by using a cleavable tag that is cleaved after protein purification, by using an expression system that applies similar post-translational modifications as *D. discoideum*, by determining whether the expressed protein assembles into a trimer via native PAGE and by expressing all three isoforms of discoidin I.

It was previously stated that discoidin I might have an affinity towards core-N-glycans carrying β 1,2-xylose (Amatayakul-Chantler et. al, 1991). These glycans with a core- β 1,2-xylose moiety are found on plant proteins, such as HRP, but not on proteins of *D. discoideum*. Previous glycan array analysis used mammalian printed arrays which do not comprise any form of xylosylated glycans. It therefore cannot be excluded that discoidin I bound to the HRP-affinity-column due to its xylose moiety.

Finally, through cloning each of the two binding domains of discoidin I separately and their successful expression in pilot experiments I laid the foundation stone for future domain specific investigations, which may help to elucidate discoidin I biological function.

VII. References

1. Ajit Varki, Richard D Cummings, Jeffrey D Esko, Hudson H Freeze, Pamela Stanley, Carolyn R Bertozzi, Gerald W Hart, and Marilynn E Etzler. *Essentials of Glycobiology*, 2nd edition; Cold Spring Harbor (NY): Cold Spring Harbor Laboratory Press; 2009. ISBN-13: 9780879697709
2. Amatayakul-Chantler Supavadee, Michael AJ Ferguson, Raymond A. Dwek, Thomas W. Rademacher, Raj B. Parekh, Ian E. Crandall, and Peter C. Newell. "Cell surface oligosaccharides on Dictyostelium during development." *Journal of Cell Science* 99, no. 3 (1991): 485-495.
3. Barondes SH, Cooper DN, Haywood-Reid PL. Discoidin I and discoidin II are localized differently in developing Dictyostelium discoideum. *J Cell Biol.* 1983 Jan;96(1):291-6. PubMed PMID: 6826651; PubMed Central PMCID: PMC2112257.
4. Barondes SH, Haywood-Reid PL, Cooper DN. Discoidin I, an endogenous lectin, is externalized from Dictyostelium discoideum in multilamellar bodies. *J Cell Biol.* 1985 Jun;100(6):1825-33. PubMed PMID: 2581974; PubMed Central PMCID: PMC2113611.
5. Baumgartner S, Hofmann K, Chiquet-Ehrismann R, Bucher P. The discoidin domain family revisited: new members from prokaryotes and a homology-based fold prediction. *Protein Sci.* 1998 Jul;7(7):1626-31. PubMed PMID: 9684896; PubMed Central PMCID: PMC2144056.
6. Blusch J, Alexander S, Nellen W. Multiple signal transduction pathways regulate discoidin I gene expression in Dictyostelium discoideum. *Differentiation.* 1995 Apr;58(4):253-60. PubMed PMID: 7641976.
7. Bonner JT. Evidence for the formation of cell aggregates by chemotaxis in the development of the slime mold Dictyostelium discoideum. *J Exp Zool.* 1947 Oct;106(1):1-26. PubMed PMID: 20268085.
8. Champion A, Griffiths K, Gooley AA, Gonzalez BY, Gritzali M, West CM, Williams KL. Immunochemical, genetic and morphological comparison of fucosylation mutants of Dictyostelium discoideum. *Microbiology.* 1995 Apr;141 (Pt 4):785-97. PubMed PMID: 7539686.
9. Chen G, Zhuchenko O, Kuspa A. Immune-like phagocyte activity in the social amoeba. *Science.* 2007 Aug 3;317(5838):678-81. PubMed PMID: 17673666; PubMed Central PMCID: PMC3291017.
10. Clark A, Nomura A, Mohanty S, Firtel RA. A ubiquitin-conjugating enzyme is essential for developmental transitions in Dictyostelium. *Mol Biol Cell.* 1997 Oct;8(10):1989-2002. PubMed PMID: 9348538; PubMed Central PMCID: PMC25659.
11. Devreotes, P. (1989). "Dictyostelium discoideum: a model system for cell-cell interactions in development." *Science* 245(4922): 1054-8.
12. Eichinger L, Noegel AA. Crawling into a new era-the Dictyostelium genome project. *EMBO J.* 2003 May 1;22(9):1941-6. Review. PubMed PMID: 12727861; PubMed Central PMCID: PMC156086.
13. Eichinger, L., J. A. Pachebat, G. Glockner, M. A. Rajandream, R. Sugang, M. Berriman, J. Song, R. Olsen, K. Szafranski, Q. Xu, B. Tunggal, S. Kummerfeld, M. Madera, B. A.

- Konfortov, F. Rivero, A. T. Bankier, R. Lehmann, N. Hamlin, R. Davies, P. Gaudet, P. Fey, K. Pilcher, G. Chen, D. Saunders, E. Sodergren, P. Davis, A. Kerhornou, X. Nie, N. Hall, C. Anjard, L. Hemphill, N. Bason, P. Farbrother, B. Desany, E. Just, T. Morio, R. Rost, C. Churcher, J. Cooper, S. Haydock, N. van Driessche, A. Cronin, I. Goodhead, D. Muzny, T. Mourier, A. Pain, M. Lu, D. Harper, R. Lindsay, H. Hauser, K. James, M. Quiles, M. Madan Babu, T. Saito, C. Buchrieser, A. Wardroper, M. Felder, M. Thangavelu, D. Johnson, A. Knights, H. Louseged, K. Mungall, K. Oliver, C. Price, M. A. Quail, H. Urushihara, J. Hernandez, E. Rabbinowitsch, D. Steffen, M. Sanders, J. Ma, Y. Kohara, S. Sharp, M. Simmonds, S. Spiegler, A. Tivey, S. Sugano, B. White, D. Walker, J. Woodward, T. Winckler, Y. Tanaka, G. Shaulsky, M. Schleicher, G. Weinstock, A. Rosenthal, E. C. Cox, R. L. Chisholm, R. Gibbs, W. F. Loomis, M. Platzter, R. R. Kay, J. Williams, P. H. Dear, A. A. Noegel, B. Barrell and A. Kuspa (2005). "The genome of the social amoeba *Dictyostelium discoideum*." *Nature* 435(7038): 43-57.
14. Feasley CL, Johnson JM, West CM, Chia CP. Glycopeptidome of a heavily N-glycosylated cell surface glycoprotein of *Dictyostelium* implicated in cell adhesion. *J Proteome Res.* 2010 Jul 2;9(7):3495-510. doi: 10.1021/pr901195c. PubMed PMID: 20443635.
 15. Fey P, Kowal AS, Gaudet P, Pilcher KE, Chisholm RL. Protocols for growth and development of *Dictyostelium discoideum*. *Nat Protoc.* 2007;2(6):1307-16. PubMed PMID: 17545967.
 16. Frazier WA, Rosen SD, Reitherman RW, Barondes SH. Purification and comparison of two developmentally regulated lectins from *Dictyostelium discoideum*. Discoidin I and II. *J Biol Chem.* 1975 Oct 10;250(19):7714-21. PubMed PMID: 1236849.
 17. Gabius HJ, Siebert HC, André S, Jiménez-Barbero J, Rüdiger H. Chemical biology of the sugar code. *Chembiochem.* 2004 Jun 7;5(6):740-64. Review. PubMed PMID: 15174156.
 18. Gabius HJ, Springer WR, Barondes SH. Receptor for the cell binding site of discoidin I. *Cell.* 1985 Sep;42(2):449-56. PubMed PMID: 2411421.
 19. Gaudet P, Fey P, Chisholm R. Extraction of RNA from *dictyostelium*. *CSH Protoc.* 2008 Dec 1;2008:pdb.prot5106. doi: 10.1101/pdb.prot5106. PubMed PMID: 21356752.
 20. Gonzalez-Yanes B, Mandell RB, Girard M, Henry S, Aparicio O, Gritzali M, Brown RD Jr, Erdos GW, West CM. The spore coat of a fucosylation mutant in *Dictyostelium discoideum*. *Dev Biol.* 1989 Jun;133(2):576-87. PubMed PMID: 2471657.
 21. Grimson MJ, Haigler CH, Blanton RL. Cellulose microfibrils, cell motility, and plasma membrane protein organization change in parallel during culmination in *Dictyostelium discoideum*. *J Cell Sci.* 1996 Dec;109 (Pt 13):3079-87. PubMed PMID: 9004042.
 22. Harvey, D. J. (2008). "Analysis of carbohydrates and glycoconjugates by matrix-assisted laser desorption/ionization mass spectrometry: an update covering the period 2001-2002." *Mass Spectrom Rev* 27(2): 125-201.
 23. Helenius A, Aebi M. Roles of N-linked glycans in the endoplasmic reticulum. *Annu Rev Biochem.* 2004;73:1019-49. Review. PubMed PMID: 15189166.
 24. Hereld D. (2005), Signal Transduction via G-Protein-Coupled Receptors, Trimeric G Proteins, and RGS Proteins, in *Dictyostelium Genomics* (Loomis W. F., Kuspa A., eds) Horizon Bioscience, 103-123
 25. Herscovics A. Importance of glycosidases in mammalian glycoprotein biosynthesis. *Biochim Biophys Acta.* 1999 Dec 6;1473(1):96-107. Review. PubMed PMID: 10580131.
 26. Holle A, Haase A, Kayser M, Höhdorf J. Optimizing UV laser focus profiles for improved

- MALDI performance. *J Mass Spectrom.* 2006 Jun;41(6):705-16. PubMed PMID: 16718638.
27. Ivatt RJ, Das OP, Henderson EJ, Robbins PW. Developmental regulation of glycoprotein biosynthesis in *Dictyostelium*. *J Supramol Struct Cell Biochem.* 1981;17(4):359-68. PubMed PMID: 7328678.
 28. Jenny RJ, Pittman DD, Toole JJ, Kriz RW, Aldape RA, Hewick RM, Kaufman RJ, Mann KG. Complete cDNA and derived amino acid sequence of human factor V. *Proc Natl Acad Sci U S A.* 1987 Jul;84(14):4846-50. PubMed PMID: 3110773; PubMed Central PMCID: PMC305202.
 29. Kessin R. H., *Dictyostelium—Evolution, Cell Biology, and the Development of Multicellularity*, Cambridge University Press, Cambridge, UK (2001)
 30. Kiedzińska A, Smietana K, Czepczynska H, Otlewski J. Structural similarities and functional diversity of eukaryotic discoidin-like domains. *Biochim Biophys Acta.* 2007 Sep;1774(9):1069-78. Epub 2007 Jul 24. Review. PubMed PMID: 17702679.
 31. Konijn T. M., van de Meene J. G. C., Chang Y. Y., Barkley D. S. and Bonner J. T. (1969), Identification of adenosine-3',5'-monophosphate as the bacterial attractant for myxamoebae of *Dictyostelium discoideum*. *J Bacteriol.* 99(2):510-2
 32. Lichty JJ, Malecki JL, Agnew HD, Michelson-Horowitz DJ, Tan S. Comparison of affinity tags for protein purification. *Protein Expr Purif.* 2005 May;41(1):98-105. PubMed PMID: 15802226.
 33. Maeda, M., H. Sakamoto, N. Iranfar, D. Fuller, T. Maruo, S. Ogihara, T. Morio, H. Urushihara, Y. Tanaka and W. F. Loomis (2003). "Changing patterns of gene expression in *Dictyostelium* prestalk cell subtypes recognized by in situ hybridization with genes from microarray analyses." *Eukaryot Cell* 2(3): 627-37.
 34. Manahan, C. L., P. A. Iglesias, Y. Long and P. N. Devreotes (2004). "Chemoattractant signaling in *Dictyostelium discoideum*." *Annu Rev Cell Dev Biol* 20: 223-53.
 35. Mathieu SV, Aragão KS, Imberty A, Varrot A. Discoidin I from *Dictyostelium discoideum* and Interactions with oligosaccharides: specificity, affinity, crystal structures, and comparison with discoidin II. *J Mol Biol.* 2010 Jul 16;400(3):540-54. doi: 10.1016/j.jmb.2010.05.042. Epub 2010 May 24. PubMed PMID: 20580724; PubMed Central PMCID: PMC2975065.
 36. Müller-Taubenberger A, Kortholt A, Eichinger L. Simple system – substantial share: The use of *Dictyostelium* in cell biology and molecular medicine. *Eur J Cell Biol.* 2013 Feb;92(2):45-53. doi: 10.1016/j.ejcb.2012.10.003. Epub 2012 Nov 27. PubMed PMID: 23200106.
 37. O'Day DH, Keszei A. Signalling and sex in the social amoebozoans. *Biol Rev Camb Philos Soc.* 2012 May;87(2):313-29. doi: 10.1111/j.1469-185X.2011.00200.x. Epub 2011 Sep 19. Review. PubMed PMID: 21929567.
 38. Paschinger K, Gutternigg M, Rendić D, Wilson IB. The N-glycosylation pattern of *Caenorhabditis elegans*. *Carbohydr Res.* 2008 Aug 11;343(12):2041-9. doi: 10.1016/j.carres.2007.12.018. Epub 2007 Dec 28. Review. PubMed PMID: 18226806.
 39. Paschinger K, Rendić D, Wilson IB. Revealing the anti-HRP epitope in *Drosophila* and *Caenorhabditis*. *Glycoconj J.* 2009 Apr;26(3):385-95. doi: 10.1007/s10719-008-9155-3. Epub 2008 Aug 26. Review. PubMed PMID: 18726691.

40. Payne S.H. (2005), Metabolic Pathways, in Dictyostelium Genomics (William F. Loomis, Adam Kuspa, eds) Horizon Bioscience, 41-57
41. Poole S, Firtel RA, Lamar E, Rowekamp W. Sequence and expression of the discoidin I gene family in Dictyostelium discoideum. J Mol Biol. 1981 Dec 5;153(2):273-89. PubMed PMID: 6279874.
42. Raines RT, McCormick M, Van Oosbree TR, Mierendorf RC. The S.Tag fusion system for protein purification. Methods Enzymol. 2000;326:362-76. PubMed PMID: 11036653.
43. Raper KB., Dictyostelium discoideum, a new species of slime mold from decaying forest leaves. Journal of Agricultural Research. 1935 Jan; 50(2):135-47.
44. Rendić, Dubravko, Mary Sharrow, Toshihiko Katoh, Bryan Overcarsh, Khoi Nguyen, Joseph Kapurch, Kazuhiro Aoki, Iain BH Wilson, and Michael Tiemeyer. "Neural-specific α -fucosylation of N-linked glycans in the Drosophila embryo requires Fucosyltransferase A and influences developmental signaling associated with O-glycosylation." *Glycobiology* 20, no. 11 (2010): 1353-1365.
45. Rosen SD, Kafka JA, Simpson DL, Barondes SH. Developmentally regulated, carbohydrate-binding protein in Dictyostelium discoideum. Proc Natl Acad Sci U S A. 1973 Sep;70(9):2554-7. PubMed PMID: 4517669; PubMed Central PMCID: PMC427054.
46. Ruoslahti E. The RGD story: a personal account. Matrix Biol. 2003 Nov;22(6):459-65. PubMed PMID: 14667838.
47. Saga Y, Yanagisawa K. Macrocyst development in Dictyostelium discoideum. I. Induction of synchronous development by giant cells and biochemical analysis. J Cell Sci. 1982 Jun;55:341-52. PubMed PMID: 6286696.
48. Sanchez JF, Lescar J, Chazalet V, Audfray A, Gagnon J, Alvarez R, Breton C, Imberty A, Mitchell EP. Biochemical and structural analysis of Helix pomatia agglutinin. A hexameric lectin with a novel fold. J Biol Chem. 2006 Jul 21;281(29):20171-80. Epub 2006 May 16. PubMed PMID: 16704980.
49. Schaap P., Evolutionary crossroads in developmental biology: Dictyostelium discoideum. Development. 2011 Feb;138(3):387-96. doi: 10.1242/dev.048934. Review. PubMed PMID: 21205784; PubMed Central PMCID: PMC3014629.
50. Schaap, P., T. Winckler, M. Nelson, E. Alvarez-Curto, B. Elgie, H. Hagiwara, J. Cavender, A. Milano-Curto, D. E. Rozen, T. Dingermann, R. Mutzel and S. L. Baldauf (2006). "Molecular phylogeny and evolution of morphology in the social amoebas." *Science* 314(5799): 661-3.
51. Schiller B, Hykollari A, Voglmeir J, Pörtl G, Hummel K, Razzazi-Fazeli E, Geyer R, Wilson IB. Development of Dictyostelium discoideum is associated with alteration of fucosylated N-glycan structures. Biochem J. 2009 Sep 14;423(1):41-52. doi: 10.1042/BJ20090786. PubMed PMID: 19614564; PubMed Central PMCID: PMC2851138.
52. Schiller B, Makrypidi G, Razzazi-Fazeli E, Paschinger K, Walochnik J, Wilson IB. Exploring the unique N-glycome of the opportunistic human pathogen Acanthamoeba. J Biol Chem. 2012 Dec 21;287(52):43191-204.
53. Schubert M, Bleuler-Martinez S, Butschi A, Wälti MA, Egloff P, Stutz K, Yan S, Collot M, Mallet JM, Wilson IB, Hengartner MO, Aebi M, Allain FH, Künzler M. Plasticity of the β -trefoil protein fold in the recognition and control of invertebrate predators and parasites by a fungal defence system. PLoS Pathog.2012;8(5):e1002706. doi:

- 10.1371/journal.ppat.1002706. Epub 2012 May 17.
54. Shevchenko, A., Henrik Tomas, J. H. S., Olsen, J. V., & Mann, M. (2007). In-gel digestion for mass spectrometric characterization of proteins and proteomes. *Nature protocols*, 1(6), 2856-2860.
 55. Shevchenko, A., Wilm, M., Vorm, O., & Mann, M. (1996). Mass spectrometric sequencing of proteins from silver-stained polyacrylamide gels. *Analytical chemistry*, 68(5), 850-858.
 56. Sobko A, Ma H, Firtel RA. Regulated SUMOylation and ubiquitination of DdMEK1 is required for proper chemotaxis. *Dev Cell*. 2002 Jun;2(6):745-56. PubMed PMID: 12062087.
 57. Stephenson SL., Stempen H., Myxomycetes: Handbook of slime molds, Timber Press, Jun 2005; ISBN-13: 978-0881924398.
 58. Sturm A, Bergwerff AA, Vliegthart JF. 1H-NMR structural determination of the N-linked carbohydrate chains on glycopeptides obtained from the bean lectin phytohemagglutinin. *Eur J Biochem*. 1992 Feb 15;204(1):313-6. PubMed PMID: 1740144.
 59. Teng-umnuay P, Morris HR, Dell A, Panico M, Paxton T, West CM. The cytoplasmic F-box binding protein SKP1 contains a novel pentasaccharide linked to hydroxyproline in *Dictyostelium*. *J Biol Chem*. 1998 Jul 17;273(29):18242-9. PubMed PMID: 9660787.
 60. Tremblay LO, Herscovics A. Cloning and expression of a specific human alpha 1,2-mannosidase that trims Man9GlcNAc2 to Man8GlcNAc2 isomer B during N-glycan biosynthesis. *Glycobiology*. 1999 Oct;9(10):1073-8. PubMed PMID: 10521544.
 61. Tsang AS, Devine JM, Williams JG. The multiple subunits of discoidin I are encoded by different genes. *Dev Biol*. 1981 May;84(1):212-7. PubMed PMID: 7250494.
 62. Urushihara, H. (2009). "The cellular slime mold: eukaryotic model microorganism." *Exp Anim* 58(2): 97-104.
 63. Van Haastert PJ, Janssens PM, Erneux C. Sensory transduction in eukaryotes. A comparison between *Dictyostelium* and vertebrate cells. *Eur J Biochem*. 1991 Jan 30;195(2):289-303. Review. PubMed PMID: 1997316.
 64. van Kuik JA, van Halbeek H, Kamerling JP, Vliegthart JF. Primary structure of the low-molecular-weight carbohydrate chains of *Helix pomatia* alpha-hemocyanin. Xylose as a constituent of N-linked oligosaccharides in an animal glycoprotein. *J Biol Chem*. 1985 Nov 15;260(26):13984-8. PubMed PMID: 4055767.
 65. Wacker M, Linton D, Hitchen PG, Nita-Lazar M, Haslam SM, North SJ, Panico M, Morris HR, Dell A, Wren BW, Aebi M. N-linked glycosylation in *Campylobacter jejuni* and its functional transfer into *E. coli*. *Science*. 2002 Nov 29;298(5599):1790-3. PubMed PMID: 12459590.
 66. Watts DJ, Ashworth JM. Growth of myxameobae of the cellular slime mould *Dictyostelium discoideum* in axenic culture. *Biochem J*. 1970 Sep;119(2):171-4. PubMed PMID: 5530748; PubMed Central PMCID: PMC1179339.
 67. West CM, McMahon D. Identification of concanavalin A receptors and galactose-binding proteins in purified plasma membranes of *Dictyostelium discoideum*. *J Cell Biol*. 1977 Jul;74(1):264-73. PubMed PMID: 559679; PubMed Central PMCID: PMC2109878.
 68. West CM, Nguyen P, van der Wel H, Metcalf T, Sweeney KR, Blader IJ, Erdos GW. Dependence of stress resistance on a spore coat heteropolysaccharide in *Dictyostelium*. *Eukaryot Cell*. 2009 Jan;8(1):27-36. doi: 10.1128/EC.00398-07. Epub 2008 Nov 7.

PubMed PMID: 18996984; PubMed Central PMCID: PMC2620749.

69. West CM, van der Wel H, Coutinho PM, Henrissat B. Glycosyltransferase Genomics. In: Loomis WF, Kuspa A, editors. *Dictyostelium Genomics*. Horizon Bioscience; 2005. pp. 235–264.
70. Wood WI, Capon DJ, Simonsen CC, Eaton DL, Gitschier J, Keyt B, Seeburg PH, Smith DH, Hollingshead P, Wion KL, Delwart E, Tuddenham EG, Vehar GA, Lawn RM. Expression of active human factor VIII from recombinant DNA clones. *Nature*. 1984 Nov 22-28;312(5992):330-7. PubMed PMID: 6438526.
71. Wright B, Simon W, Walsh BT. A kinetic model of metabolism essential to differentiation in *Dictyostelium discoideum*. *Proc Natl Acad Sci U S A*. 1968 Jun;60(2):644-51. PubMed PMID: 5248821; PubMed Central PMCID: PMC225095.
72. Xu Y, Brown KM, Wang ZA, van der Wel H, Teygong C, Zhang D, Blader IJ, West CM. The Skp1 protein from *Toxoplasma* is modified by a cytoplasmic prolyl 4-hydroxylase associated with oxygen sensing in the social amoeba *Dictyostelium*. *J Biol Chem*. 2012 Jul 20;287(30):25098-110. doi: 10.1074/jbc.M112.355446. Epub 2012 May 30. PubMed PMID: 22648409;
73. Yan S, Bleuler-Martinez S, Plaza DF, Künzler M, Aebi M, Joachim A, Razzazi-Fazeli E, Jantsch V, Geyer R, Wilson IB, Paschinger K. Galactosylated fucose epitopes in nematodes: increased expression in a *Caenorhabditis* mutant associated with altered lectin sensitivity and occurrence in parasitic species. *J Biol Chem*. 2012 Aug 17;287(34):28276-90.
74. Yanagishita M. Function of proteoglycans in the extracellular matrix. *Acta Pathol Jpn*. 1993 Jun;43(6):283-93. Review. PubMed PMID: 8346704.
75. Zhang P, McGlynn AC, Loomis WF, Blanton RL, West CM. Spore coat formation and timely sporulation depend on cellulose in *Dictyostelium*. *Differentiation*. 2001 Mar;67(3):72-9. PubMed PMID: 11428129.

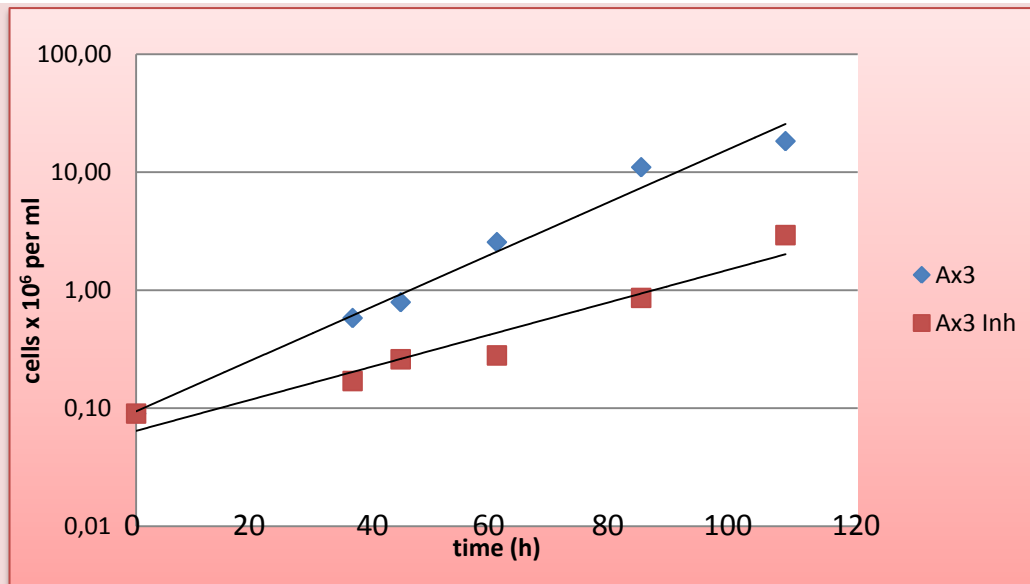
VIII. Appendix

8.1 Growth Kinetics of Ax3

According to Ashworth and Watts 1970, axenic growing *Dictyostelium discoideum* have a doubling time of 8 to 12 hours depending on the exact temperature, medium and presence of selective drugs. To confirm that simple growth kinetics measurements were done with the used Ax3 strain. Ax3 was cultured as described in chapter 4.1 with an initial number of 9×10^4 cells per ml. The cells were grown for about 4 and a half day (108 hours) till they reached the stationary phase of over 10^7 cells per ml. The results are shown in table 5.1.1 and figure 5.1.1. Excluding the non-log-phase growth, which is reached above 8×10^6 cells per ml, the doubling time was calculated. In comparison the growth kinetics of Ax3 grown in the presence of N-butyl-deoxynojirimycin (NB-DNJ) glucosidase II inhibitor revealed a decrease in growth rate. The doubling times for Ax3 and Ax3 with glucosidase II inhibitor are 11.39 hours and 17.82 hours respectively.

Table 5.1.1 Growth kinetics	0h	36h	44h	60h	84h	108h
Ax3	9×10^4	5.8×10^5	7.9×10^5	2.55×10^6	1.1×10^7	1.83×10^7
Ax3 with NB-DNJ	9×10^4	1.7×10^5	2.6×10^5	2.8×10^5	8.6×10^5	2.93×10^6

Figure 5.1.1 Growth curve Ax3 and Ax3 with glucosidase inhibitor



On logarithmic scale growth kinetics of Ax3 (blue diamonds) and Ax3 treated with glucosidase inhibitor (red square) are shown. The cells were grown for 108 hours at room temperature with constant shaking in HL5 media containing streptomycin.

As clearly shown by the graph due to the slower growth rate a gap in cell number of up to ten fold arose.

Glucosidase II removes distal glucoses, rendering fucosylation possible. The reason for the impaired growth rate in presence of glucosidase II inhibitor remains unsolved, but it might correlate with a reduction of the core- α -1,3-fucose moiety or other effects.

8.2 Abstract in German

Dictyostelium discoideum ist eine seit vielen Jahren erforschte Amöbe, welche, ausgelöst durch Hungerstress, in der Lage ist in einen Lebenszyklus zu wechseln, in welchem es mit tausenden anderen Zellen aggregiert und einen echten vielzelligen Organismus bildet. In dieser vielzelligen Entwicklungsphase differenzieren und spezialisieren sich einzelne Zellverbände unterschiedlich, was zu intra- und extrazellulären Veränderungen führt. Zum Beispiel verändert sich das N-Glykom. Während in der einzelligen Amöbe die neutralen N-Glykane vor allem α -1,3-Kern-fucosyliert sind und bis zu acht Mannosen und sogenannte „intersecting“ und „bisecting“ N-Acetylglucosamine tragen, tragen die neutralen N-Glykane der differenzierten Zellen keine „intersecting“ und „bisecting“ N-Acetylglucosamine und nur noch bis zu fünf Mannosen. Lediglich die α -1,3-Kern-fucosylierung bleibt unverändert.

Die Funktion dieser α -1,3-Kern-fucosylierung ist nachwievor unklar, jedoch scheint es sicher, dass in *Dictyostelium discoideum* zumindest ein Lektin existiert, welches an dieser funktionellen Gruppe binden kann. In meiner Arbeit bekräftige ich diese Annahme mittels Westernblot-Experimenten. Des Weiteren habe ich durch Affinitätschromatographie im *D. discoideum* Lysat nach Lektinen gesucht die in der Lage sind an HRP, einem Pflanzenprotein das α -1,3-Kern-fucosylierte N-Glykane trägt, zu binden. Die so isolierten Proteine wurden anschließend massenspektrometrisch analysiert. Hierdurch konnte ich tatsächlich ein potentiell α -1,3-Kern-fucosylierungs-bindendes Lektin identifizieren mit dem Namen Discoidin I. Um weitere biochemische Analysen mit dem Protein durchzuführen wurde eines der drei Discoidin I Gene, das dscA-1 Gen, mit einem N-terminalen His-tag in dem *E. coli* Expressionsstamm BL21 exprimiert und mittels Ni-NTA-Säule aufgereinigt. Abschließend wurden einige einfache Versuche über das Bindungsverhalten des Proteins durchgeführt die zu unerwarteten Ergebnissen führten. Da Discoidin I einen relativ komplexen Aufbau hat, bestehend aus zwei Zuckerbindungsstellen, eine N- und eine C-Terminal, wurden zusätzlich die Termini separat kloniert.

In dieser Arbeit erbringe ich Beweise für einen neuen, natürlich vorkommenden Bindungspartner von Discoidin I, und stelle der wissenschaftlichen Nachwelt rekombinante Discoidin I Expressionsstämme zur Verfügung mit deren Hilfe große Fortschritte in der entwicklungsbiologischen Aufklärung von *Dictyostelium discoideum* gemacht werden könnten.

8.3 Curriculum Vitae of the Author

Stefan **Mereiter**, BSc

education

Since January 2013

BOKU, Vienna, Austria

Master thesis: Glycan interactions in amoebae

Expected graduation: Summer 2013

October 2011 – September 2012

Tohoku University, Sendai, Japan

Cooperative Laboratory Study Programme (COLABS)

Graduate with AA-Levels

Since December 2010

University of Vienna, Austria

Field of Study: Molecular Biology

Programme: Postgraduate, Master Programme

October 2007 – November 2010

University of Vienna, Austria

Field of Study: Biology

Major: Molecular Biology

Bachelor thesis: Analysis of mitochondrial proteins and proteins of the protein degradation mechanism in plectin deficient muscles and characterisation of a plectin deficient myoblast cell line

Academic degree: Bachelor of Science

August 2006 – February 2007

Compulsory Military Service, VPW-Kaserne, Vienna, Austria

September 1997 – June 2006

Realgymnasium, Diefenbachgasse 19, Vienna, Austria

Austrian secondary education school type with emphasis on science

Graduate with A-Levels

professional experience

- Since January 2013 **BOKU, Vienna, Austria (master thesis)**
Wilson Group
Tasks: D. discoideum cultivation, affinity chromatography, MALDI-TOF, proteomics, recombinant protein expression in E. coli
- October 2011 – September 2012 **Tohoku University, Sendai, Japan (guest researcher)**
Higashitani Group
Tasks: C. elegans cultivation, western-blotting, RNA-isolation, cDNA, RT-PCR, epigenetical assays
- November 2010 – December 2010 **Max F. Perutz Laboratories, Vienna, Austria (internship)**
Barta Group
Tasks: PCR, RNA-Isolation, cDNA, transformation, mini-prep
- July 2010 – August 2010 **Max F. Perutz Laboratories, Vienna, Austria (bachelor thesis)**
Wiche Group
Tasks: western-blotting, cell culture, immunostaining, fluorescence microscopy
- August 2009 – September 2009 **Baxter, Vienna, Austria (internship)**
Incoming goods inspection
Tasks: Chemical and physical analysis of chemicals in terms of quality and purity
www.baxter.at

publication

Authors: Suetomi K, Mereiter S, Mori C, Takanami T, Higashitani A.
Title: Caenorhabditis elegans ATR checkpoint kinase ATL-1 influences life span through mitochondrial maintenance.
Journal: Mitochondrion. 2013 Feb 19. doi:pII: S1567-7249(13)00028-7.